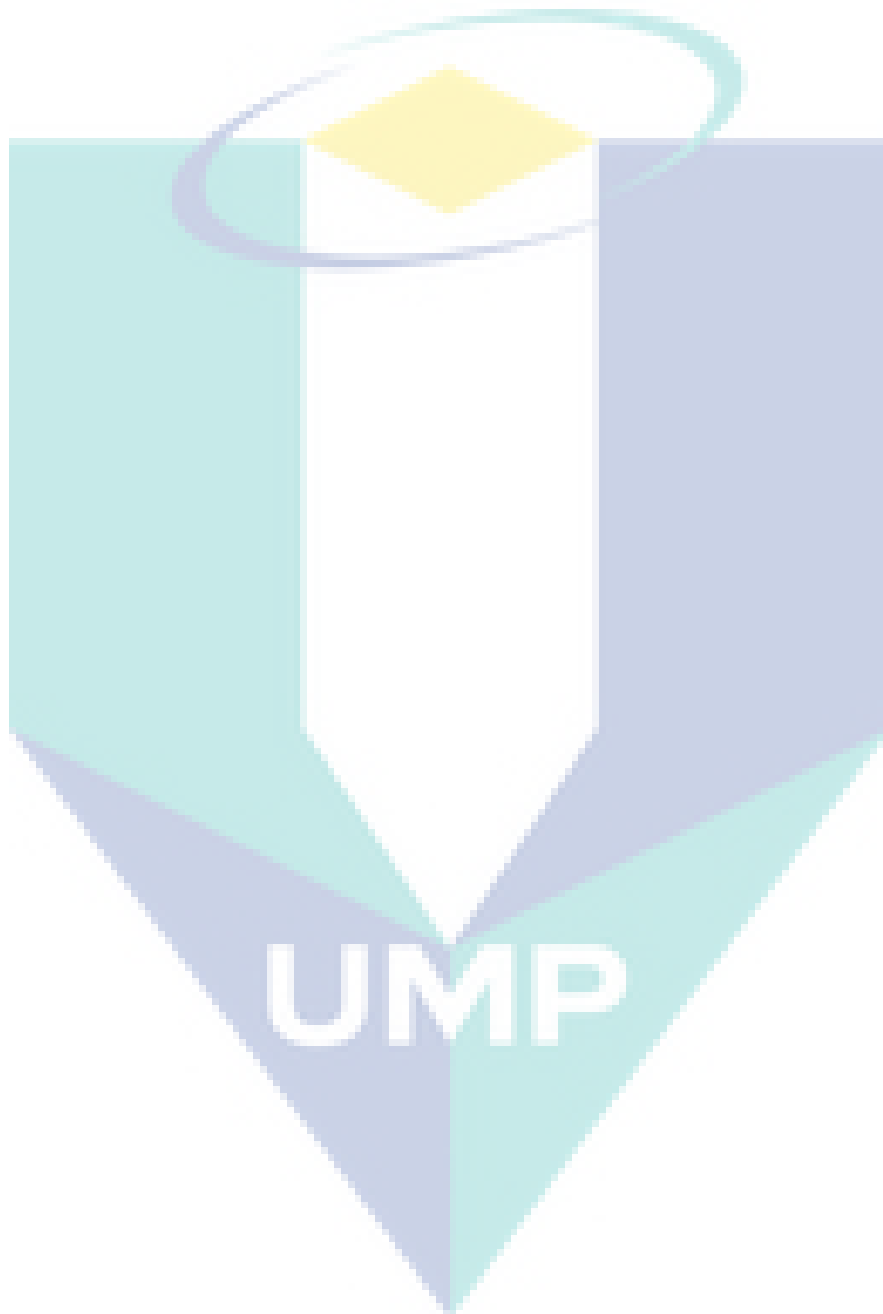


Thermal Management of Vehicle Radiator by Nanofluid

UMP

Click here to enter text.



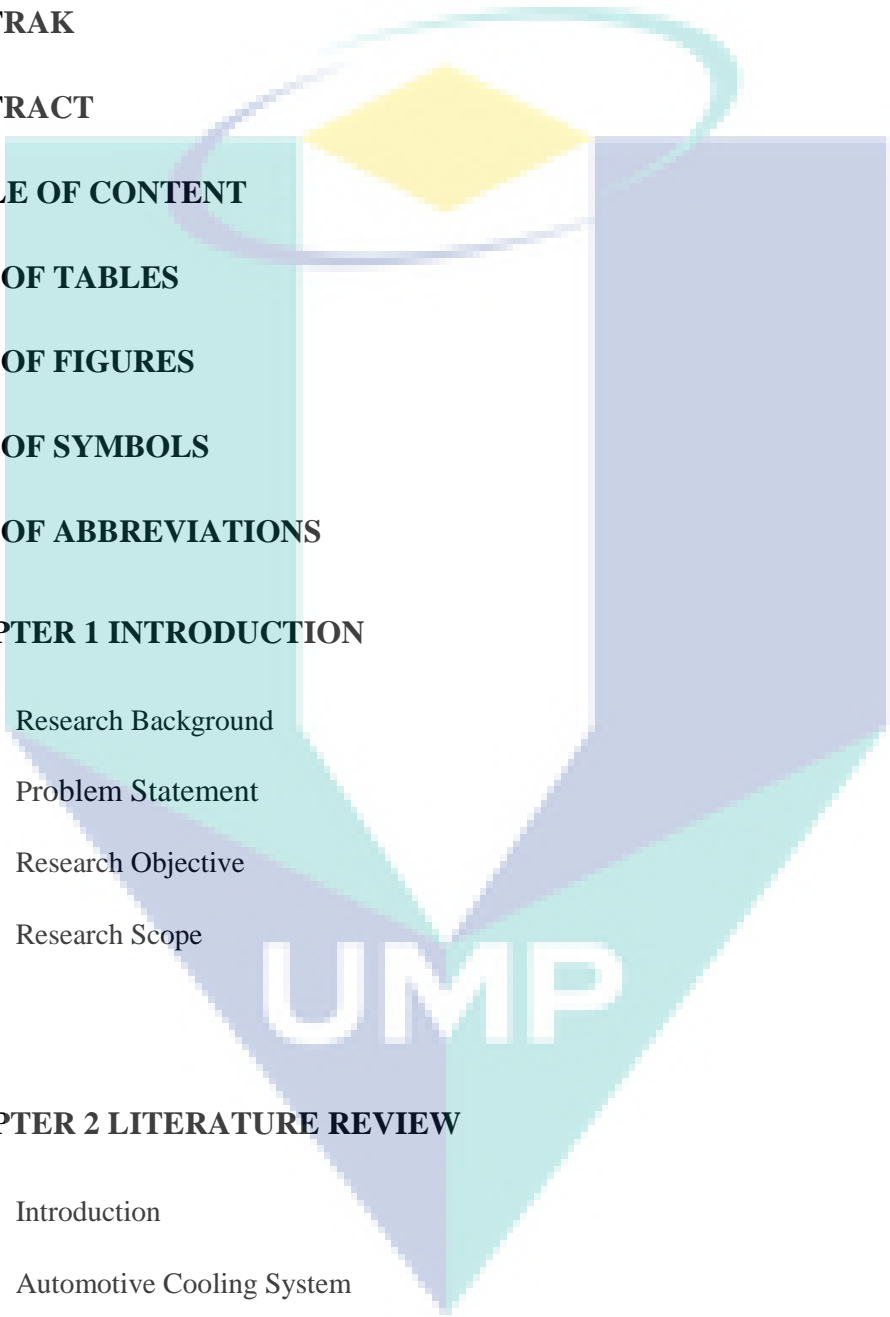
ABSTRAK

Kenderaan dilengkapi dengan sistem penyejukan untuk menyerap haba yang berlebihan dari enjin. Kajian menunjukkan bahawa penambahbaikan radiator telah mencapai tahap maksima dan sebarang pengubahsuaian tidak akan meningkatkan penyerapan haba. Manakala, nilai termofizikal yang rendah di dalam cecair penyejuk konvensional dikaitkan dengan penyerapan haba yang rendah. Oleh itu, permintaan untuk cecair penyejuk yang mempunyai nilai termofizikal yang tinggi semakin meningkat. Jika cecair penyejuk dengan nilai termofizikal yang tinggi dapat dihasilkan, saiz radiator boleh dikecilkan justeru ia akan membantu mengurangkan berat kenderaan. Dalam beberapa dekad yang lalu, penyelidikan terhadap bendalir nano mendapat perhatian penyelidik dari seluruh dunia. Bendalir nano ialah penyebaran bahan yang bersaiz nano di dalam larutan yang dapat membantu meningkatkan nilai termofizikal. Dalam kajian ini, bendalir nano yang diluputi oleh “nanocellulose” diekstrak daripada tumbuhan bernama “Hemlock Western” pada nisbah berat sebanyak 8.0% telah digunakan untuk meningkatkan nilai termofizikal. Bendalir nano dapat dihasilkan dengan mencampurkan “nanocellulose” dalam campuran Etilina glikol-air suling pada nisbah isipadu 40:60. Bendalir nano disediakan dengan menggunakan kaedah penyediaan dua langkah. Kestabilan bendalir nano telah dinilai dengan menggunakan kaedah kualitatif dan kaedah kuantitatif. Keputusan kestabilan bendalir nano menunjukkan bahawa ianya stabil lebih daripada satu bulan. Nilai termofizikal untuk bendalir nano telah diukur pada pelbagai kepekatan isipadu terdiri daripada 0.1, 0.5, 0.9 dan 1.3% yang diukur pada suhu diantara 30°C ke 80°C. Kadar penyerapan haba akan dibandingkan antara bendalir nano dan cecair konvensional di dalam radiator. Analisis statistik menunjukkan bahawa kepekatan isipadu 0.5% mempunyai nilai termofizikal yang optimum dan akan digunakan sebagai cecair penyejuk di dalam radiator untuk dibandingkan dengan cecair penyejuk konvensional. Eksperimen ini dijalankan pada dua keadaan yang berbeza iaitu tanpa pengaruh kipas dan dengan pengaruh kipas. Keputusan eksperimen menunjukkan bahawa nilai pekali pemindahan haba, pemindahan haba perolakan, nombor “Reynolds”, nombor “Nusselt” mempunyai hubungan berkadar terus dengan kadar aliran isipadu. Manakala, faktor geseran mempunyai hubungan songsang dengan kadar aliran isipadu. Pemindahan haba maksimum yang diperolehi dalam eksperimen ialah sebanyak 66.85% untuk keadaan tanpa pengaruh kipas dan 55.27% untuk keadaan dengan pengaruh kipas. Oleh itu, bendalir nano menyerap haba secara lebih berkesan jika dibandingkan dengan cecair penyejuk konvensional. Di samping itu, peningkatan pemindahan haba maksimum yang melibatkan aliran bendalir dalam radiator sebanyak 39.75% untuk keadaan tanpa pengaruh kipas dan 43.24% dalam keadaan pengaruh kipas. Selain itu, nilai “performance factor” untuk keadaan tanpa dan dengan pengaruh kipas ialah 2.15 dan 2.28. Oleh itu, bendalir nano yang dihasilkan daripada “nanocellulose” sesuai dijadikan sebagai bahan penyejuk dan boleh digunakan untuk aplikasi penyejukan enjin kerana ia mempunyai nilai penyerapan haba yang baik jika dibandingkan dengan cecair penyejuk konvensional.

ABSTRACT

The excess heat produced in an internal combustion engine is removed by mean of an automotive cooling system. A literature survey shows that improvement on fins and microchannel in the radiator already reaches it limitation and any further modification would not make any difference. On the other hand, it is reported that conventional thermal transport fluid has poor thermophysical property and another reason for low heat dissipation from engine. Thus, demand for thermal transport fluid with high thermophysical property is increasing as it able to enhance heat transfer performance. Besides, by using an improved thermal transport fluid, size of the radiator could be miniaturized which also reduces weight of the vehicle. Literally, it helps to improve engine performance of vehicle. Few decades ago, nanofluid is widely have been researched to be used in heat transport applications. Nanofluid is prepared by dispersing nano-scaled material into a basefluid which enhances thermophysical property. In this research, nanosubstance used was nanocellulose extracted from Western Hemlock plant at weight concentration of 8.0% to be used as novel thermal transport fluid in radiator. The nanosubstance is dispersed into ethylene glycol-distilled water mixture at volume ratio of 40:60, respectively. Heat transfer performance of nanofluid and conventional ethylene glycol-water mixture is compared in a fabricated radiator test rig. Nanofluid is prepared by using two-step preparation method. Stability of nanofluid is evaluated through qualitative and quantitative method. The stability results prove that nanofluid can be stable for more than a month. Thermophysical property measurement for nanofluid is measured for volume concentration of 0.1, 0.5, 0.9 and 1.3% at temperature ranged from 30°C to 80°C. Analysis from statistical tool shows that volume concentration 0.5% has an optimized thermophysical property and it had been used as nanofluid (thermal transport fluid) in radiator. Then, experiment for heat transfer performance comparison for nanofluid and conventional thermal transport fluid is conducted in the automotive radiator test rig. Experiment for heat transfer analysis is conducted under two different circumstances; without the influence of draft fan and with the influence of draft fan. The experiment result shows that experimental heat transfer coefficient, convective heat transfer, Reynolds number, Nusselt number has proportional relation with volumetric flow rate. Meanwhile, friction factor has inverse relation with the volumetric flow rate. Maximum convective heat transfer enhancement recorded is 66.85% for without the influence of fan circumstance and 55.27% with the influence of fan circumstance. Thus, nanofluid able to remove heat efficiently in automotive cooling system. On the other side, maximum heat transfer enhancement involving ratio of convective heat transfer against conductive heat transfer in radiator is 39.75% for without the influence of draft fan circumstance and 43.24% with the influence of fan circumstance. Besides, maximum thermal and hydraulic performance factor without and with the influence of fan is 2.15 and 2.28 respectively. Thus, nanocellulose based nanofluid is suitable for automotive cooling application since it has a better heat transfer performance than conventional thermal transport fluid.

TABLE OF CONTENT

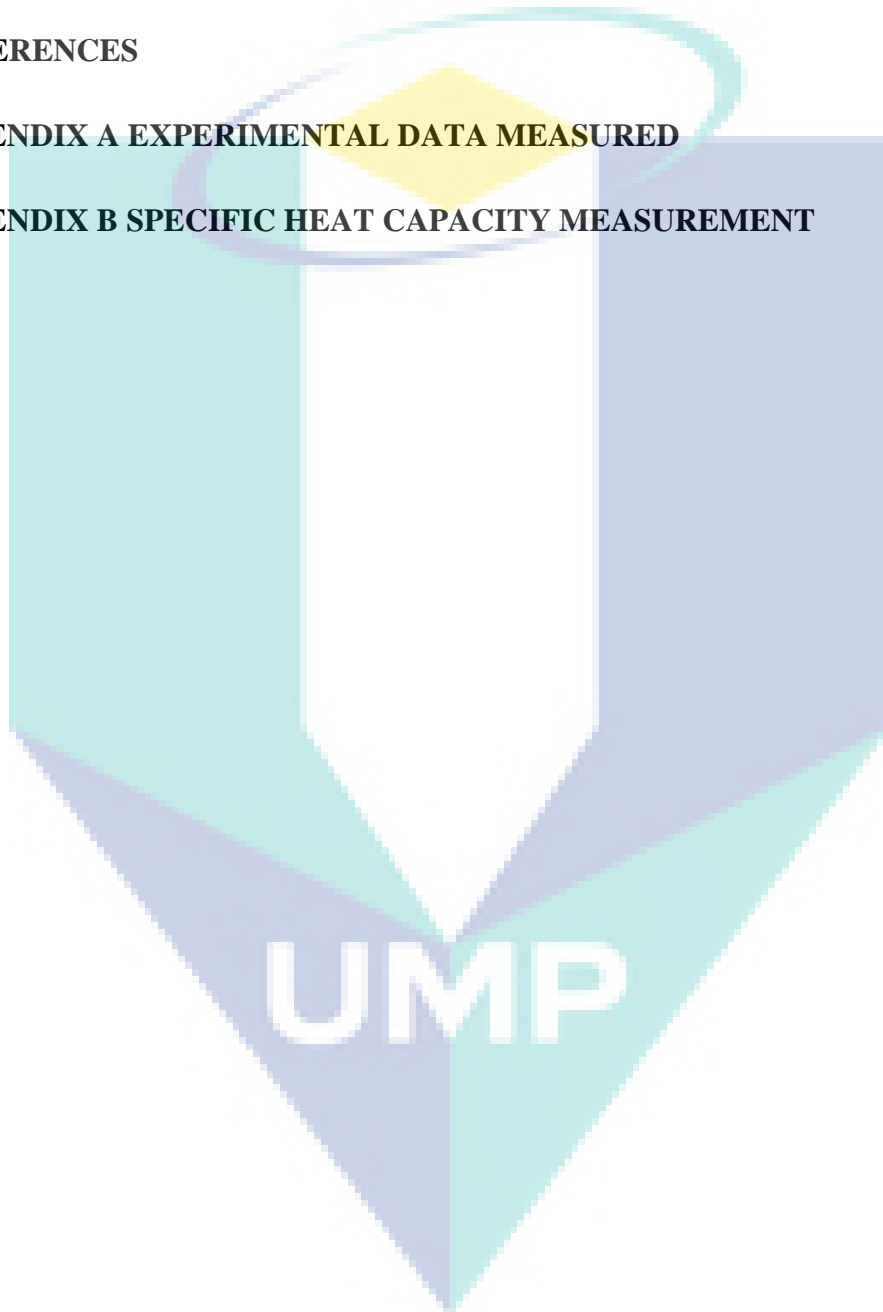


ABSTRAK	iii
ABSTRACT	iv
TABLE OF CONTENT	v
LIST OF TABLES	ix
LIST OF FIGURES	x
LIST OF SYMBOLS	xiv
LIST OF ABBREVIATIONS	xv
CHAPTER 1 INTRODUCTION	1
1.1 Research Background	1
1.2 Problem Statement	3
1.3 Research Objective	4
1.4 Research Scope	4
CHAPTER 2 LITERATURE REVIEW	6
2.1 Introduction	6
2.2 Automotive Cooling System	6
2.3 Nanofluids	9
2.3.1 Nanofluid Application	10
2.3.2 Preparation method of Nanofluid	11

2.3.3	Nanofluid Stability	13
2.3.4	Nanofluid Stability Evaluation	14
2.4	Improvement on Nanofluid Stability	16
2.5	Thermophysical Property of Nanofluid	17
2.5.1	Thermal Conductivity	18
2.5.2	Dynamic Viscosity	21
2.5.3	Density	23
2.5.4	Specific Heat Capacity	24
2.6	Flow Behaviour of Fluid	25
2.6.1	Reynolds Number	25
2.6.2	Nusselt Number	26
2.7	Convection Heat Transfer of Nanofluids	27
2.8	Experimental Study on Automotive Radiator	28
2.9	Conclusions	31
CHAPTER 3 METHODOLOGY		33
3.1	Introduction	33
3.2	Research Flow Chart	33
3.3	Nanofluid Preparation	35
3.4	Thermophysical Property Measurement	37
3.4.1	Thermal Conductivity	37
3.4.2	Dynamic Viscosity	39
3.4.3	Density	40
3.4.4	Specific Heat Capacity	41
3.5	Nanofluid Stability Measurement	42
3.5.1	Sedimentation Observation	42

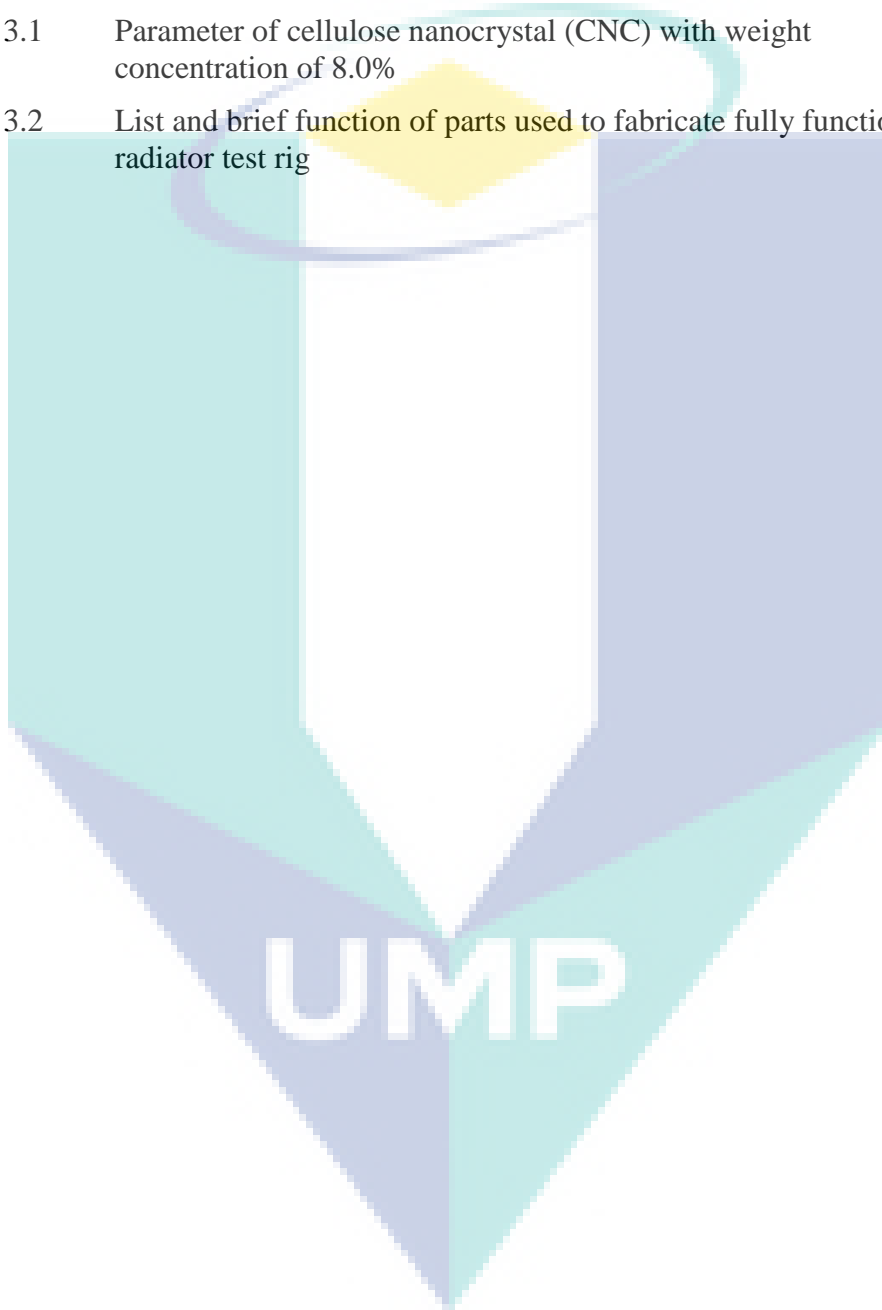
3.5.2	Ultra Violet-Visible Spectrophotometry	43
3.6	Experimental Setup	43
3.7	Fabrication of Radiator Test Rig	46
3.7.1	Experimental Procedure	47
3.8	Data Collection and Analysis	47
CHAPTER 4 RESULTS AND DISCUSSION		51
4.1	Introduction	51
4.2	Nanofluid Stability	51
4.2.1	Sedimentation Observation	52
4.2.2	Ultraviolet-visible Spectrophotometry	53
4.3	Thermophysical Property of Nanofluid	55
4.3.1	Thermal Conductivity	55
4.3.2	Dynamic Viscosity	57
4.3.3	Density	59
4.3.4	Specific Heat Capacity	60
4.4	Nanofluid optimization	61
4.5	Heat Transfer Performance and Flow Behaviour Analysis	63
4.5.1	Experimental Heat Transfer Coefficient	64
4.5.2	Convection Heat Transfer	67
4.5.3	Reynolds Number	69
4.5.4	Nusselt Number	71
4.5.5	Friction Factor	74
4.5.6	Heat Transfer Enhancement	75
4.5.7	Thermal and Hydraulic Performance Factor	77
4.5.8	Temperature Distribution Analysis on Automotive Radiator	79

CHAPTER 5 CONCLUSIONS	83
5.1 Introduction	83
5.2 Conclusions	83
5.3 Recommendations	85
REFERENCES	86
APPENDIX A EXPERIMENTAL DATA MEASURED	94
APPENDIX B SPECIFIC HEAT CAPACITY MEASUREMENT	95



LIST OF TABLES

Table 2.1	Review of thermal conductivity enhancement for various type of nanofluid at varying temperature and volume concentration	20
Table 2.1	Review of dynamic viscosity enhancement for various type of nanofluid at varying temperature and volume concentration	22
Table 3.1	Parameter of cellulose nanocrystal (CNC) with weight concentration of 8.0%	35
Table 3.2	List and brief function of parts used to fabricate fully function radiator test rig	46



LIST OF FIGURES

Figure 2.1	Vital parts in automotive cooling system	7
Figure 2.2	Direction of coolant flow from engine block to radiator in a closed loop	8
Figure 2.3	List of common challenges found in nanofluid	9
Figure 2.4	Various nanofluid application for industrial and commercial purposes	10
Figure 2.5	Preparation technique through one-step preparation method	12
Figure 2.6	Preparation technique through two-step preparation method	12
Figure 2.7	Effect of surface charge on producing various type of dispersion level	13
Figure 2.8	Gradual settlement of nanosubstance at bottom of the container over time	15
Figure 2.9	Position of potential charges and layers in a diagrammatic zeta potential concept	16
Figure 2.10	Graphical illustration of nanomaterial settlement at bottom of test tube over time in which absorbance drop will <u>be measured</u> by using spectrophotometry	16
Figure 2.11	Relationship between isoelectric, pH value and zeta potential	17
Figure 2.12	Various thermal conductivity measurement method for liquid solution	18
Figure 2.13	Percentage of thermal conductivity measurement method used in nanofluid based to published literature	19
Figure 2.14	Principle factor that influence thermal conductivity enhancement in nanofluid	21
Figure 2.15	Principle factor that influence dynamic viscosity enhancement in nanofluid	23
Figure 2.16	Type of fluid flows and its pattern	25
Figure 2.17	Relationship between Nusselt number and Reynolds number at varying microchannel dimension	27
Figure 2.18	Schematic diagram and dimension of radiator used to study effect of Al ₂ O ₃ based nanofluid on heat transfer enhancement	29
Figure 2.19	Illustration of experiment setup to study influence of CuO based nanofluid on heat transfer convection and radiator used in the experiment	30
Figure 2.20	Schematic diagram of experimental setup to study influence of ZnO based nanofluid on heat transfer enhancement	31
Figure 3.1	Research process flowchart used in this experiment	34

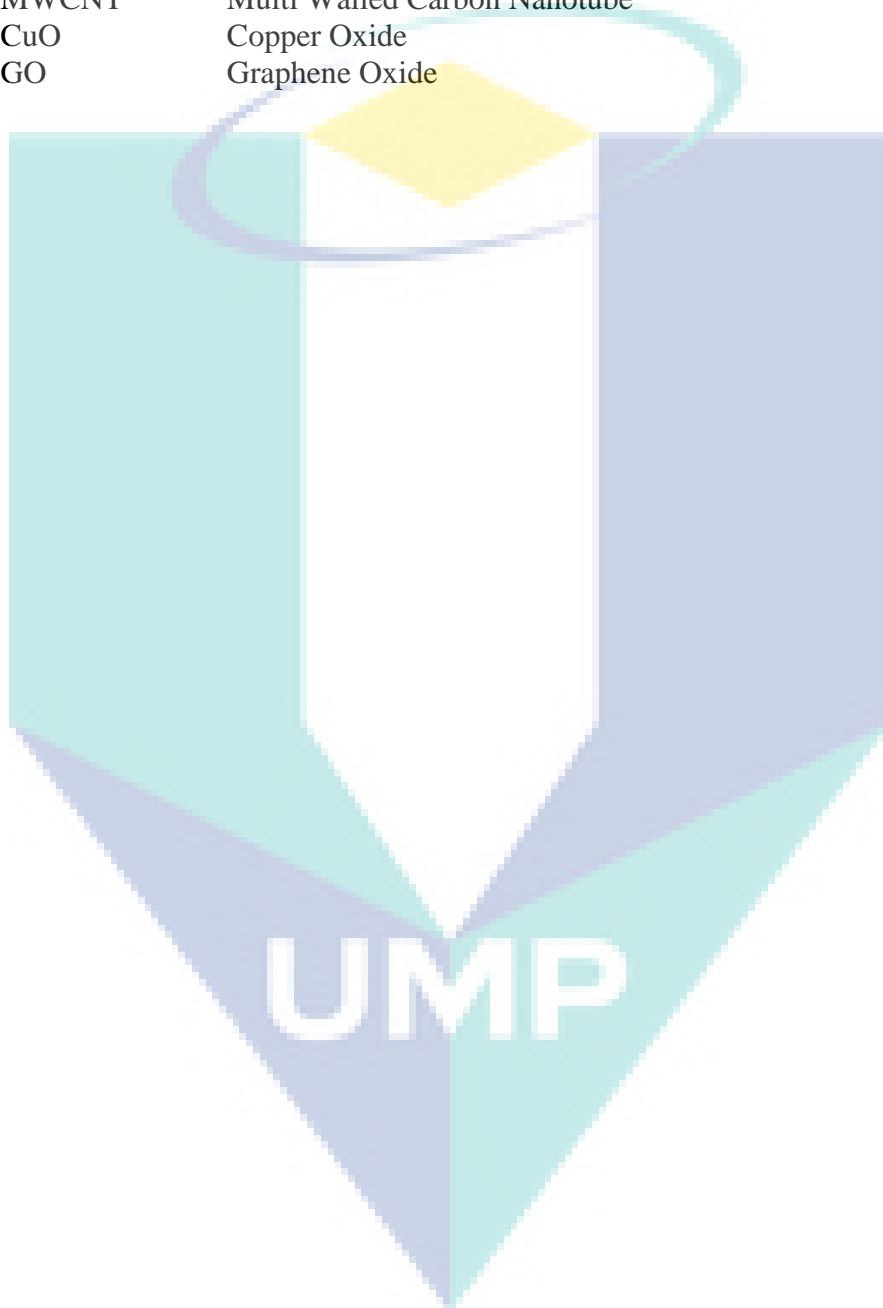
Figure 3.2	Micrographic evaluation of CNC under 120kV Bio-TEM microscope	36
Figure 3.3	Thermal conductivity measurement technique by using KD2 Pro Thermal Analyser	38
Figure 3.4	Error comparison for thermal conductivity measurement between ethylene glycol-water mixture (base fluid) and ASHRAE data	38
Figure 3.5	Equipment and measuring technique for dynamic viscosity by using Brookfield LVDV-III Ultra Programmable Rheometer	39
Figure 3.6	Error comparison for dynamic viscosity measurement between ethylene glycol-water mixture (base fluid) and ASHRAE data	39
Figure 3.7	Experiment setup for density measurement	40
Figure 3.8	Error comparison for density measurement between ethylene glycol-water mixture (base fluid) and ASHRAE data	41
Figure 3.9	Differential scanning calorimetry (DSC) model number (Perkin Elmer DSC-8000) that had been used to determine specific heat capacity value	41
Figure 3.10	Nanofluid is poured in test tubes and left undisturbed to observe settlement of nanofluid for one month	42
Figure 3.11	Spectrophotometry model name (Shimadzu UV2600) that had been used to measure absorbance drop value in nanofluid	43
Figure 3.12	Schematic diagram of fabricated radiator test rig in this experiment	44
Figure 3.13	Location of major diameter, minor diameter and length in radiator used in this research	44
Figure 3.14	Volumetric flow rate measurement at various operating voltage	45
Figure 3.15	Parts that had been used to fabricate fully function radiator test rig to study heat transfer performance	46
Figure 4.1	Photographs shows comparison of appearance taken at different timeline which shows no settlement of nanosubstance at bottom of test tube	52
Figure 4.2	Peak absorbance value is measured at 254 nm for all the volume concentration	53
Figure 4.3	Absorbance drop of 5.51% is measured for volume concentration 0.1% after one month of nanofluid preparation	54
Figure 4.4	Absorbance drop of 1.14% is measured for volume concentration 1.3% after one month of nanofluid preparation	54
Figure 4.5	Comparison of thermal conductivity at varying temperature and volume concentration	55
Figure 4.6	Comparison of thermal conductivity enhancement at varying temperature and volume concentration	56
Figure 4.7	Comparison of dynamic viscosity measurement at varying temperature and volume concentration	58

Figure 4.8	Comparison of relative dynamic viscosity measurement at varying temperature and volume concentration	58
Figure 4.9	Comparison of density measurement at varying temperature and volume concentration	59
Figure 4.10	Comparison of specific heat capacity measurement at varying temperature and volume concentration	61
Figure 4.11	Results from statistical analysis for composite desirability, D	62
Figure 4.12 (a)	Results from statistical analysis for individual desirability for thermal conductivity	63
Figure 4.12 (b)	Results from statistical analysis for individual desirability for specific heat capacity	63
Figure 4.12 (c)	Results from statistical analysis for individual desirability for density	63
Figure 4.12 (d)	Results from statistical analysis for individual desirability for dynamic viscosity	63
Figure 4.13	Comparison of experimental heat transfer coefficient results for CNC and EGW against flow rate (without influence of fan)	64
Figure 4.14	Relative experimental heat transfer coefficient results against varying flow rate (without influence of fan)	65
Figure 4.15	Comparison of experimental heat transfer coefficient results for CNC and EGW against flow rate (with influence of fan)	66
Figure 4.16	Results of relative experimental heat transfer coefficient against flow rate (with influence of fan)	66
Figure 4.17	Comparison of convective heat transfer results for CNC and EGW against varying flow rate (without influence of fan)	68
Figure 4.18	Comparison of convective heat transfer results for CNC and EGW against varying flow rate (with influence of fan)	68
Figure 4.19	Overall convective heat transfer enhancement comparison at two experiment circumstances (with and without influence of fan)	69
Figure 4.20	Results for Reynolds number against varying flow rate (conventional ethylene glycol - EGW)	70
Figure 4.21	Results for Reynolds number against varying flow rate (Nanofluid –CNC)	71
Figure 4.22	Comparison of Nusselt number against varying flow rate for nanofluid and EGW under without fan circumstance	72
Figure 4.23	Comparison of Nusselt number against varying flow rate for nanofluid and EGW under with fan circumstance	72
Figure 4.24	Results for Nusselt number against varying Reynold number for EGW under two different circumstances	73
Figure 4.25	Results for Nusselt number against varying Reynold number for CNC under two different circumstances	73

Figure 4.26	Results for friction factor against varying Reynolds number for EGW	74
Figure 4.27	Results for friction factor against varying Reynolds number for CNC	75
Figure 4.28	Results of heat transfer enhancement against flow rate (without influence of fan)	76
Figure 4.29	Results of heat transfer enhancement against flow rate (with influence of fan)	76
Figure 4.30	Overall comparison of heat transfer enhancement against varying flow rate under two different circumstances	77
Figure 4.31	Results of overall cooling system efficiency against flow rate (without influence of fan)	78
Figure 4.32	Results of overall cooling system efficiency against flow rate (with influence of fan)	78
Figure 4.33	Overall comparison of performance factor against varying flow rate under two circumstances	79
Figure 4.34	Temperature distribution at flow rate 3.5 LPM – EGW (without fan)	80
Figure 4.35	Temperature distribution at flow rate 3.5 LPM – CNC (without fan)	80
Figure 4.36	Temperature distribution at flow rate 4.5 LPM – EGW (without fan)	80
Figure 4.37	Temperature distribution at flow rate 4.5 LPM – CNC (without fan)	80
Figure 4.38	Temperature distribution at flow rate 5.5 LPM – EGW (without fan)	80
Figure 4.39	Temperature distribution at flow rate 5.5 LPM – CNC (without fan)	80
Figure 4.40	Temperature distribution at flow rate 3.5 LPM – EGW (with fan)	81
Figure 4.41	Temperature distribution at flow rate 3.5 LPM – CNC (with fan)	81
Figure 4.42	Temperature distribution at flow rate 4.5 LPM – EGW (with fan)	81
Figure 4.43	Temperature distribution at flow rate 4.5 LPM – CNC (with fan)	81
Figure 4.44	Temperature distribution at flow rate 5.5 LPM – EGW (with fan)	81
Figure 4.45	Temperature distribution at flow rate 5.5 LPM – CNC (with fan)	81

LIST OF SYMBOLS

TiO ₂	Titanium Dioxide
ZnO	Zinc Oxide
SiO ₂	Silicon Dioxide
CNT	Carbon Nanotube
MWCNT	Multi Walled Carbon Nanotube
CuO	Copper Oxide
GO	Graphene Oxide



LIST OF ABBREVIATIONS

CNC	Cellulose Nanocrystals
EGW	Ethylene glycol-distilled water mixture
TEM	Transition Electron Microscope
SEM	Scanning Electron Microscope
UV-Vis	Ultra Violet visible Spectrometry
ASHRAE	American Society of Heating, Refrigeration, and Air Conditioning Engineers
DSC	Differential Scanning Calorimetry
STA	Simultaneous Thermal Analyzer
IEP	Isoelectric Point
LPM	Liter per Minute
RPM	Rotation per Minute
RSM	Response Surface Methodology



UMP

CHAPTER 1

INTRODUCTION

1.1 Research Background

According to a version in first law of Thermodynamics, known as conservation of energy defines that energy cannot be created nor destroyed but can transfer from one state to another (Cengel et al., (2006). In real life, extensive engineering applications such as semiconductor industry, power generation industry, manufacturing industry and automotive industry produces excessive heat energy which is an unwanted element. In those cases, thermal transport fluid plays an important role for heat absorption from the system. Common conventional heat transfer fluid that is widely being used is ethylene glycol, water, various type of coolant etc.

In this 21st century, technology advancement in automotive industry is very impressive as high-efficiency engines with better performance is achievable. Unfortunately, engine with high performance requires extra fuel to be burned which results in excessive heat exposure in combustion chamber. In automobile, heat in engine blocks is being carried away with the help of automotive cooling system. Engine coolant (thermal transport fluid) flows over the engine blocks and eventually carries the heat from the engine block. The process ends at radiator where thermal transport fluid from engine block cools down the excessive heat as it enters microchannel and fins assembled together the radiator. According to Kulkarni et al., (2008), improvement on fins and micro channel in radiator already reaches its limitation and any further modification would not make any difference. Meanwhile, K. Y. Leong et al., (2010) suggests novel and innovative thermal transport fluid is required to improve heat transfer rate in automobile radiator.

Innovation remedy for thermophysical property is found by Maxwell, (1881) by suspending micro sized particles into the basefluid. Hence, this development faces great

challenges as it faces few drawbacks. The major problem with the micro sized suspension is high sedimentation, clogging and causes erosion. Micro sized particle is heavy which causes it to settle at bottom of solution which leads to high sedimentation. Low stability is not preferable as it affects thermophysical measurement. Meanwhile, these large particles causes erosion on rotating mechanical parts (Godson et al., 2010).

In 1993, nanofluid is introduced by Masuda et al., (1993) as it becomes a great breakthrough for the researchers around the world. Nanofluid able to produce drastic thermal conductivity enhancement which helps for conduct heat more efficiently from thermal transport applications. It can be formed by suspending nanomaterial ranged between 1 – 100 nm into base fluid. The selection of nanosubstance and base fluid depends on the application. Preliminary research conducted by Eastman et al., (2001), proves that suspension of Cu nanoparticle enhances thermal conductivity around 40% in ethylene glycol based fluid. Meanwhile, Putra et al., (2003) proves that dispersion of CuO nanoparticle in water produces maximum thermal conductivity enhancement of 29%. Recently, Aravind & Ramaprabhu, (2013) conducted an experiment through nanocomposite approach by dispersing carbon nanotube and GO into ethylene glycol. The maximum thermal conductivity enhancement of 24% is measured at 50°C and volume concentration of 0.04%.

In fact, nanosubstance can be categorized into nanoparticle, nanorod, nanowire, nanosheet and nanotube. Each category is differentiated by its physical appearance such as size, shape and aspect ratio. Thus, variation in physical appearance produces different amount of thermophysical enhancement. The selected type of nanosubstance and base fluid plays a major role in thermophysical property enhancement. Experiment conducted by Murshed et al., (2008) reveals that nanoparticle in sphere size enhances thermal conductivity better than cylinder shaped nanoparticle. It can be best explained by variation of surface area to volume ratio among type of nanosubstances. Thus, nanoparticle with high surface area produces better thermal conductivity enhancement (Murshed et al., 2008).

Cellulose Nanocrystals (CNC), a cellulosic extract from biosynthesis product remarked as renewable and environmentally benign material at the nanoscale (Abitbol et al., 2016). They publicized to have tailored mechanical and physical property that endorses them for diversity applications focusing towards green nature-based activities.

Moreover, CNC's characteristics such as biodegradable, nontoxic, large surface area, film forming, and high strength, stand out from nanoparticle (Rodionova et al., 2012). There are some promising rooms for CNC based solution to have better thermophysical property to exhibit good heat conductivity. Thus, CNC based nanofluid can be used in thermomechanical systems such as automobiles, air conditioners etc as a thermal transport fluid.

1.2 Problem Statement

In automobile cooling system, radiator plays a significant role to dissipate heat from thermal transport fluid. The construction of radiator with high surface area helps to remove heat from thermal transport fluid as it flows. According to Kulkarni et al., (2008), modification on radiator reaches its limitation and further modification doesn't causes significant effect on heat transfer performance. Alternatively, heat transfer can be enhanced by using bigger radiator with high number of fins and tubes. Unfortunately, this technique consumes space in the vehicle. Besides, increasing thermal management system increases drag coefficient and fuel consumption eventually reduces engine performance.

Conventionally, ethylene glycol-water mixture has been used as thermal transport fluid for heat removal in car radiator. However, these conventional thermal transport fluid exhibits low thermal conductivity and specific heat capacity value which is responsible for poor heat performance in engine cooling system. Thus, conventional thermal transport fluid is incapable to absorb heat efficiently in high-performance engines. In addition, demands for novel thermal transport fluid with enhanced thermophysical property is increasing for a better heat removal cooling system.

Besides, by using an improved thermal transport fluid, small sized radiator could be used which also reduces weight of the vehicle. Moreover, it helps to improve engine performance of vehicle. According to Mathivanan et al., (2017), usage of nanofluid in heat transfer applications able to improve cooling rate in thermal management system. Nanocellulose based nanofluid has good site for chemical modification which is expected suitable to be used for thermal transport applications (Siró & Plackett, 2010). Besides, nanocellulose has hydrophilic characteristics which helps the cellulose to dissolve in ethylene glycol-distilled water mixture well (Duran et al., 2012).

1.3 Research Objective

The objectives of this research are as follows:

- i) To optimize formation of stable condition from dispersion of Cellulose Nanocrystals (CNC) in diluted ethylene glycol
- ii) To determine thermophysical properties (thermal conductivity, dynamic viscosity, density and specific heat capacity)
- iii) To analyse heat transfer performance of nanofluid in a radiator test rig

1.4 Research Scope

The scope of this work are as follows:

- i) The preparation of a stable nanofluid by using Cellulose Nanocrystals (CNC) extracted from Western Hemlock plant at weight concentration of 8.0% as a dispersant.
- ii) The ethylene glycol-distilled water mixture at volume ratio 40:60 as basefluid and prepared by using two-step preparation method.
- iii) The thermophysical property measurement and optimization of nanofluid for volume concentration up to 1.3%.
- iv) The experiment is conducted at an operating temperature of 80°C at varying volumetric flow rate of 3.5, 4.5 and 5.5 LPM.
- v) This study focuses on heat transfer performance between nanofluid and conventional thermal transport fluid in a fabricated radiator test rig.

CHAPTER 2

LITERATURE REVIEW

2.1 Introduction

The chapter begins with explanation of automotive cooling system. Vital parts in automotive cooling system are water pump, thermostat, pressure cap, fan and radiator. Then, history and preparation of nanofluid is highlighted. Nanofluid can be prepared via one-step and two-step preparation methods. During preparation, physical agitation is important to homogenize nanofluid. In fact, nanofluid stability determine its quality and can be validated through qualitative and quantitative method. Examples of qualitative method is sedimentation observation and micrographic visual evaluation. Meanwhile, examples of quantitative method are zeta potential evaluation, absorbance drop evaluation through UV-visible spectrophotometry and monitoring changes in pH value. Thus, procedures to measure nanofluid stability is explained with the visual aids. Thermophysical property is consists of measurement of thermal conductivity, dynamic viscosity, specific heat capacity and density. These thermophysical property measurement is vital to understand nanofluid behaviour at varying temperature and volume concentration. The chapter ends with highlights of reported forced heat convection experiments in car radiator using nanofluids.

2.2 Automotive Cooling System

In automobile, engine is the most vital component that requires proper care and maintenance to prevent major overhaul. During combustion, 33% of thermal energy is converted to heat energy (Yadav & Singh, 2011). Literally, high heat energy causes overheating in engine. In fact, overheating is an unwanted element in combustion chamber because it brings catastrophic consequences such as knocking, wear and formation in piston and cylinder which reduces life span of engine (Joseph & Isaac,

2016). Thus, overheating in engine should be avoided at any cost. The most promising and reliable method to control overheating in engine is by having a well-designed heat exchanger (radiator) with efficient thermal transport fluid.

Automotive cooling system consists of water pump, thermostat, pressure cap, draft fan and radiator as depicted in Figure 2.1. As engine reaches maximum allowable temperature, thermostat valve opens and let thermal transport fluid flows through the engine blocks. Simultaneously, pump is turned on which is responsible to drive hot thermal transport fluid from engine compartment to radiator. Meanwhile, pressure cap loaded with spring ensure cooling system is kept at high pressure which increases thermal transport fluid's boiling point. Besides, the crucial part in automotive cooling system is radiator, which act as a heat exchanger that dissipates heat by flowing thermal transport fluid through it.

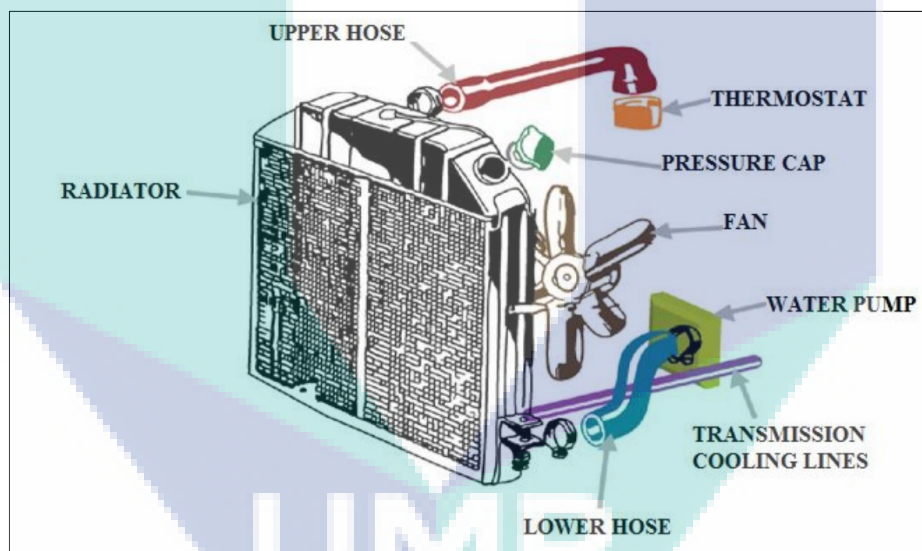


Figure 2.1 Vital parts in automotive cooling system

Source: Yadav & Singh (2011).

As illustrates in Figure 2.2, thermal transport fluid or in another term coolant transmits through engine block and cylinder head to remove excessive heat. Meanwhile, flow rate of coolant and fan speed determine the radiators heat transfer performance. This is because heat removal in radiator is related with heat conduction and forced heat convection principle. Thermal transport fluid that make contacts with tubes inside the radiator remove heat by conduction process and further heat removal is achieved by forced convection process by absorbing heat through the fins. High count of fins increases

surface area of contact and ensures maximize heat removal from the thermal transport fluid. Thus, cooling rate of the system is enhanced by modifying micro channel and fins in radiator. Conventionally, ethylene glycol and water is being used as engine coolant in automotive applications. The major drawback with these coolants is corrosion on cooling channel due to high acidic level and has limited thermophysical property that slows down the heat transfer process.

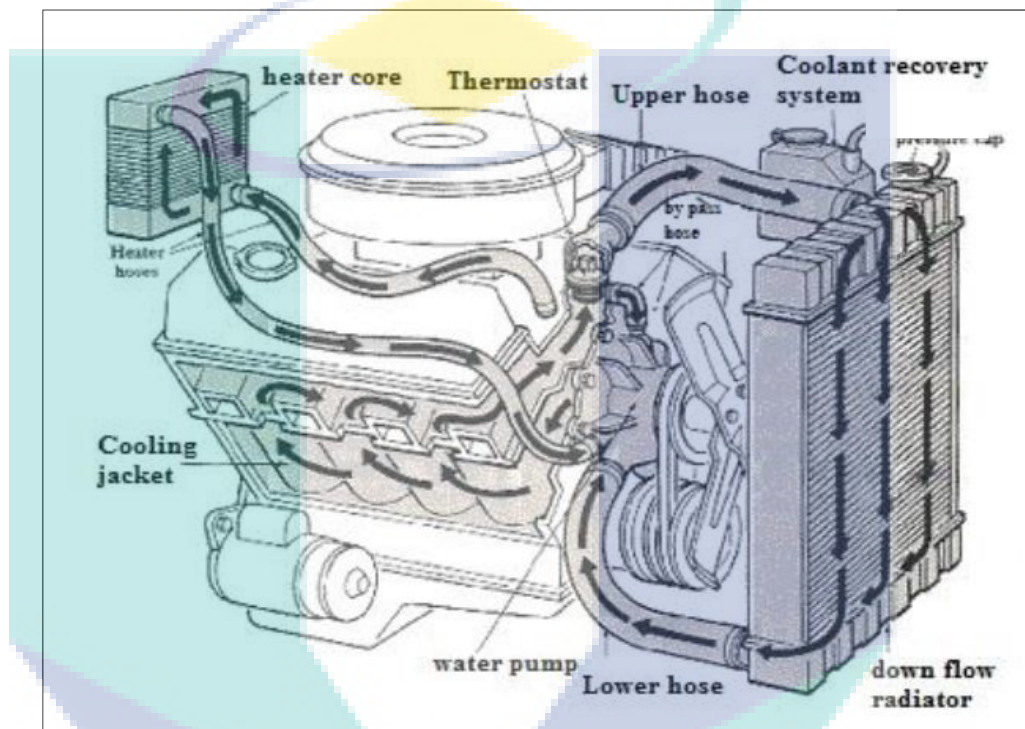


Figure 2.2 Direction of coolant flow from engine block to radiator in a closed loop
Source: Yadav & Singh (2011).

As a remedy, the use of nanofluid in radiator, enhances heat removal and increases effectiveness of overall cooling system (Hussein et al., 2014). Experiment conducted by S.M. Peyghambarzadeh et al., (2011) enhance heat transfer efficiency up to 45% compared to pure water by using Al_2O_3 nanoparticle at low volume concentration. In another experiment conducted in radiator test rig, Naraki et al., (2013) manage to enhance overall heat transfer coefficient up to 8% as CuO nanoparticle based nanofluid was used. Recent research by Shi et al., (2017) proves that nanofluid, made up of SiO_2 nanoparticle has a potential to dissipate heat 1.17 times better than pure water as basefluid. Thus, dispersion of nanomaterial into basefluid enhances thermophysical property of nanofluid. This is because enhanced thermal conductivity and specific heat capacity increases heat removal rate which also improves performance factor of a cooling system.

2.3 Nanofluids

In 1881, excessive thermal problem is solved by dispersing micro sized particle into basefluid which produces a better heat absorption performance (Maxwell, 1881). This modification helps to eliminate excessive thermal problem in most applications. Per se, micro sized dispersion causes some major drawback such as high sedimentation, clogging on cooling passageway and produces erosion on moving parts (Godson et al., 2010). Two-decade later, introduction of nanofluid by Masuda et al., (1993) which is through colloidal suspension of nanoparticles in range of 1-100nm into basefluid enhances thermophysical property which exhibits great potential for thermal transport applications.

Nevertheless, there are several problems that can be commonly found in nanofluid as illustrates in Figure 2.3. In fact, nanoparticle has high reactivity which increases agglomeration and cluster formation. Eventually, this phenomenon causes high sedimentation to occur and causes the nanofluid to have low stability (Mahbubul et al., 2017). Besides that, addition of nanomaterial into basefluid increases dynamic viscosity in nanofluid. High viscosity is not preferable since high pumping power is required which literally reduce efficiency of the system (Azmi et al., 2016). On the other side, nanoparticle is expensive which also increases the production cost.

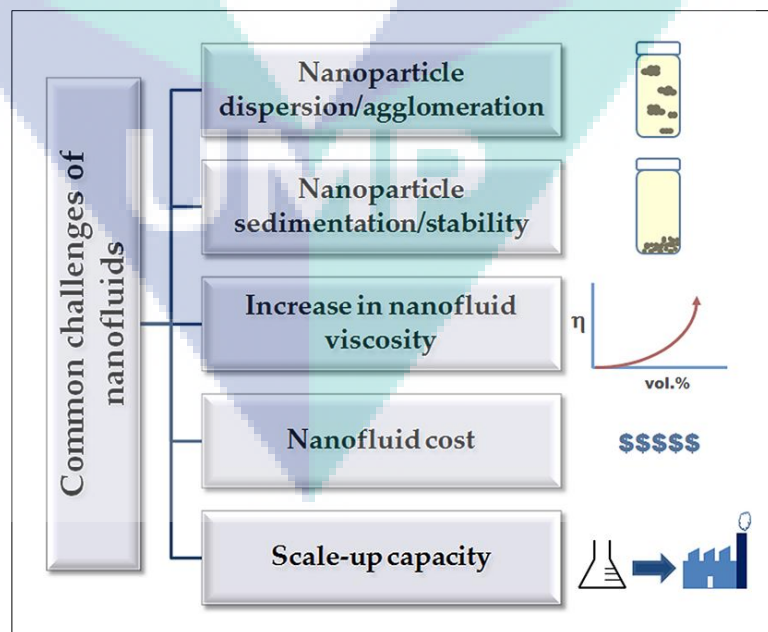


Figure 2.3 List of common challenges found in nanofluid

Source: Taha-Tijerina, Peña-Parás, & Maldonado-Cortés (2016).

2.3.1 Nanofluid Application

In this modern world, nanofluid is widely been used in vast applications for industrial and commercial purposes. Globally, industries such as power plant, semiconductor, automotive and manufacturing largely relying on thermal transport fluid for their daily production involving massive thermal exchange. Indeed, a small thermal property enhancement give a big impact on their production rate. Since, nanofluid has better thermophysical property which able to produce better thermal absorbance performance, it is most suitable for thermal transport application as coolant. Figure 2.4 depicts various nanofluid application.

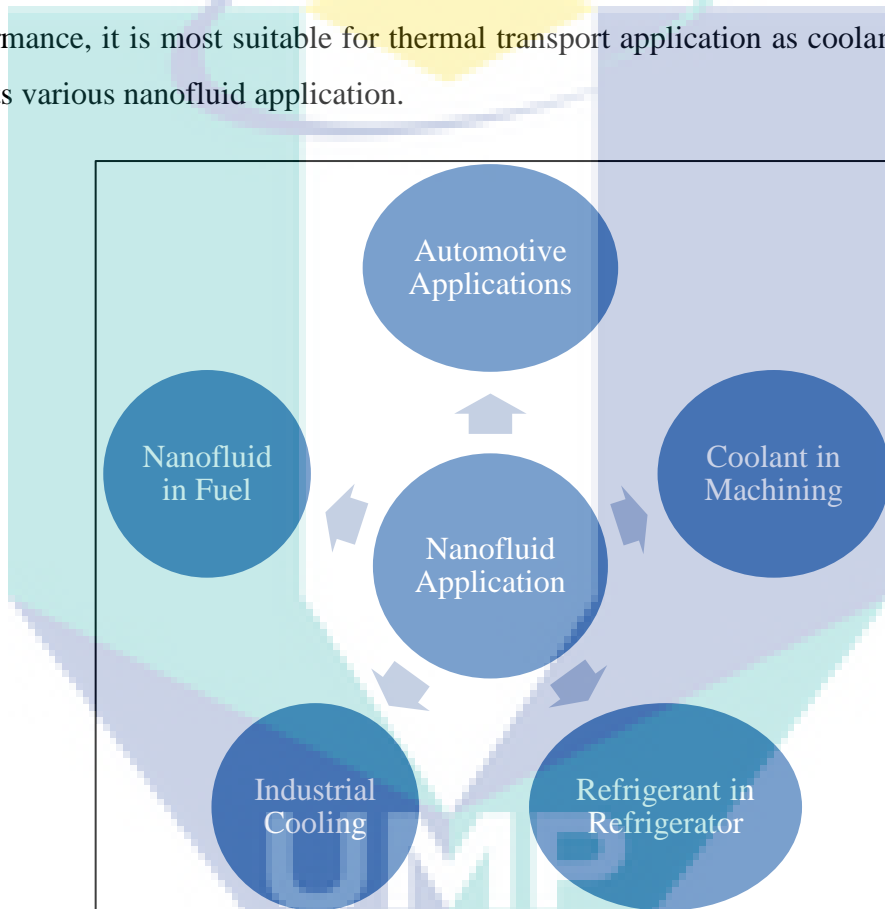


Figure 2.4 Various nanofluid application for industrial and commercial purposes

Statistics shows that heat dissipation in electronic chip increased 36.54% in 4 years (J. H. Lee, 2009). This shows that development of high-performance chip dissipates more heat than usual. Unfortunately, heat dissipation result through conventional heat removal method such as air cooling, liquid cooling and two-phase cooling is not promising. Conversely, C. Nguyen et al., (2007) has suspended Al_2O_3 nanoparticle in water for cooling microelectronic components which shows promising result. In addition, nanofluid is also being used for chiller performance improvement in air conditioning systems. Meanwhile, Saidur et al., (2011) explained that use of nanofluid in chiller able

to produce better performance as nanofluid has better heat transfer characteristics under dynamic conditions.

Besides, nanofluid is also being used as lubrication in domestic refrigerator applications. R. Wang et al., (2003) used TiO_2 nanoparticle to produce stable nanofluid in HFC134a refrigerant basefluid which give better performance and more lubrication property. Research by K.-J. Wang et al., (2006) reveals that dispersing of Al_2O_3 in R22 refrigerant produce better lubrication property hence reduces bubble formation near heat transfer surface. On the other side, nanofluid can be used in machining as coolant to enhance heat transfer removal on cutting tool.

In addition, C. Choi et al., (2008) comes with an idea to use nanofluid as engine coolant in automobile thermal management system. In addition, S. Peyghambarzadeh et al., (2011) used Al_2O_3 nanoparticle in ethylene glycol as base fluid to study heat performance of nanofluid in car radiator. This is because high thermal conductivity and specific heat capacity value of nanofluid is always being highlighted by the researches which is suitable for most of thermal transfer application. Demands for novel thermal transport fluid is increasing as most thermal application requires massive heat removal.

2.3.2 Preparation method of Nanofluid

Since then, a lot of researches being investigated involving various type of nanomaterial such as nanoparticle, nanofibers, nanorod, nanotube, nanowire and nanosheet. For example, L.Syam Sundar et al., (2013) used Fe_3O_4 nanoparticle in ethylene glycol and water mixture and found 46% of thermal conductivity enhancement. Then, experiment conducted by Fakoor Pakdaman et al., (2012) using nanotube, MWCNT enhances kinematic viscosity about 67% compared to basefluid at 40°C . Moreover, Chen et al., (2009) attempts to increase boiling heat transfer by using Si and Cu nanowires.

The nanofluid preparation method is vital and it can be prepared through one-step preparation method and two-step preparation method. In one-step preparation method, nanomaterial is synthesized and basefluid is added during the production itself generally through vapor condensation method (Eastman et al., 2001). In this preparation method, unnecessary process such as drying, storage and separate dispersion can be avoided. The direct dispersion of nanomaterial ensures nanofluid has a better stability with minimal

agglomeration formation (Y. Li et al., 2009). Unfortunately, it is difficult to be produced in bulk quantity and the production cost is expensive. Figure 2.5 shows one-step preparation method for nanofluid.

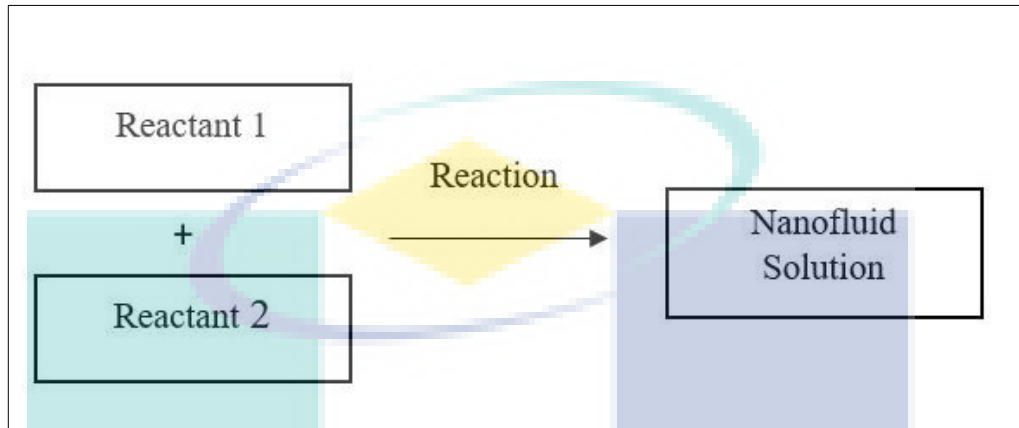


Figure 2.5 Preparation technique through one-step preparation method
Source: Mukherjee & Paria, (2013).

Meanwhile, most of the nanofluid is prepared through two-step preparation method. Firstly, nanomaterial will be produced through physical or chemical method. Then, it will be dispersed into basefluid with the help of intensive magnetic force agitation, homogenizing, uniform high shear mixing, ultrasonic agitation for a stable nanofluid by breaking cluster formation upon mixing (Yu & Xie, 2012). Since nanomaterial has high surface area with active surface charge, the tendency for agglomeration formation is high. On the good side, this method is the most economical and fastest way to produce nanofluid in bulk quantity. Figure 2.6 shows two-step preparation method for nanofluid.

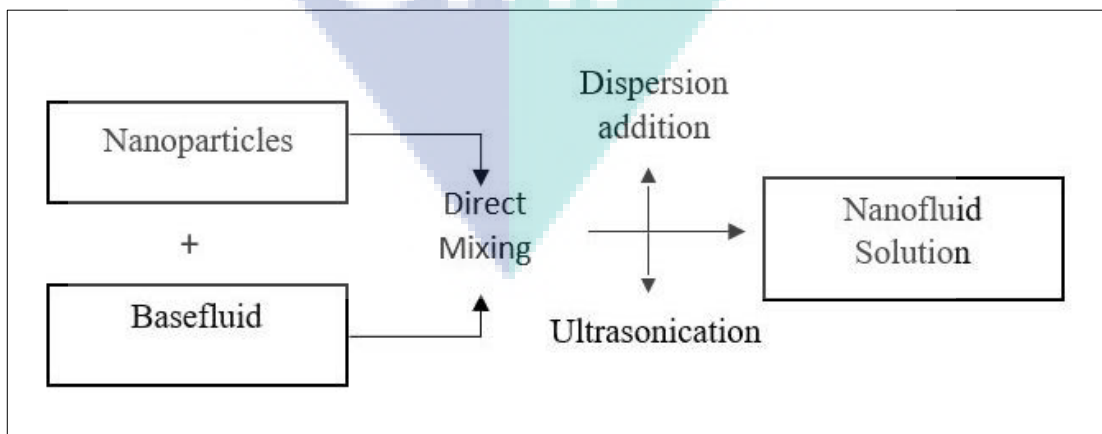


Figure 2.6 Preparation technique through two-step preparation method
Source: Mukherjee & Paria, (2013).

2.3.3 Nanofluid Stability

Nanofluid is made up of two-phase system; solid (nanosubstance) and liquid (basefluid). The challenging part in nanofluid is to achieve a desired stability for a certain period depending on the applications. Thus, study on nanofluid stability is eventually significant before it can be used for practical usage. Meanwhile, nanofluid stability measurement helps to evaluate nanofluid's quality. Nanofluid is labelled as stable if able to prevent any settlement of nanomaterial at the bottom of container. Nanofluid stabilization can be achieved through four techniques such as electrostatic stabilization, steric stabilization, depletion stabilization and ultrasonic agitation.

In electrostatic stabilization technique, nanofluid is controlled by changing chemical characteristics of the solution through pH and concentration alteration of existing ions. Thus, with the help of zeta potential, Isoelectric Point (IEP) and optimum pH value is determined. A stable nanofluid should have zeta value far away from IEP (Witharana et al., 2013). Besides, pH of the nanofluid can be adjust by adding hydrochloric acid for acidic circumstance and sodium hydroxide for alkaline condition requirement (Mui et al., 2016). Figure 2.7 shows effect of surface charge on producing various type of dispersion level.

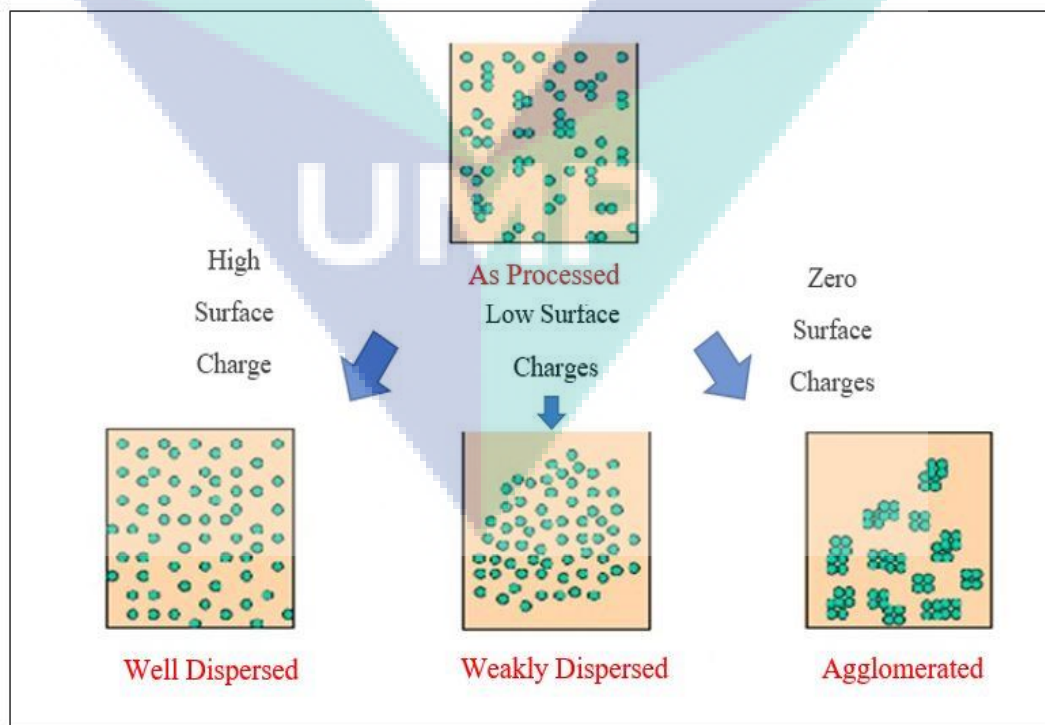


Figure 2.7 Effect of surface charge on producing various type of dispersion level

Meanwhile, in steric stabilization method, nanofluid stability is achieved by controlling interaction among nanoparticles. Cohesive behaviour particles such as surfactant and dispersant were added to the nanofluid to slow down aggregation process to achieve a stable nanofluid (D. Zhu et al., 2009). Addition of surfactant ensure electrostatic repulsive force and hydrophobic force between particles prevents agglomeration (Sakamoto et al., 2002).

Depletion stabilization is another technique that alters intermolecular force between nanoparticles (Lin et al., 2011). Smaller nanoparticle has higher surface energy which has great potential for rapid aggregation formation. By enhancing electrostatic repulsive force on the nanoparticle, the chances for particle fusion will be reduced which produces a stable nanofluid.

Finally, the easiest and promising method is ultrasonic agitation. In this technique, agitation equipment such as ultrasonic bath and homogenizer were used to break the cluster formation into smaller piece. By doing so, the sedimentation period can be greatly reduced. Agitation procedure is influenced by ultrasound power, sonication frequency and sonication period (Palabiyik et al., 2011). According to Hong et al., (2006), sonication time has proportional relation with nanofluid stability. Conversely, after an optimum sonication time, nanofluid stability tend to reduce. Finding an optimum sonication time is a mandatory process before nanofluid is exposed with any agitation.

In nutshell, stability is influenced by preparation method, molecular behaviour modification, addition of surfactant and pH value alteration. Aggregation easier to form on nanomaterials as they have high surface charges on them (Ghadimi et al., 2011). Thus, aggregation formation need to be avoided to make nanofluid stable for a longer period. According to Ghadimi et al., (2011), nanofluid with higher electrostatic repulsive force will be stable compared to nanofluid with higher Van Der Waals attraction force.

2.3.4 Nanofluid Stability Evaluation

As stated previously, nanofluid stability is the most vital element in nanofluid that need to be figured out before can be used in applications. Methods for stability evaluation can be divided into qualitative measurement and quantitative measurement. Qualitative measurement is the simplest and easiest method to determine nanofluid stability. Examples of qualitative measurement is sedimentation observation and micrographic

image evaluation. In sedimentation observation technique, nanofluid is left undisturbed for certain period in a test tube to monitor any occurrence of sedimentation. Besides, tendency of sedimentation to form supernatant in nanofluid observed visually. Figure 2.8 illustrates gradual settlement of nanosubstance at bottom of the container over time. High sedimentation is influenced by large size of nanomaterial and cluster formation due to high surface energy on particles. Meanwhile, in microscopic evaluation, images from Scanning Electron Microscopy (SEM) and Transition Electron Microscopy (TEM) were used to study aggregation and distribution of nanomaterial with basefluid.

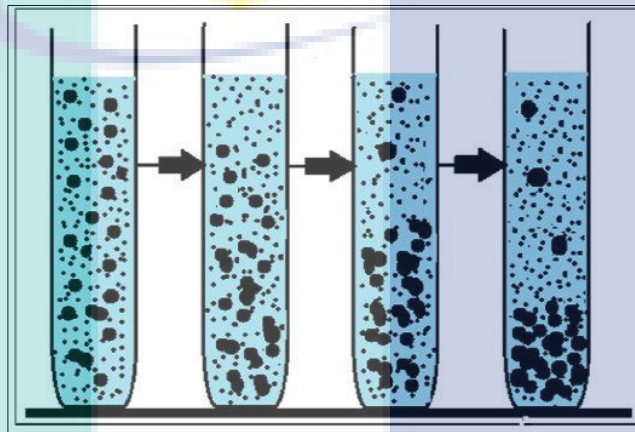


Figure 2.8 Gradual settlement of nanosubstance at bottom of the container over time

Source: Sharma & Gupta (2016).

Stability results obtained in quantitative measurement is much more reliable because the validation is done scientifically. Zeta potential analysis measures surface boundary's potential to resist ions from entering the surface boundary. Figure 2.9 illustrates position of potential charges and layers in a diagrammatic zeta potential concept. Around the nanoparticle, liquid layer is divided into two; stern layer and diffuse layer. Stern layer has strong ion bound meanwhile diffuse layer has slightly loose ions attached together.

As the boundary gets bigger, it increases more resistance for ions to enter surface boundary. The nanofluid entity is stable as zeta potential value increases (H. Zhu et al., 2007). Another interesting stability evaluation s through UV-vis spectroscopy evaluation. Figure 2.10 shows graphical illustration of UV-vis technique. In this method, UV-vis spectrophotometer is used to determine peak absorbance value at varying wavelength from 190-1100 nm. Then, the relative stability is studied from the prepared nanofluid.

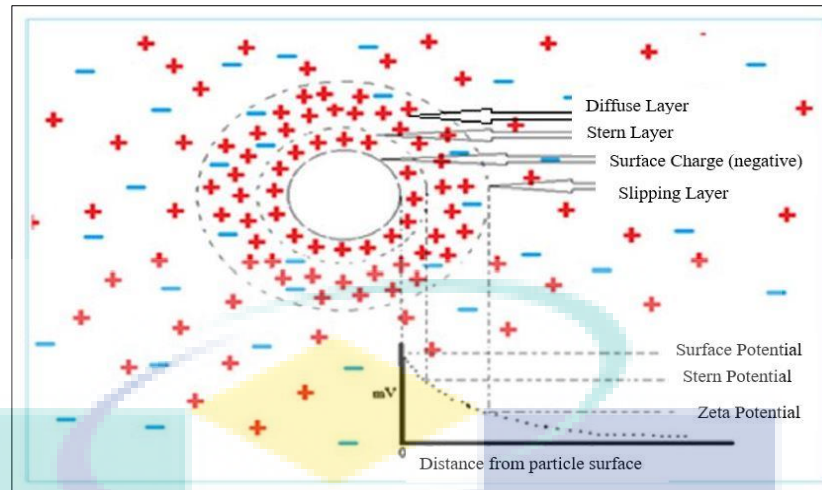


Figure 2.9 Position of potential charges and layers in a diagrammatic zeta potential concept

Source: Sharma & Gupta (2016).

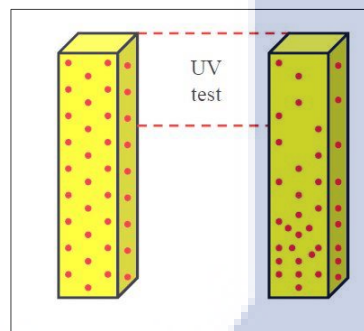


Figure 2.10 Graphical illustration of nanomaterial settlement at bottom of test tube over time in which absorbance drop will be measured by using spectrophotometry

Source: Mansour & Atiya (2016).

2.4 Improvement on Nanofluid Stability

As highlighted by Sharma & Gupta, (2016), stability of nanofluid can be improved by chemical treatment and physical treatment. Addition of surfactant is the primary remedy for unstable nanofluid. In nature, nanomaterial can be classified as hydrophilic and hydrophobic. Meanwhile, basefluid is divided into polar and non-polar. Hydrophobic nanomaterial easily disperses into non-polar basefluid such as oil. On the other side, hydrophilic nanomaterial molecules dispersed well with polar basefluid such as water without need of third component additive.

Stability improvement can be achieved by physical treatment through agitations on nanofluid. During preparation, sonication and homogenization help to breaks cluster

formation which helps to obtain a stable nanofluid. Rashmi et al., (2011) mention that optimum sonication time need to be determined to produce a stable nanofluid because further sonication beyond that affects thermophysical property. In the experiment conducted by Hong et al., (2006), nanofluid sonicated in high powered pulse produces less particle clustering which enhances thermal conductivity.

In addition, surfactant can be used to increase nanofluid stability. Besides, surfactant act as thermal bridge in between nanomaterial and basefluid creates a continuity which enhances nanofluid stability. The suitability of surfactant is subjective and depends on head group of surfactant charge. Another method is through chemical treatment by altering nanofluid's pH value. According to Yousefi et al., (2012), pH value that is far away from pH of isoelectric point produces positive results. Figure 2.11 depicted relationship between pH and zeta potential. In thermal transport applications, the ideal pH for nanofluid is 7, where it has neutral property to prevent damages on cooling system (Wen & Ding, 2005).

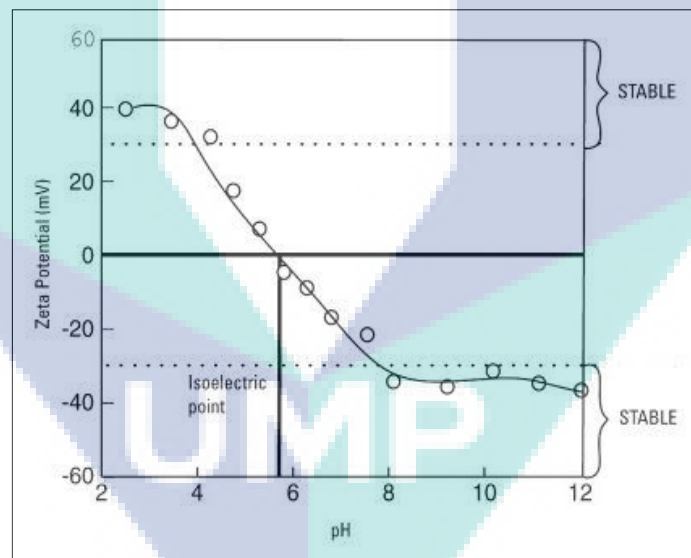


Figure 2.11 Relationship between isoelectric, pH value and zeta potential
Source: Colloids (2012).

2.5 Thermophysical Property of Nanofluid

Thermophysical property is comprises of thermal conductivity, dynamic viscosity, density and specific heat capacity measurement. Measurement of these four parameters is vital to validate the suitability of nanofluid for any required engineering application. Improvement of thermophysical property increases heat transfer coefficient

value during heat transfer. During cluster or aggregation formation, particles are fuse together and increases sedimentation process. Eventually, faster sedimentation leads to an unstable nanofluid that has tendency to reduce thermophysical property.

2.5.1 Thermal Conductivity

According to Fourier’s Law of heat conduction as shown in Equation 2.1, thermal conductivity of material, k , has proportional relation with heat transfer. In this equation, Q denotes heat transfer and $\frac{dT}{dx}$ indicates temperature gradient. Thus, enhancement in thermal conductivity value enhances heat transfer augmentation. Thermal conductivity measurement in nanofluid helps to determine the capability of nanofluid to be used for massive heat removal especially in thermal transport applications.

$$Q = k \frac{dT}{dx} \tag{2.1}$$

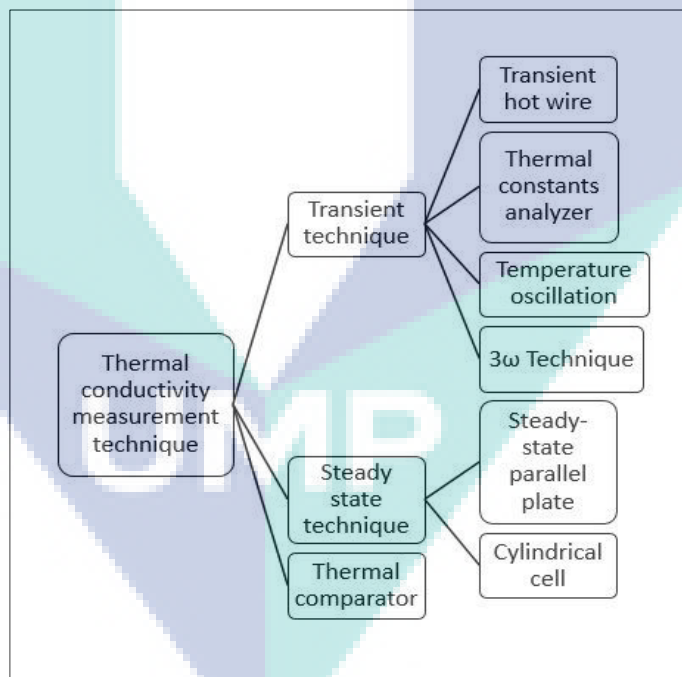


Figure 2.12 Various thermal conductivity measurement method for liquid solution

Source: Paul, Chopkar, Manna, & Das (2010)

Over the years, there are several techniques to measure thermal conductivity of liquid such as transient technique, steady state technique and thermal comparator as depicted in Figure 2.12. In steady state technique, test cells need to be constructed first

before thermal conductivity can be measured (X. Wang et al., 1999). Thermal comparator uses principle of thermal comparator by bringing two materials at various temperature together over a small area and let heat transfer take place from hot region to cold region. Temperature difference from heat transfer is computed for thermal conductivity measurement (Powell, 1957).

Among these measuring techniques, statistics shows that transient hot wire method is the most widely used method by the researchers with 65% as reported in published literature as illustrates in Figure 2.13. In transient hot wire method, a probe will be inserted into the nanofluid and left undisturbed to avoid micro convection effect. Probe acts as heat source where constant current is supplied to heat up nanofluid. Heat dissipates from probe rises nanofluid to required temperature. This measuring technique is preferable as the measurement can be done faster and errors caused by natural convection effect can be eliminated. Initially, this technique is invented by Horrocks & McLaughlin, (1963) to measure absolute thermal conductivity in powders. As the technology development, this technique is modified to give much accurate data for liquids.

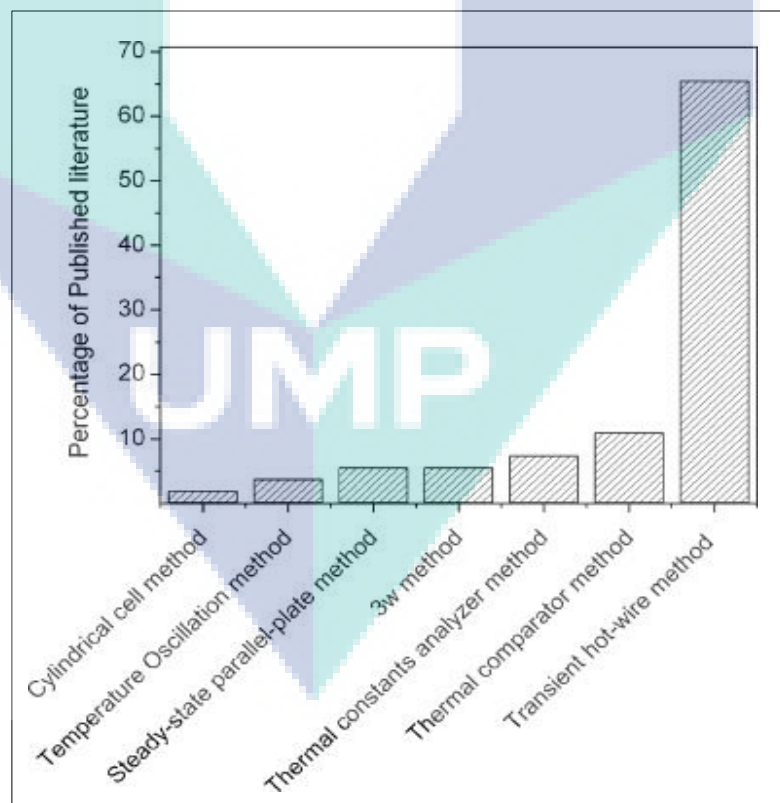


Figure 2.13 Percentage of thermal conductivity measurement method used in nanofluid based to published literature

Source: Paul, Chopkar & Das (2010).

In recent years, studies show that dispersion of nanomaterial into basefluid enhance thermal conductivity enhancement which improves heat transfer rate. Table 2.1 list downs thermal conductivity enhancement of nanofluid using various type of nanosubstance. Results proves that dispersion of nanomaterial produces drastic thermal conductivity enhancement.

Table 2.1 Review of thermal conductivity enhancement for various type of nanofluid at varying temperature and volume concentration

Author	Nanofluid	Material Concentration	Temperature	Maximum Thermal Conductivity Enhancement
(Azmi et al., 2016)	EGW-TiO ₂	0.5 – 1.5 vol%	30 – 80 °C	15.4 %
(L. Syam Sundar et al., 2013)	EGW-Fe ₃ O ₄	0.2 – 2.0 vol%	20 – 60 °C	33 %
(L. Syam Sundar et al., 2013)	EGW-Fe ₃ O ₄	0.2 – 2.0 vol%	20 – 60 °C	46 %
(L. Syam Sundar et al., 2013)	EGW-Fe ₃ O ₄	0.2 – 2.0 vol%	20 – 60 °C	42 %
(Singh et al., 2015)	PG-TiO ₂	0.1 – 0.5 vol%	20 – 80 °C	13.33 %
(Teng & Yu, 2013)	EG	0.1 – 0.4 vol%	80 – 95 °C	49.6%
(Duangthongsuk & Wongwises, 2009)	W-TiO ₂	0.2 – 2.0 vol%	15 – 35 °C	7 %
(Yu et al., 2011)	EG-AiNs	0.1 – 10 vol%	60 °C	38.71 %
(Yu et al., 2011)	PG-AiNs	0.1 – 10 vol%	60 °C	40.2 %
(Syam Sundar et al., 2013)	W-Fe ₃ O ₄	0.2 – 2.0 vol%	20 – 60 °C	48%
(Van Trinh et al., 2017)	EG-CNT	0.005 – 0.035 vol%	30 – 60 °C	41%
(Afrand, 2017)	EG-CNT & MgO	0.05 – 0.6% vol%	25 – 50 °C	21%
(Aravind & Ramaprabhu, 2013)	EG-MWNT & GO	0.011– 0.04 vol%	25 – 50 °C	24%

The anomaly behind thermal conductivity enhancement can be related with physical appearance of nanomaterial, Brownian motion and interfacial layer. In the research conducted by Murshed et al., (2005), they reveal that shape and size of nanoparticle influences thermal conductivity enhancement. Smaller size nanoparticle enhances thermal conductivity better than nanoparticle in larger size. Meanwhile, effect

of nanoparticle shape is related with surface area to volume ratio. Nanoparticle with higher surface area exposed well with the basefluid and eventually enhances thermal conductivity.

Meanwhile, Jang & Choi, (2004) research proves that Brownian motion produces rapid collusion among particles which enhances thermal conductivity. In addition, thermal conductivity enhancement is also related with formation of interfacial layer between solid nanoparticle and liquid basefluid (Leong et al., 2006). This layer act as thermal bridge which reduce thermal resistance hence improve thermal conductivity in nanofluid. Figure 2.14 summarizes principle factor that affecting thermal conductivity in nanofluid.

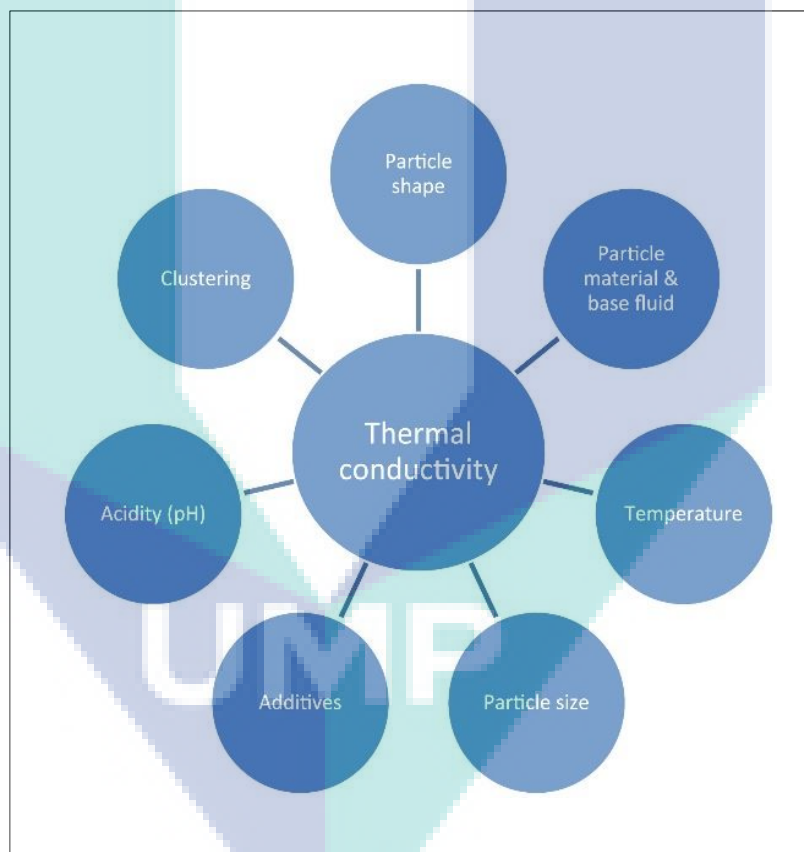


Figure 2.14 Principle factor that influence thermal conductivity enhancement in nanofluid

Source: Gupta, Singh, Kumar, & Said (2017).

2.5.2 Dynamic Viscosity

Dynamic viscosity is essential thermophysical property that determines rheological behaviour of fluid motion. Besides, dynamic viscosity influencing important

flow property such as pumping power, pressure drop and convective heat transfer. Dynamic viscosity property is also important for rheological based applications to evaluate the nanofluid effectiveness. Nanofluid with minimum dynamic viscosity value has less internal resistance during fluid flow (Mahbubul et al., 2012). Table 2.2 shows review of dynamic viscosity enhancement for various type of nanofluid.

The anomaly behind dynamic viscosity enhancement can be related with many factors such as volume concentration, temperature, physical of nanomaterial and nanofluid preparation. According to Gupta et al., (2017), volume concentration has linear relation with dynamic viscosity enhancement and inverse relation with temperature. In experiment conducted by Azmi et al., (2016) dispersing of TiO₂ in water obtained proportional relation with volume concentration and inverse relation with temperature trend. As more nanoparticle is dispersed into the basefluid, there is more particle has contacts with the liquid particle which promotes more dynamic viscosity enhancement.

Table 2.2 Review of dynamic viscosity enhancement for various type of nanofluid at varying temperature and volume concentration

Author	Nanofluid	Material Concentration	Temperature	Maximum Dynamic Viscosity Enhancement
(Azmi et al., 2016)	EGW-TiO ₂	0.5 – 1.5 vol%	30 – 80 °C	33.3%
(Teng & Yu, 2013)	EG-WCNT	0.1 – 0.4 vol%	80 – 95 °C	9.3%
(Duangthongsuk & Wongwises, 2009)	W- TiO ₂	0.2 – 2.0 vol%	15 – 35 °C	15%
(S. W. Lee et al., 2011)	W-SiC	0.1 – 3 vol%	30 – 70 °C	102%
(Syam Sundar et al., 2013)	W- Fe ₃ O ₄	0.2 – 2 vol%	20 – 60 °C	(2.96 times more)
(Chandrasekar et al., 2010)	W-Al ₂ O ₃	1 – 5 vol%	30 °C	136%
(Garg et al., 2008)	EG – Cu	0.4 – 2 vol%	-	24%
(Pastoriza-Gallego et al., 2011)	W-CuO	1-10 wt%	50 °C	73%
(Turgut et al., 2009)	W-TiO ₂	0.2 – 3 vol%	50 °C	135%
(He et al., 2007)	W-TiO ₂	0.024 – 1.18 vol%	22 °C	11%

Besides, temperature rise in nanofluid causes gain in kinetic energy which weakens the intermolecular adhesion force which causes low dynamic viscosity in high temperature (Thomas & Sobhan, 2011). In addition, physical morphology especially size and shape of nanomaterial also plays an important role in determining dynamic viscosity. Nguyen et al., (2008) measured dynamic viscosity by using Al₂O₃ nanoparticle with 36 nm and 47 nm and revealed that higher viscosity is found on bigger size nanoparticle. This can be best explained by occurrence of low interforce resistance on smaller nanoparticle (Agarwal et al., 2013).

In another experiment, Ferrouillat et al., (2013b) studied influence of shape factor by using rod and polygonal sized ZnO nanoparticle. It is proven that nanoparticle with low surface area to volume ratio produces lower viscosity (Timofeeva et al., 2011). Thus, physical of nanoparticle consists of size, shape and surface to volume ratio influences dynamic viscosity in nanofluid. of the nanoparticle also determines the Figure 2.15 illustrates principle factor that affecting dynamic viscosity in nanofluid.

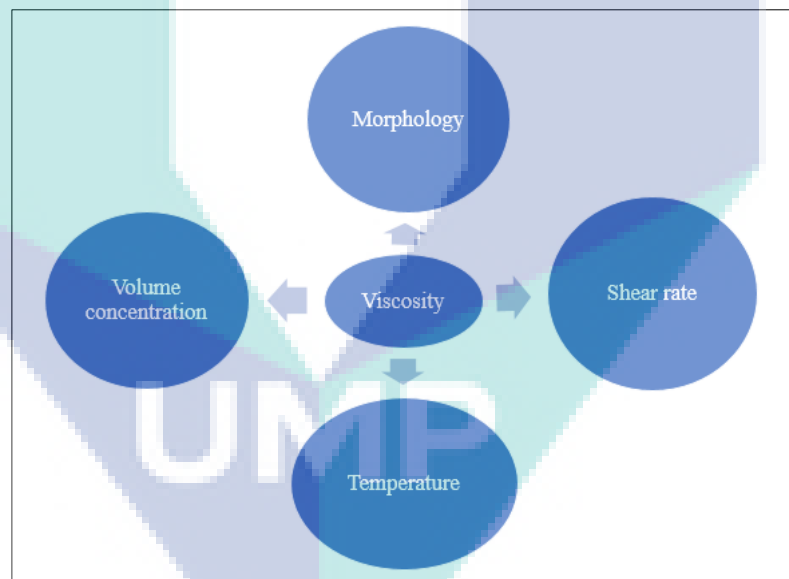


Figure 2.15 Principle factor that influence dynamic viscosity enhancement in nanofluid

Source: Gupta, Singh, Kumar, & Said (2017).

2.5.3 Density

Density is defined as ratio of mass against volume. It is another vital thermophysical property that is used for heat transfer performance determination of nanofluid for heat transfer performance validation. Density is used to calculate some of

the fluid characteristics such as Reynolds number, Nusselt number and friction factor. Usually, nanofluid density is predicted from Pak and Cho model as shown in Equation 2.2, where ϕ denote the volume concentration, ρ_p denotes density of nanoparticle, ρ_f is density of basefluid and ρ_{nf} indicates density of nanofluid. This model is suitable for volume concentration less than 4.5%.

$$\rho_{nf} = \phi\rho_p + (1-\phi)\rho_f \quad 2.2$$

In experiment conducted by Vajjha et al., (2009), experiments for density measurement for Al_2O_3 , Sb_2O_5 and ZnO nanoparticle is done and the model using Equation 2.2 has good agreement with the experimental data. Besides, Pastoriza-Gallego et al., (2009) dispersed Al_2O_3 nanoparticle in water by using various weight concentration from 0.5 to 7% and reported highest weight concentration records the highest density. Thus, density has proportional relation with volume concentration. According to Singh et al., (2015) experiment using dispersion of CuO in water, density has inverse relation with temperature. In fact, only limited literature on nanofluid density had been published. Thus, the need for experimental studies on nanofluid density is required to obtain a reliable data for novel nanosubstance.

2.5.4 Specific Heat Capacity

The most vital thermophysical property that plays a significant role in heat transfer of nanofluid is specific heat. It is defined as amount of heat required to increase temperature by one degree Celsius for one kilogram of nanofluid. There are two model that is widely being used for theoretical specific heat determination as shown in Equation 2.3 and Equation 2.4. The first model is known as Pak and Cho model and the second model is known as Xuan and Roetzel model. In these equations, C_p denotes specific heat, ϕ denotes volume concentration and ρ denotes density.

$$C_{p,nf} = \phi(C_p)_p + (1-\phi)(C_p)_{bf} \quad 2.3$$

$$C_{p,nf} = \frac{(1-\phi)(\rho C_p)_{bf} + \phi(\rho C_p)_p}{(1-\phi)\rho_{bf} + \phi\rho_p} \quad 2.4$$

In experiment conducted by Tiznobaik & Shin, (2013) they used differential scanning calorimetry (DSC) to measure specific heat capacity value for SiO₂ dispersed in molten salt eutectic for various nanoparticle size (5, 10, 30 and 60 nm). Experiment results shows that nanomaterial enhanced 25% compared to base fluid. Besides, size of nanoparticle doesn't influence specific heat enhancement in nanofluid (K.-J. Wang et al., 2006). Conversely, Saeedinia et al., (2012) conduct an experiment using CuO nanoparticle in oil with varying volume concentration from 0.2-2% weight concentration and result shows decline in specific heat capacity value around 23%. They insist specific heat capacity decreases as nanoparticle concentration increases.

2.6 Flow Behaviour of Fluid

Fluid behaviour differs for various type of fluid motion. Besides, it also important to evaluate heat transfer performance. In most cases, flow behaviour properties such as Reynolds number and Nusselt number is calculated in the formulas to validate heat transfer performance.

2.6.1 Reynolds Number

Reynolds number is a dimensionless number that is used to study fluid flow pattern according to flow situation. Literally, Reynold number measures ratio of inertial force to viscous force. It can be classified into laminar flow, transitional flow and turbulent flow by nature. Reynolds number less than 2300 indicates laminar flow whereby more than 4000 indicates turbulent flow. Meanwhile, transitional flow is in between these value, normally 2000 to 4000.

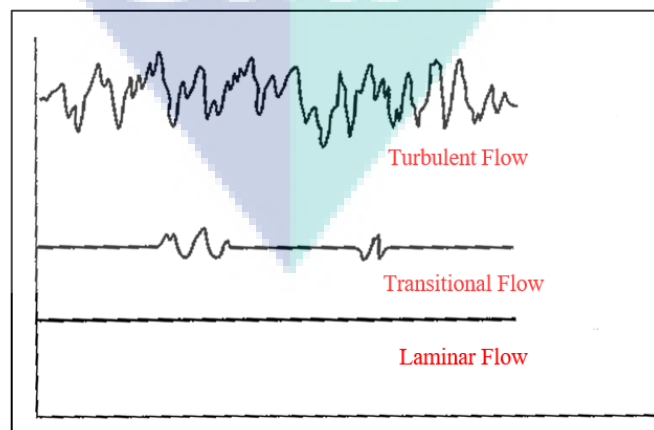


Figure 2.16 Type of fluid flows and its pattern

Source: Aerodynamics (2015).

Flow pattern of dye at varying type flow is depicted as in Figure 2.16. Various type of fluid flow can be achieved at varying Reynolds number. Laminar flow has parallel layer with decent and smooth fluid flow without disruption between the layers (Batchelor, 2000). Besides, laminar flow is much influenced by high momentum diffusion than momentum convection. On the other side, turbulent flow has irregular pattern and fluctuation. In any turbulent flow, kinetic energy is high which causes to overcome damping effect of fluid's viscosity (Ting & Kirby, 1996). Thus, the type of fluid flow affects heat removal in heat transfer applications. The trend for heat removal is various depending on type of fluid flow.

Meanwhile, Peyghambarzadeh et al., (2013) used CuO to disperse in water. Author reported that at Reynolds number of 1000, overall heat transfer coefficient is increased by 9% than basefluid. In an experiment conducted by Namburu et al., (2009), they disperse copper oxide (CuO) in ethylene glycol-water mixture to study effect of turbulent flow in heat transfer performance. At Reynolds number of 20000, the heat transfer coefficient enhanced 1.35 times than basefluid. Moreover, Saedinia et al., (2012) found maximum heat transfer enhancement of 12.7% at high Reynolds number than the base fluid.

2.6.2 Nusselt Number

Nusselt number is a dimensionless number which is defined as ratio of convective heat transfer to conductive heat transfer. According to Ferrouillat et al., (2013a) Reynolds number has proportional relation with Nusselt number. Besides, Pak & Cho, (1998) reveals that Nusselt number increases volume concentration of nanofluid increase. Figure 2.17 depicts relationship of Nusselt number depends on Reynolds number at varying microchannel dimension.

In an experiment conducted by S. Peyghambarzadeh et al., (2011), Nusselt number for nanofluid enhanced 40% than water based basefluid. In addition, Q.Li et al., (2003) dispersed Al₂O₃ nanoparticle into water and found 39% enhancement of Nusselt number than basefluid in a microchannel. The author elucidates that high increase in Nusselt number is due to turbulence flow effect on the channels. Enhancement in Nusselt number can be elucidated with high impact of forced convection heat transfer compared to conduction heat transfer.

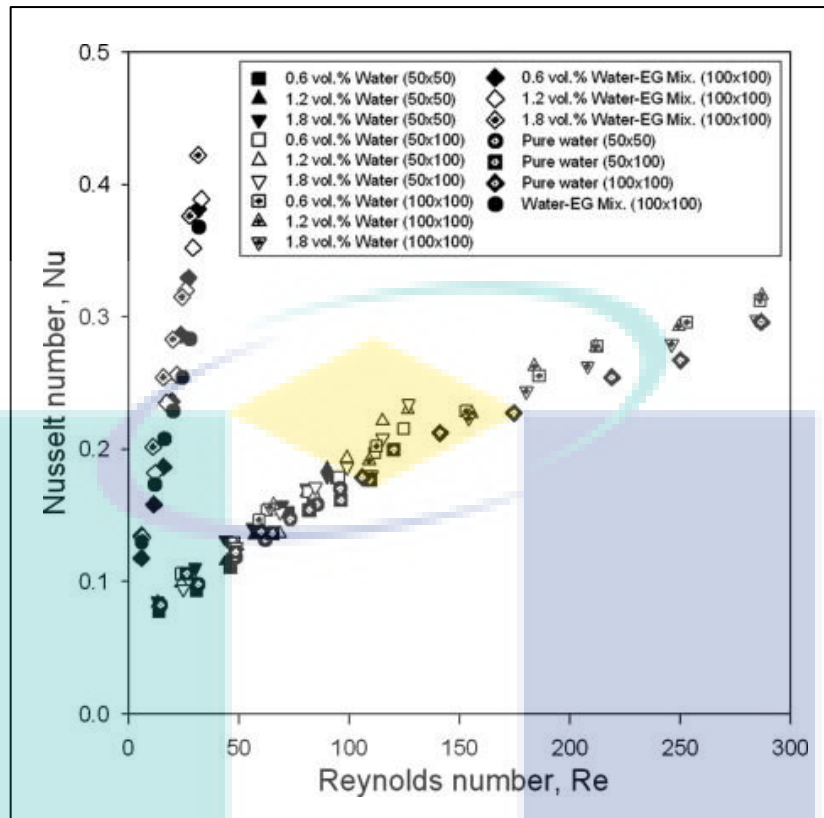


Figure 2.17 Relationship between Nusselt number and Reynolds number at varying microchannel dimension

Source: Jung, Oh, & Kwak (2009).

2.7 Convection Heat Transfer of Nanofluids

According to Newton's law of cooling, heat transfers from solid surface to adjacent fluid which is known as convection heat transfer as shown in Equation 2.5. Convection heat transfer is also defined as combined effect of conduction and flow motion. In this formula, Q , denotes rate of heat transfer, h denotes heat transfer coefficient, A denotes exposed surface area, T_w is the wall temperature (solid) and T_f is bulk fluid temperature (liquid). Convection heat transfer also defined as combined effect of conduction and flow motion. In fact, convection heat transfer mechanism can occur in two different mechanism; naturally and forced convection with the help of fluid motion. In natural convection, the heat dissipates by the boundary force because of temperature variation. Meanwhile, forced heat transfer convection is caused by external force which tend to absorb heat.

$$Q = hA(T_w - T_f) \quad 2.5$$

In experiment conducted by Esfe et al., (2014), they found maximum enhancement of 35.93% for MgO particle dispersed in water with volume concentration of 1.0% under turbulence flow. Meanwhile, in another experiment conducted by Fotukian & Esfahany, (2010), heat transfer enhancement of 25% and pressure drop enhancement of 20% were reported as CuO were dispersed into water under turbulence flow. According to Duangthongsuk & Wongwises, (2009), Reynolds number as linear relation with heat transfer coefficient.

In addition, type of fluid flow also influences friction factor, pressure drop, heat transfer performance. J. Wang et al., (2013) used MWNT in horizontal circular tube and found effective thermal conductivity doesn't influences convective heat transfer enhancement. Besides, Nusselt number and friction factor has proportional relation with particle concentration and Reynold number under turbulent flow (L Syam Sundar et al., 2014). Meanwhile, under laminar flow convective heat transfer has proportional relation with nanomaterial's aspect ratio and inverse relation with thermal conductivity of basefluid (Halelfadl et al., 2014).

2.8 Experimental Study on Automotive Radiator

The use of nanofluid for thermal transport application especially for automotive applications is no more bizarre. In fact, nanofluid is suitable to be used as thermal transport fluid since it has high thermal conductivity value with acceptable rheological behaviour which helps to conduct heat efficiently from heat exchanger. In those days, water is used as heat transfer agent but it has some drawbacks in long run. Water is not advisable to be used as thermal transport fluid as it cause radiator parts to corrode easily. As a remedy, water is substituted with ethylene glycol-water mixture. Ethylene glycol has anti freezing agent and prevent corrosion in micro channels. However, convectional coolant mixture has poor thermophysical property which reduces heat performance in thermal applications.

S. Peyghambarzadeh et al., (2011) investigate the influence of Al₂O₃ nanoparticle dispersed in ethylene glycol and water on automotive radiator. Schematic diagram of the experiment setup is as depicted in Figure 2.18. In the experiment, they enhanced maximum heat transfer enhancement of 40% for nanoparticle dispersed in water. The flow rate used was from 2 to 6 LPM at varying fluid inlet temperature.

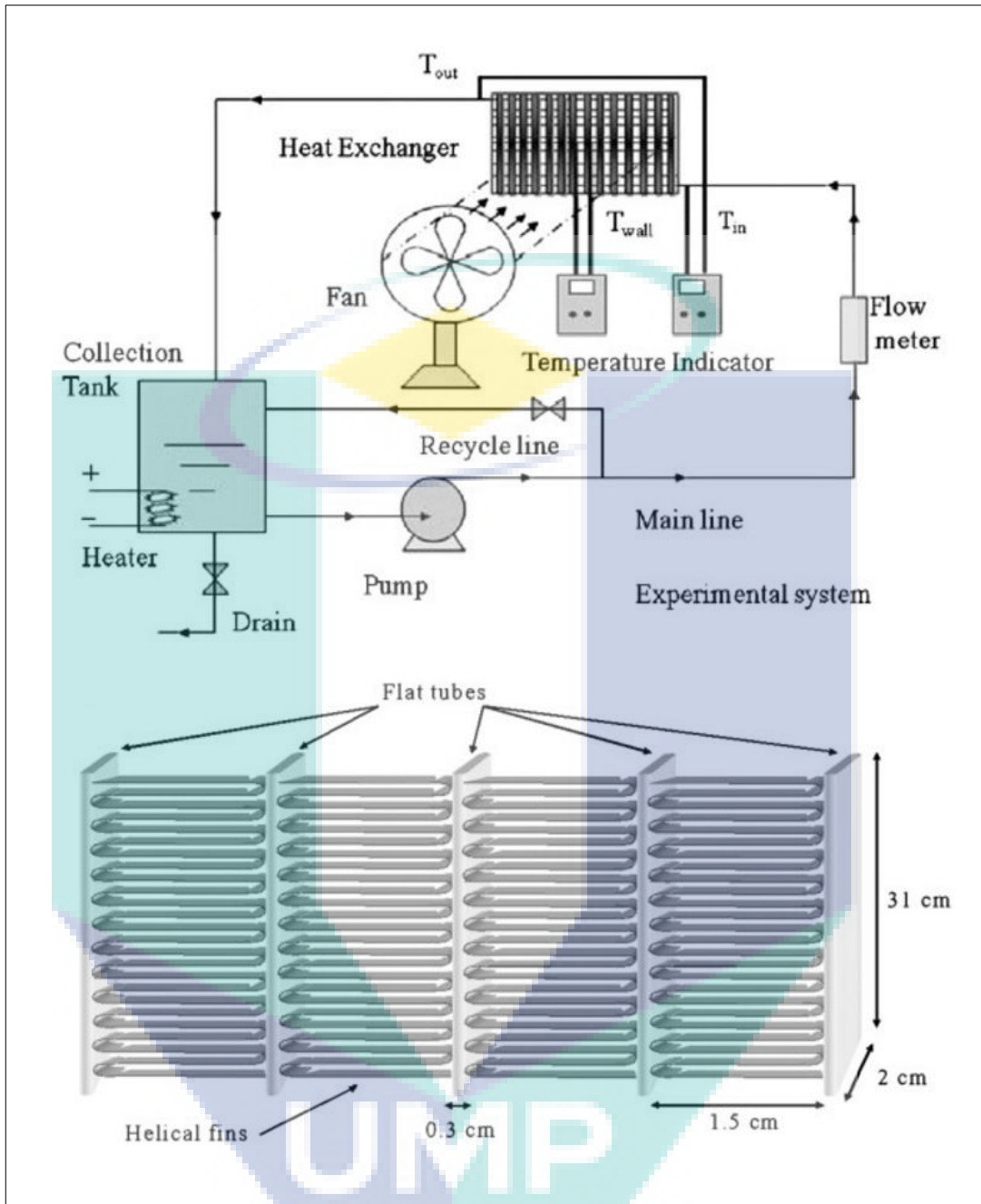


Figure 2.18 Schematic diagram and dimension of radiator used to study effect of Al_2O_3 based nanofluid on heat transfer enhancement

Source: Peyghambarzadeh, Hashemabadi & Hoseini (2011).

In another experiment, Peyghambarzadeh et al., (2013) used CuO and Fe_2O_3 nanoparticle at varying volume concentration from 0.15 to 0.65%. The flow rate used was laminar flow with Reynolds number 50-1000. Figure 2.19 illustrates experiment setup for heat transfer convection determination. From the experiment, the author reveals overall heat transfer coefficient is affected by nanoparticle concentration, flow rate and air velocity.

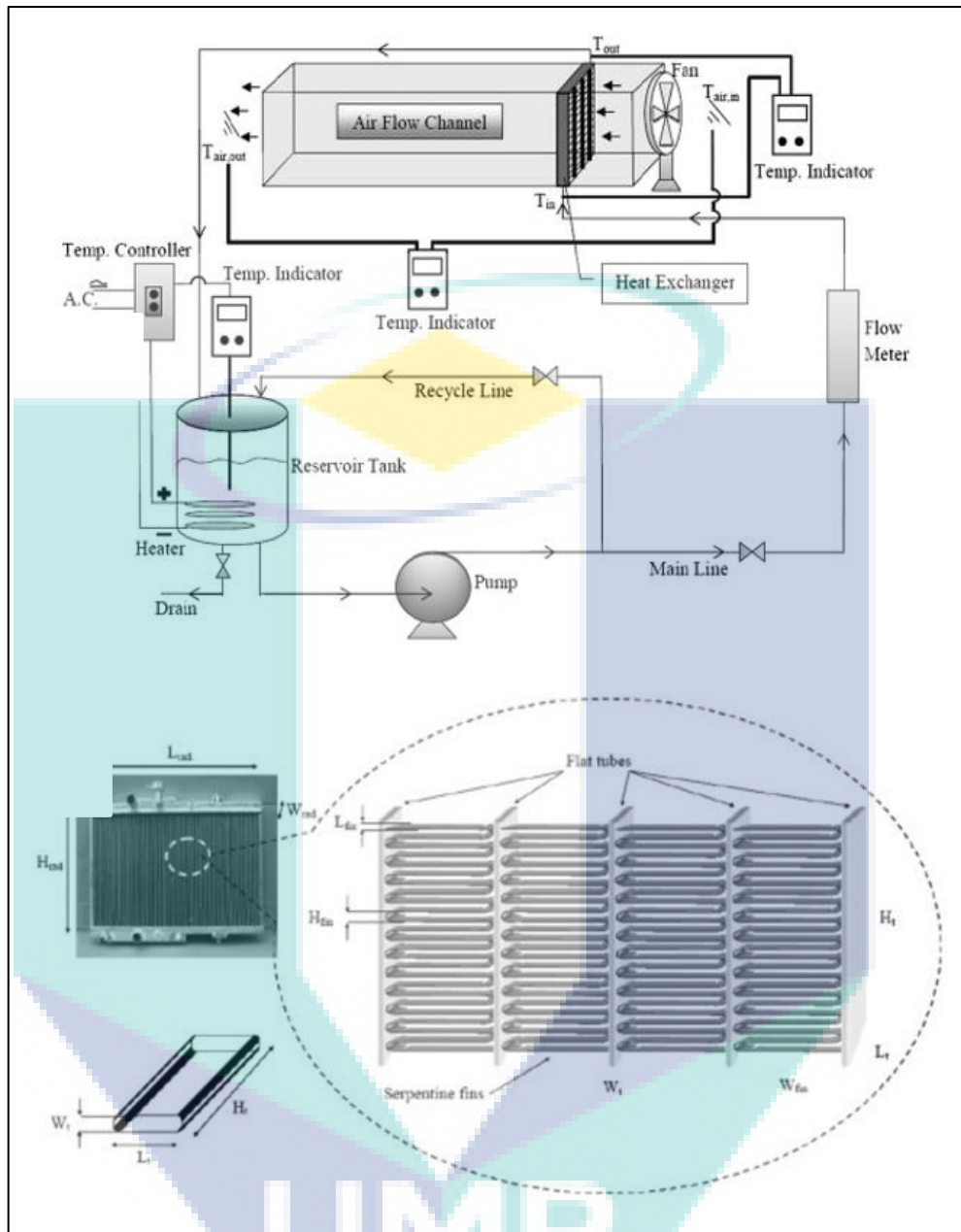


Figure 2.19 Illustration of experiment setup to study influence of CuO based nanofluid on heat transfer convection and radiator used in the experiment

Source: Peyghambarzadeh, Hashemabadi & Hoseini (2013).

Meanwhile, Ali et al., (2015) used ZnO -water based nanofluid to study heat performance of nanofluid in car radiator. Varying volume concentration from 0.01% - 0.3% at varying flow rate ranged 7 – 11 LPM were used in the car radiator to determine optimized heat transfer enhancement. From the study, nanofluid with 0.2% of volume concentration enhanced up to 46% compared to basefluid. Meanwhile, highest volume concentration (3%) shows a decrease heat transfer enhancement. This can be explained with decreasing specific heat capacity value after certain volume concentration range.

Author also elucidate that heat transfer enhancement is highly depends on volume concentration of nanofluid. In addition, heat transfer is depending on inlet temperature of the fluid. Increase from 45°C to 55°C inlet temperature enhance heat transfer rate by 4%. Figure 2.20 shows illustration experiment setup to study influence of volume concentration on heat transfer enhancement. Heat transfer enhancement by using nanofluid may reduce capital cost and operation cost.

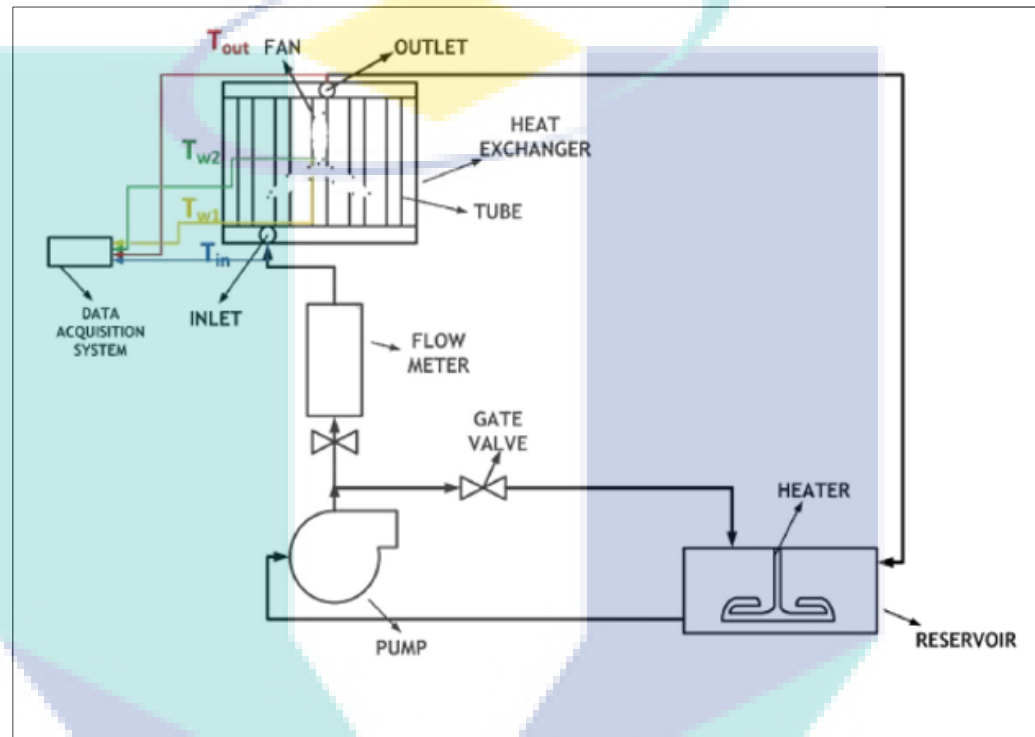


Figure 2.20 Schematic diagram of experimental setup to study influence of ZnO based nanofluid on heat transfer enhancement

Source: Ali, Liaquat &Nadir (2015).

2.9 Conclusions

Internal combustion process in automobile produces excessive heat in automobile. Studies reveals that about 33% of thermal energy is converted to heat energy which results in excess heat problem. Thus, this excessive heat problem is controlled by having a thermal management system especially through the heat exchanger (radiator).

Per se, literature reveal that modification on radiator and fins already reaches its limitation and further alteration would not bring any significant result. Conversely, novel thermal transport fluid should be promising method to control this excessive heat problem since conventional thermal transport fluid has limited thermophysical property.

Nanofluid, produced from dispersion of nanomaterial into basefluid is reported to have better thermal conductivity and specific heat capacity. Though, researchers were only been conducted by using non-renewable type of nanomaterials. Examples of non-renewable nanomaterials are nanoparticles, nanowires, nanorods and nanocarbon tubes. Conversely, cellulose nanocrystals extracted from plant is a renewable material which has advantages over non-renewable.

Celluloses naturally has good physical and morphology which will homogenise well with water based liquid. This light material is biodegradable and contains no toxics. Thus, an attempt to optimize formation of stable condition from dispersion of Cellulose Nanocrystals (CNC) in diluted ethylene glycol is proposed in this research. In addition, heat transfer performance among novel nanofluid and conventional thermal transport fluid will be analysed.

The logo for UIMP (Universiti Malaysia Perlis) is a large, downward-pointing arrow shape. It is composed of four triangular sections meeting at a central point. The top-left and bottom-right sections are light blue, while the top-right and bottom-left sections are a darker, muted blue. The letters 'UIMP' are printed in white, bold, sans-serif font across the center of the arrow.

UIMP

CHAPTER 3

METHODOLOGY

3.1 Introduction

The chapter begins with graphical illustration of research flow chart which highlights sequence of activity carried out throughout this research. Then, method used to prepare nanofluid which is through two-step preparation method is described. In addition, nanofluid stability is evaluated through qualitative method (sedimentation observation) and quantitative method (absorbance drop evaluation using UV-Vis Spectrometry). Another vital subtopic in this chapter is data collection from the experiments. Data collection in this research is divided into two parts; thermophysical property measurement for nanofluid and obtaining experimental data from radiator test rig. In addition, experimental setup that includes fabrication and specification of radiator test rig is explained with the help of visual aids. Besides, formulas used in this experiment for the data analysis is listed at the end of the chapter.

3.2 Research Flow Chart

Figure 3.1 illustrates flow chart in this research. First step in this research is the preparation of the nanofluid. The scope of this research to prepare nanofluid with volume concentration up to 1.3%. Thus, four nanofluid volume concentration is prepared with 0.4 interval among each other starting from 0.1%. Nanofluid is prepared by using two-step preparation method. During preparation, magnetic stirrer is used for a uniform high shear mixing and physical agitation technique in ultrasonic bath to break down cluster formation. Nanofluid stability is measured through qualitative and quantitative method involving sedimentation observation and absorbance drop evaluation using UV-Vis spectrophotometry. If the nanofluid appears to be stable for more than one month, research can proceed with thermophysical measurement.

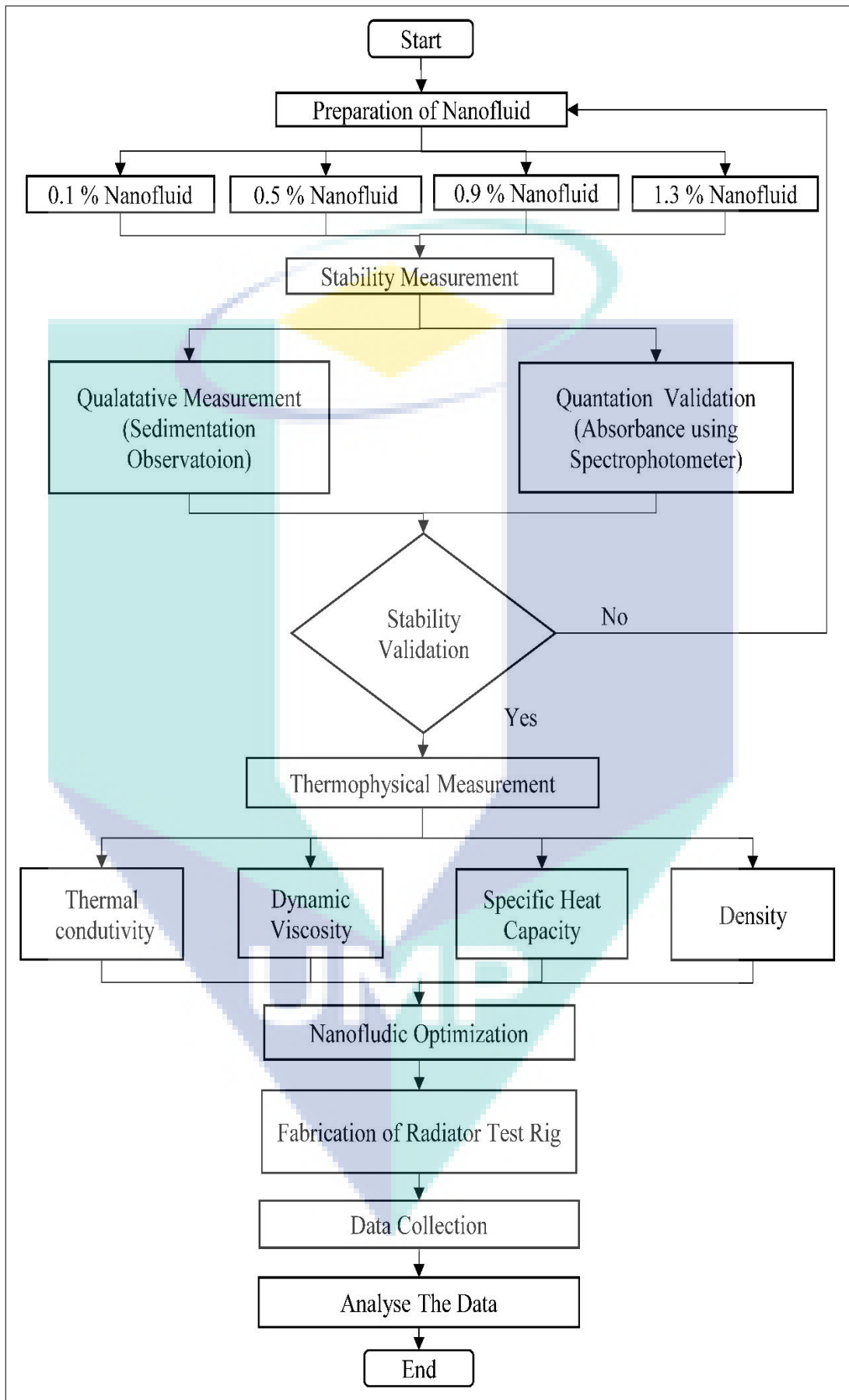


Figure 3.1 Research process flowchart used in this experiment

Conversely, if nanofluid become unstable, alternation on preparation method is required until stable nanofluid is prepared. Stabilization techniques such as electrostatic, depletion, steric and physical agitation can be used to improve nanofluid stability. After thermophysical property of the volume concentration is measured individually, optimized nanofluid is obtained by using statistical analytical tool, Minitab. On the other hand, radiator test rig will be fabricated which imitates the actual radiator application. Conventional ethylene glycol-water mixture (EGW) and optimized nanofluid (CNC) will be used as thermal transport fluid in radiator test rig to study heat transfer performance and fluid behaviour. Besides, effect of forced convection heat transfer is studied by using draft fan at constant velocity. In this experiment, influence of forced convection heat transfer will be studied to understand the influence of draft fan in heat transfer analysis.

Some of the data can be collected directly such as bulk temperature, average radiator wall temperature, mass flow rate and draft fan constant velocity. Other data can be calculated by using equations to study and analysis heat transfer performance. The research ends with data analysis and discussion. At the end of research, conclusion will be drawn for heat transfer performance analysis for EGW and CNC in automotive radiator test rig.

3.3 Nanofluid Preparation

In this research, nanofluid is prepared by using two-step preparation method. Nanosubstance used is Cellulose Nanocrystal which is procured from Blue Goose Biorefineries Inc with weight concentration of 8.0%. This nanocellulose is extracted from Western Hemlock plant. Table 3.1 specify cellulose nanocrystal parameter that is provided by the supplier. Meanwhile, Figure 3.2 depicted images of Transition Electron Microscopy (TEM) 120kV under Bio-TEM Microscope. According to Duran et al., (2012) research, cellulose has good physical and morphology which able to dissolve with water since it is hydrophilic.

Table 3.1 Parameter of cellulose nanocrystal (CNC) with weight concentration of 8.0%

Parameter	Value
Crystallinity Index	80%
Crystal length	100 - 150 nm
Crystal Diameter	9 - 14 nm
Density	1.6 g/ml

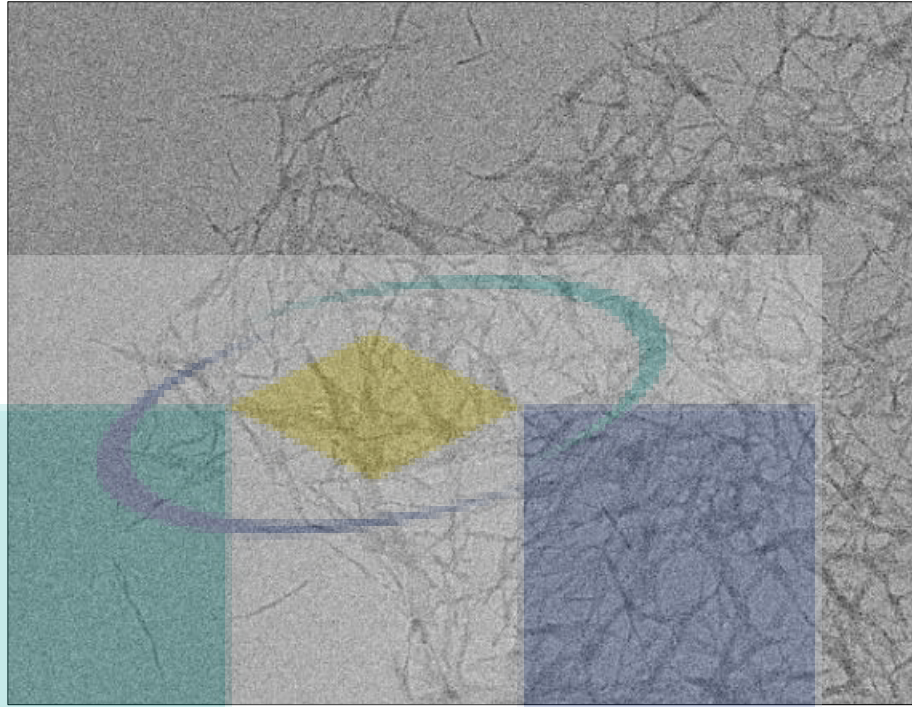


Figure 3.2 Micrographic evaluation of CNC under 120kV Bio-TEM microscope

The basefluid used to disperse CNC is ethylene glycol-distilled water mixture at volume ratio of 40:60 respectively. The ethylene glycol is purchased from QReC Chemicals, Grade AR that has 95% of purity. Meanwhile, distilled water used is prepared at Advance Automotive Liquid Laboratory (A²LL), Universiti Malaysia Pahang. Double distillation was done to ensure high quality of collected distilled water. Since, the procured Cellulose Nanocrystal in weight concentration, it need to be converted to volume concentration by using Equation 3.1. Then, Equation 3.2 is used to dilute volume concentration of nanomaterial into desired value. Nanofluid with volume concentration of 0.1, 0.5, 0.9 and 1.3% is prepared for this research.

$$\phi = \frac{\omega \rho_{bf}}{\left(1 - \frac{\omega}{100} \rho_p\right) + \left(\frac{\omega}{100} \rho_{bf}\right)} \quad 3.1$$

Where;

ϕ = volume concentration (vol.%)

ω = weight concentration (wt.%)

ρ_{bf} = base Fluid density (kg/m³)

ρ_p = density of nanomaterial (kg/m³)

$$\Delta V = (V_2 - V_1) = V_1 \left(\frac{\phi_1}{\phi_2} \right)$$

Where;

ΔV = change of volume (ml)

V_2 = total volume (ml)

V_1 = volume needed to be add (ml)

ϕ_1 = actual volume concentration (vol.%)

ϕ_2 = desired volume concentration (vol.%)

The prepared nanofluid is stirred by using magnetic stirrer for 30 minutes and sonicated in ultrasonic bath for 2 hours individually by using Fisherbrand (FB15051) that has frequency of 30kHz and peak power of 320W (Azmi, W.H et al., 2016). According to Duran et al., (2012), nanofluid involves dispersion of Celluloses has hydrophilic characteristics which able to dissolve with water mixture well.

3.4 Thermophysical Property Measurement

Primary thermophysical property for nanofluid consist of measurement of thermal conductivity, dynamic viscosity, density and specific heat capacity. During nanofluid preparation, changes on surface chemistry occurs which causes changes in thermophysical property. Thus, nanomaterial should be dispersed evenly (J. Lee & Mudawar, 2007). In this research thermophysical property is vital to compare nanofluid property with ethylene glycol. By comparing thermophysical property itself, the capability of nanofluid can be pre-evaluated without conducting further experiments.

3.4.1 Thermal Conductivity

Thermal conductivity is measured by using transient hot wire method. Thermal analyser device, KD2 Pro by Decagon Devices was used to measure thermal conductivity. This equipment fulfils ASTM D5334 and IEEE 442-1981 standard for thermal conductivity measurement. As shown in Figure 3.3, single 60 mm long needle with 1.3 mm diameter was immersed into the vial filled with nanofluid. Then, the vial was immersed into Memmert water bath to provide uniform heating to the nanofluid. The functionality of the equipment is validated by using glycerine provided by the supplier.

Equipment validation is done by using EGW mixture at 40:60 ratio and compared with ASHRAE data sheet. The maximum deviation is 1.6% which shows high precision of the equipment measurement as shown in Figure 3.4. Error bar with 2% is included whereby all measurement lies within the error bar. Minimum of 20 thermal conductivity measurement was taken for varying volume concentration from 0.1 – 1.3% to ensure minimal error during experiment.

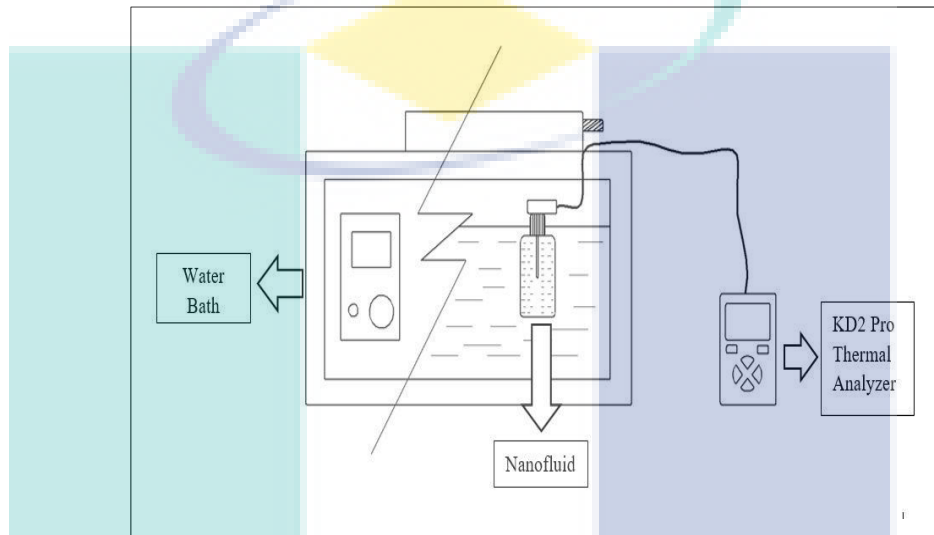


Figure 3.3 Thermal conductivity measurement technique by using KD2 Pro Thermal Analyser

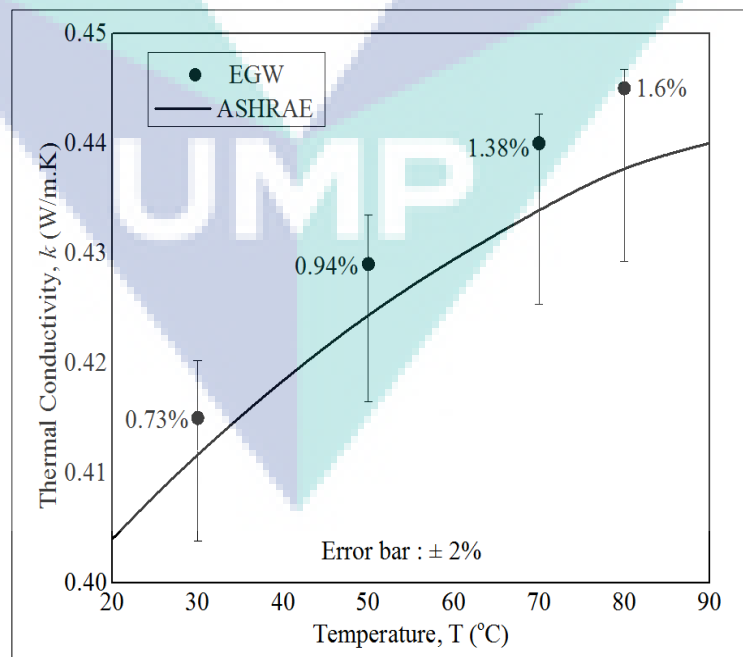


Figure 3.4 Error comparison for thermal conductivity measurement between ethylene glycol-water mixture (base fluid) and ASHRAE data

3.4.2 Dynamic Viscosity

In internal fluid flow applications, dynamic viscosity value is important because the pumping power and efficiency is relying on it. Dynamic viscosity is measured by using Brookfield viscometer model name LVDV-III Ultra Programmable Rheometer. Figure 3.5 shows parts for the dynamic viscosity measurement. Dynamic viscosity is measured by viscous drag created by the spindle rotation. Meanwhile, fluid bath provided a uniform heating in the jacket. Data collection is done by using personal computer connected with rheometer. Minimum of 5 precision reading is averaged to obtain an accurate data. The collected data achieved maximum deviation of 12.19% when compared with ASHRAE data as shown in Figure 3.6.

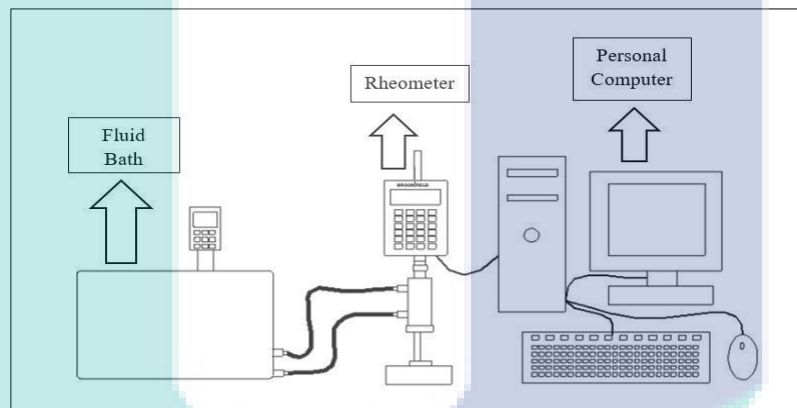


Figure 3.5 Equipment and measuring technique for dynamic viscosity by using Brookfield LVDV-III Ultra Programmable Rheometer

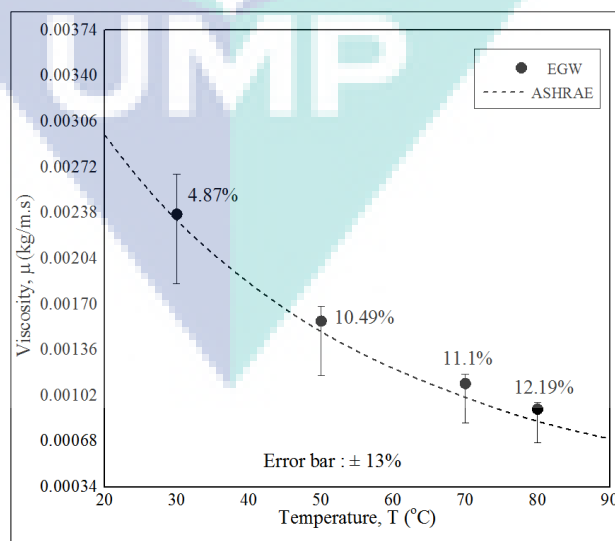
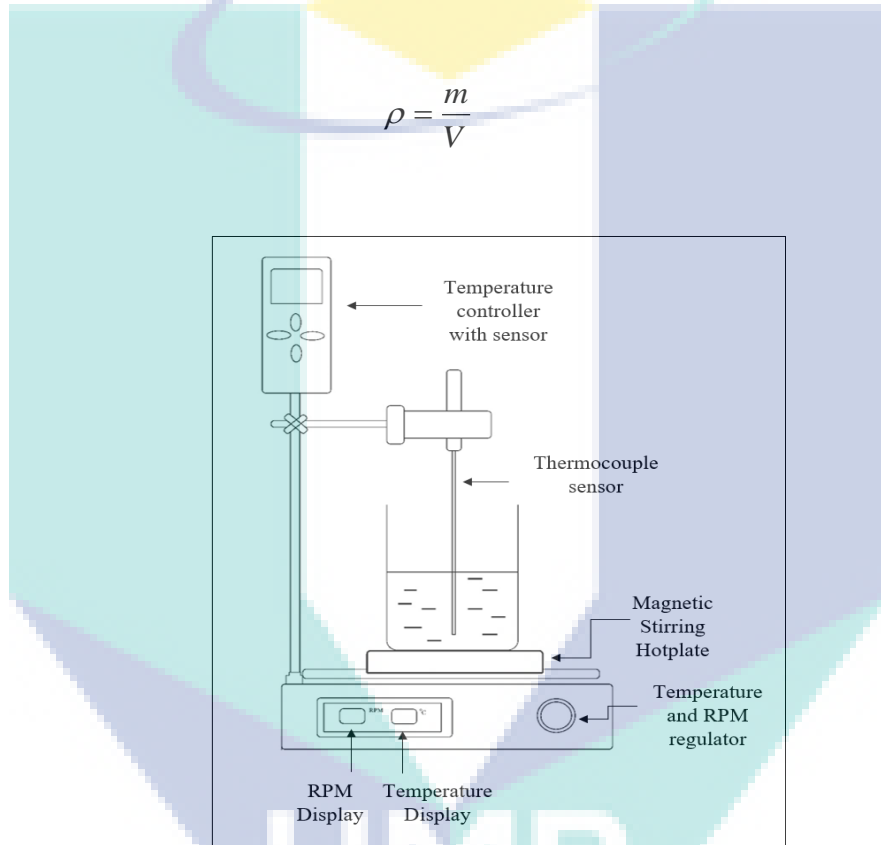


Figure 3.6 Error comparison for dynamic viscosity measurement between ethylene glycol-water mixture (base fluid) and ASHRAE data

3.4.3 Density

Density (ρ) measurement for this experiment is calculated by measuring mass (m) and volume (V) as shown in Equation 3.3. During density measurement, equipment needed is magnetic stirrer for uniform mixing, thermometer for temperature measurement and high precise weighing scale. Kumaresan & Velraj, (2012) experiment results show measuring density by weighing nanofluid able to produce good results with minimal error.



3.3

Figure 3.7 Experiment setup for density measurement

Experiment setup for density measurement as shown in Figure 3.7. Beaker in this experiment is insulated with aluminium foil to prevent heat loss during measurement to increase the experiment accuracy. Meanwhile, the solution is stirred at constant rotation per minute (RPM). RPM used in this experiment is 350 for all the experiments. Density for nanofluid is calculated for volume of 100 mm^3 and 200 mm^3 to obtain a reliable data. As a procedure validation, density results for EGW at volume ratio of 40:60 is compared with ASHRAE data. Meanwhile, Figure 3.8 shows errors comparison among ethylene glycol-water mixture with ASHRAE data for density measurement. The maximum error deviation occurs at 0.85% at 80°C .

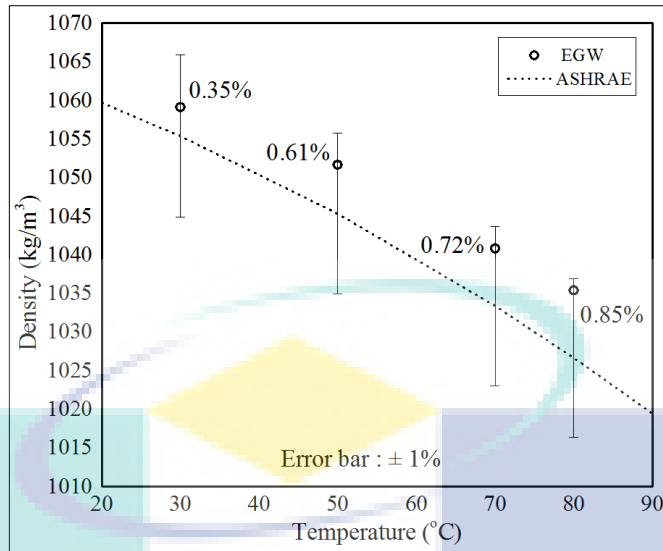


Figure 3.8 Error comparison for density measurement between ethylene glycol-water mixture (base fluid) and ASHRAE data

3.4.4 Specific Heat Capacity

Specific Heat Capacity is measured by using Differential Scanning Calorimetry (DSC) by using Perkin Elmer model name DSC-8000 as shown in Figure 3.9. This equipment is very suitable to provide fusion heat and endothermic peak's property under various heat rates. Besides, DSC-800 has capability to provide real time analysis for heat flux by considering weight loss. It also has temperature accuracy of 0.0001mg and 0.01°C which able to provide very accurate data.

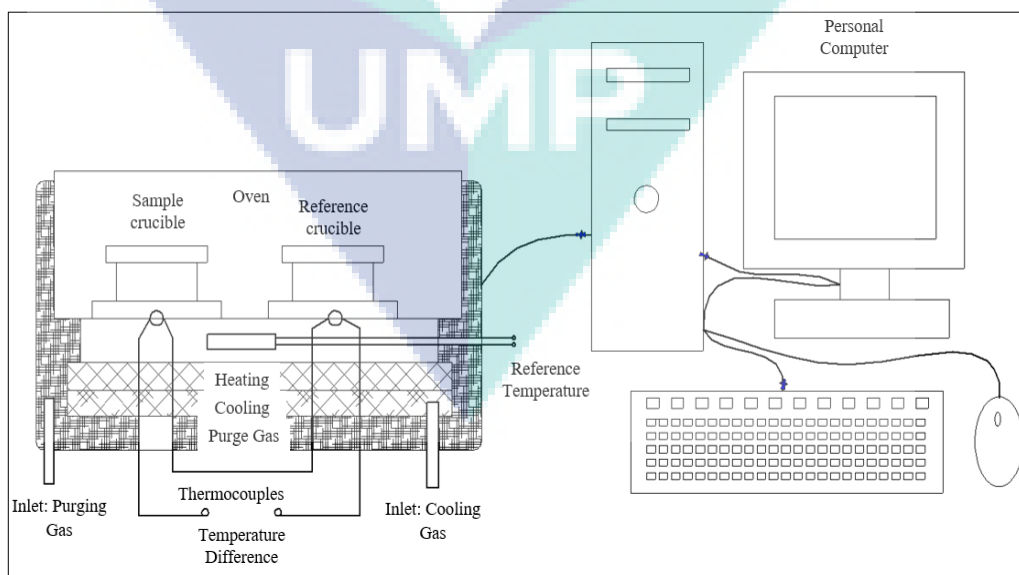


Figure 3.9 Differential scanning calorimetry (DSC) model number (Perkin Elmer DSC-8000) that had been used to determine specific heat capacity value

The specific heat capacity is measured by heating sample from 30°C to 80°C at rate of 10°C/minute under purged Nitrogen (N₂) gas. The equipment validation is performed by using benzophenone and caffeine for better reading accuracy. Indium was used for heat flow calibration. Zhou & Ni, (2008) experiment results show measuring specific heat capacity for nanofluid using DSC able to produce good results with minimal error.

3.5 Nanofluid Stability Measurement

In this research, nanofluid stability is determined through qualitative and quantitative method. Qualitative method chosen was sedimentation observation and for quantitative method absorbance drop evaluation by ultra violet spectrophotometry (UV-Vis). In sedimentation observation, nanofluid is poured in test tube and left undisturbed for one month. Accumulation of nanosubstance will cause sedimentation at the bottom of test tube. Meanwhile, in absorbance drop evaluation technique, nanomaterial will drop to the bottom as time passes and causes instability of nanofluid.

3.5.1 Sedimentation Observation

Sedimentation observation method is the most simple and easiest nanofluid stability validation method. In this method, the prepared nanofluid sample is poured into test tube and left undisturbed for one month to observe any physical change on nanofluid as shown in Figure 3.10. During the left-over period, any sedimentation drop is observed visually with naked eye. Usually, nanomaterial will accumulate at the bottom of test tube caused by gravity pull.

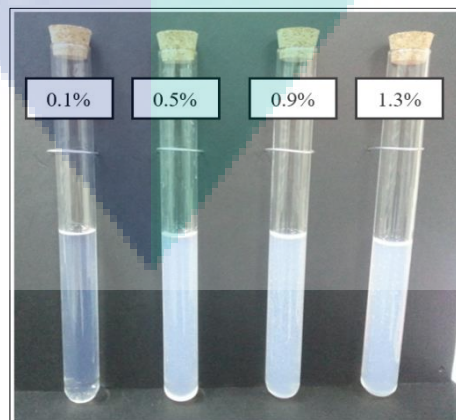


Figure 3.10 Nanofluid is poured in test tubes and left undisturbed to observe settlement of nanofluid for one month

3.5.2 Ultraviolet-Visible Spectrophotometry

In addition, Ultraviolet- visible (UV-Vis) test is required in this research to prove the nanofluid stability scientifically in quantitative manner. In this test, samples will be poured in cuvette and absorbance drop will be measured for one month. Shimadzu UV-2600 Spectrophotometry is used to find peak wavelength of nanofluid to be used for absorbance value determination as shown in Figure 3.11. Lin et al., (2011) used the same method to determine stability in nanofluid.



Figure 3.11 Spectrophotometry model name (Shimadzu UV2600) that had been used to measure absorbance drop value in nanofluid

Once peak wave length is obtained, it is used to determine the absorbance value drop for lowest and highest volume concentration of nanofluid. The idea is to take the smallest and highest volume concentration and record absorbance drop for one month. nanofluid that has absorbance value drop less than 30% considered as stable nanofluid (Sharif et al., 2017).

3.6 Experimental Setup

As a core of this research, it is mandatory to fabricate radiator test rig to test nanofluid capability in automotive car radiator as cooling agent. Thus, car radiator selection is important to achieve research's objective and problem statement. During selection, several criteria is kept in mind such as size and weight of radiator. The selected radiator should be small with lighter weight so that the heat transfer performance of

nanofluid in smaller radiator can be studied. Figure 3.12 shows schematic diagram of fabricated radiator test rig in this experiment.

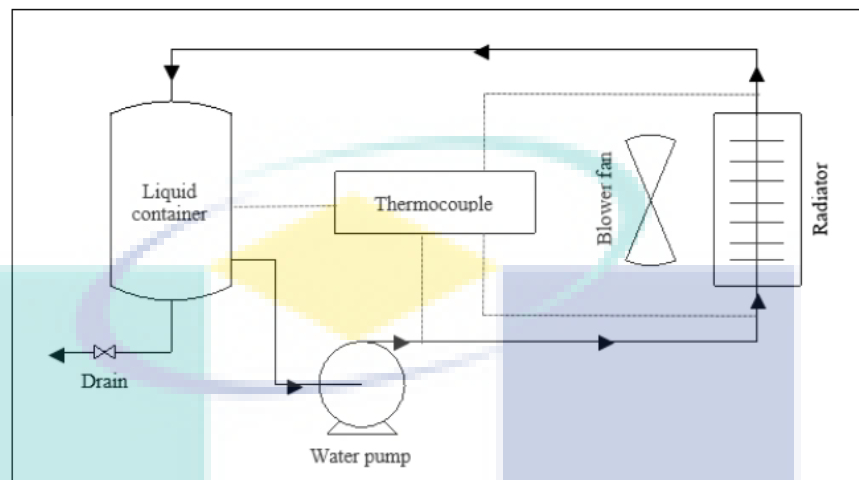


Figure 3.12 Schematic diagram of fabricated radiator test rig in this experiment

Figure 3.13 depicts radiator chosen for heat transfer study in this research. It has 31 flat tube with inlet and outlet diameter of $\frac{3}{4}$ ". The radiator has major diameter, D is 0.022mm and minor diameter, d of 0.002mm with length, L of 0.375mm. Fins is made of up aluminium with 1mm thickness to enhance heat dissipation. The experiment temperature is manipulated by using STC-1000 Thermostat, a digital temperature controller with accuracy of $\pm 0.1^\circ\text{C}$ that can control temperature up to 100°C .

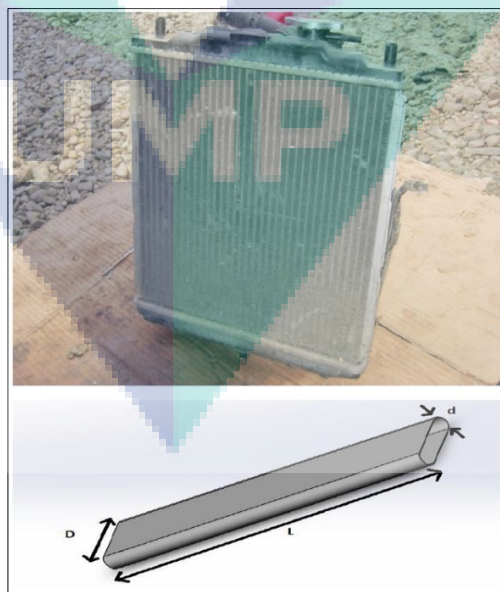


Figure 3.13 Location of major diameter, minor diameter and length in radiator used in this research

An electrical heater with heat capacity of 15000W is used to resemble the hot thermal transport fluid on engine blocks. K-type waterproof thermocouple, DS18B20 is been used to measure temperature at inlet and outlet of radiator. It is able to measure temperature from range of -55°C to 125°C with accuracy of $\pm 0.5^{\circ}\text{C}$. This digital thermocouple doesn't require any temperature calibration. Meanwhile, LM-35 thermocouple is placed at four different point on the radiator to study temperature distribution of nanofluid. It can be operated from temperature range of -55°C to 150°C with accuracy of $\pm 0.1^{\circ}\text{C}$. Since, it is analogue temperature sensor; calibration need to be done before conducting experiment each time.

A brushless water pump, JT-800D is used to provide constant flow rate of nanofluid to radiator in a closed loop. This water pump can be operated at temperature range of -20°C to 90°C and capable of providing maximum flow rate of 1000 LPM. In addition, flow rate sensor is used to monitor the flow rate of working fluid to ensure the data accuracy. Figure 3.14 shows volumetric flow rate measurement at various operating voltage.

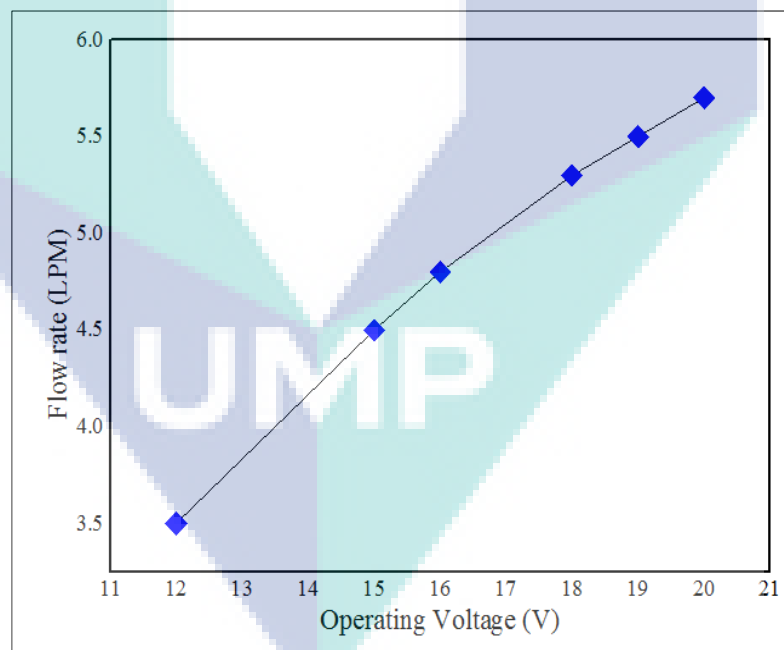


Figure 3.14 Volumetric flow rate measurement at various operating voltage

Volumetric flow rate is measured by using flow rate sensor which has maximum working pressure of 1.75MPa. Besides, the volumetric pump can be used for working range from 1 to 30 Litre per minute.

3.7 Fabrication of Radiator Test Rig

Radiator test rig is fabricated to study nanofluid heat transfer performance on automotive radiator. Figure 3.15 shows parts on fabricated radiator test rig. Meanwhile, Table 3.2 shows parts list and its function.

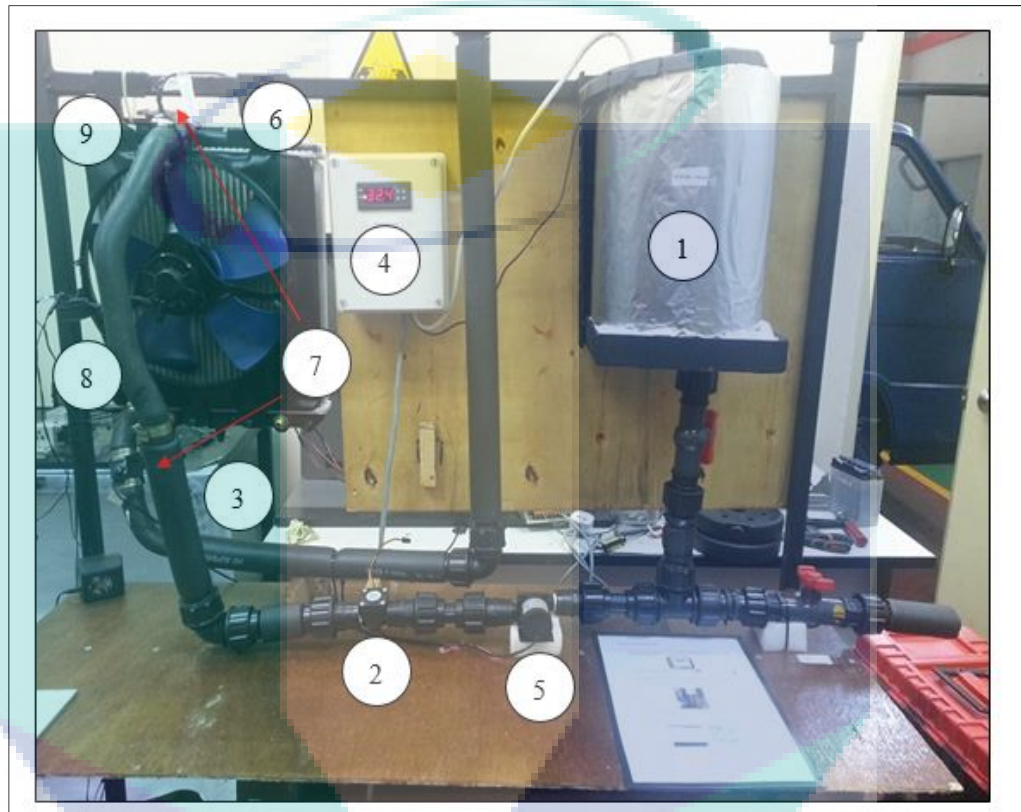


Figure 3.15 Parts that had been used to fabricate fully function radiator test rig to study heat transfer performance

Table 3.2 List and brief function of parts used to fabricate fully function radiator test rig

Label in Diagram	Part Name	Function
1	Electric heater	To heat up the fluid
2	Flow rate Sensor	To measure flow rate
3	Draft fan	To provide constant air flow to remove heat
4	Temperature controller	To control temperature inlet
5	Pump	To vary flow rate supply to radiator
6	LM-35 thermocouple	To measure radiator surface temperature
7	K-type DS18B20 thermocouple	To measure bulk temperature at inlet and outlet of radiator
8	U-tube manometer	To measure pressure drop
9	Radiator	To remove heat from working fluid

3.7.1 Experimental Procedure

The experiment begins as working fluid is pumped into the radiator until steady state is achieved. Then, heater with constant power is used to heat working fluid until equilibrium temperature reach 80°C at radiator inlet. This experiment is conducted at two different circumstances; influence of draft fan and without influence of fan. Foremost, experiment is conducted without the influence of fan. Once done, fan is used to draft air from radiator at constant velocity of 0.5m/s. The experiment begins with volumetric flow rate of 3.5 LPM. Then, the experiment is repeated for volumetric flow rate 4.5 LPM and 5.5 LPM under same condition.

Once steady state is reached, raw data acquisition for inlet temperature, outlet temperature and surface temperature at four places is taken with the help of PLX-DAQ integrated with Microsoft Excel software. Meanwhile, infra camera is also used to capture images of the radiator to study temperature distribution profile on radiator for each different parameter and circumstance. Finally, the collected data is used for data analysis and discussion.

3.8 Data Collection and Analysis

Convection heat transfer is calculated by using Equation 3.4 and Equation 3.5 as stated below to study heat transfer performance analysis (Bejan, 2013).

$$\dot{Q}_C = nA(\Delta T) = nhA_s(T_b - T_s) \quad 3.4$$

$$\dot{Q}_C = \dot{m}C_p(\Delta T) = \dot{m}C(T_{in} - T_{out}) \quad 3.5$$

Where;

Q_c = convection heat transfer (W)

h = heat transfer coefficient (W/m²K)

T_b = bulk temperature (K)

T_s = surface temperature (K)

\dot{m} = mass flow rate (kg/s)

C_p = specific heat capacity (J/kg.K)

Mass flow rate, \dot{m} (kg/s) is calculated by multiplying density, ρ (kg/m³) and volume flow rate, \dot{V} (m³/s) as shown in Equation 3.6.

$$\dot{m} = \rho \dot{V} \quad 3.6$$

Bulk temperature, T_b is mean of temperature inlet and temperature outlet as shown in Equation 3.7.

$$T_b = \frac{T_{in} + T_{out}}{2} \quad 3.7$$

Where;

T_{in} = temperature inlet (K)

T_{out} = temperature outlet (K)

Surface temperature, T_s is wall temperature on radiator surface and calculated by averaging temperature on it as shown is Equation 3.8.

$$T_s = \frac{1}{4} \sum_{i=1}^4 T_i \quad 3.8$$

Where;

T_{in} = temperature inlet (K)

T_{out} = temperature outlet (K)

Experimental heat transfer coefficient, h_{exp} is calculated by dividing Equation 3.9 with Equation 3.5 as shown in Equation 3.4.

$$h_{exp} = \frac{\dot{m}C(T_{in} - T_{out})}{nA_s(T_b - T_s)} \quad 3.9$$

Hydraulic diameter, D_h , is computed by using geometrical radiator dimension as shown in Equation 3.10. Major diameter, D and minor diameter, d is measured by using

digital caliper. The measured major diameter is 0.022mm and minor diameter is 0.002mm.

$$D_h = \frac{4(\text{Area})}{\text{Perimeter}} = \frac{4 \left[\frac{\pi}{4} d^2 (D - d) \right]}{\pi d + 2(D - d)} \quad 3.10$$

Meanwhile, Reynolds number and Nusselt number is calculated by using Equation 3.11 and Equation 3.12.

$$Re = \frac{\rho v D_h}{n \mu} = \frac{4 \dot{m}}{n \pi D_h \mu} \quad 3.11$$

Where;

Re = Reynold number

v = flow velocity (m/s)

μ = dynamic viscosity (kg/ms)

$$Nu = \frac{h_{exp} D_h}{k} \quad 3.12$$

Where;

Nu = Nusselt number

D_h = hydraulic diameter (m/s)

k = thermal conductivity (W/m. K)

h_{exp} = Experimental heat transfer coefficient (W/m²K)

Meanwhile, pressure drop is calculated as shown in Equation 3.13. Meanwhile, friction factor, f is calculated as shown in Equation 3.14 for turbulent flow.

$$\Delta P = \rho g h \quad 3.13$$

Where;

ΔP = pressure drop (Pa)

ρ = density of fluid (kg/m³)

g = gravity acceleration (m/s²)

h = height of fluid column (m)

$$f = \frac{2 \Delta P}{L \rho u^2} \quad 3.14$$

Equation 3.15 shows calculation for heat transfer enhancement of thermal transport fluid in automotive radiator (Adnan Mohammed, 2014).

$$E\% = \frac{Nu_{nf} - Nu_f}{Nu_f} \times 100 \quad 3.15$$

Finally, overall performance of the automotive cooling system influenced by thermal and hydraulic factor which is calculated as shown in Equation 3.16 (Seyf & Mohammadian, 2011).

$$\eta = \frac{\left(\frac{Nu_{nf}}{Nu_f}\right)}{\left(\frac{f_{nf}}{f_f}\right)^{1/3}} \quad 3.16$$

CHAPTER 4

RESULTS AND DISCUSSION

4.1 Introduction

This chapter begins with nanofluid stability results obtained through sedimentation observation and absorbance drop evaluation using UV-Vis spectrophotometry. Stability results reveal that the prepared nanofluid from nanocellulose dispersant into ethylene glycol-distilled water mixture produces highly stable nanofluid. Besides, thermophysical property that comprises of thermal conductivity, dynamic viscosity, density and specific heat capacity is measured individually for each volume concentration at varying temperature. Statistical analytical tool, Minitab is used to determine the optimized volume concentration to be used as thermal transport fluid to study heat transfer performance and compared with conventional thermal transport fluid in a radiator test rig. The collected heat transfer performance results are heat transfer coefficient, convection heat transfer, Reynolds number, Nusselt number, friction factor, heat transfer enhancement and overall performance factor. In addition, temperature distribution profile results for nanofluid has high cooled area compared to conventional thermal transport fluid.

4.2 Nanofluid Stability

Nanofluid stability for this research is done through qualitative method (sedimentation observation) and quantitative method (drop in absorbance evaluation). In sedimentation observation, visual inspection of any settlement at the bottom of test tube is observed for duration of one month. In addition, nanofluid stability need be supported with scientifically approaches to obtain a trustable and reliable data (Lin et al., 2011). The simplest method to do so is by absorbance drop evaluation using UV-Vis spectrometry for duration of one month. Nanofluid should have acceptable stability

characteristics results since reduction in it could give negative effects on thermophysical property.

4.2.1 Sedimentation Observation

Sedimentation tend to occur fast at lower volume concentration. This can be related with high sedimentation velocity in nanofluid for lower volume concentration compared to higher volume concentration. Thus, volume concentration plays an important role in determining nanofluid stability (Richardson & Zaki, 1954). Figure 4.1 shows comparison photographs between nanofluid after preparation and one month after preparation. It is observed that there is no accumulation or settlement of nanomaterial at the bottom of test tube. In addition, there are no significant change in appearance or multilayer formation on the nanofluids. This means that nanofluid shows an excellent stability characteristics under sedimentation observation technique. Thus, the preparation method is proper and able to produce stable nanocellulose based nanofluid which is proven through sedimentation observation method.

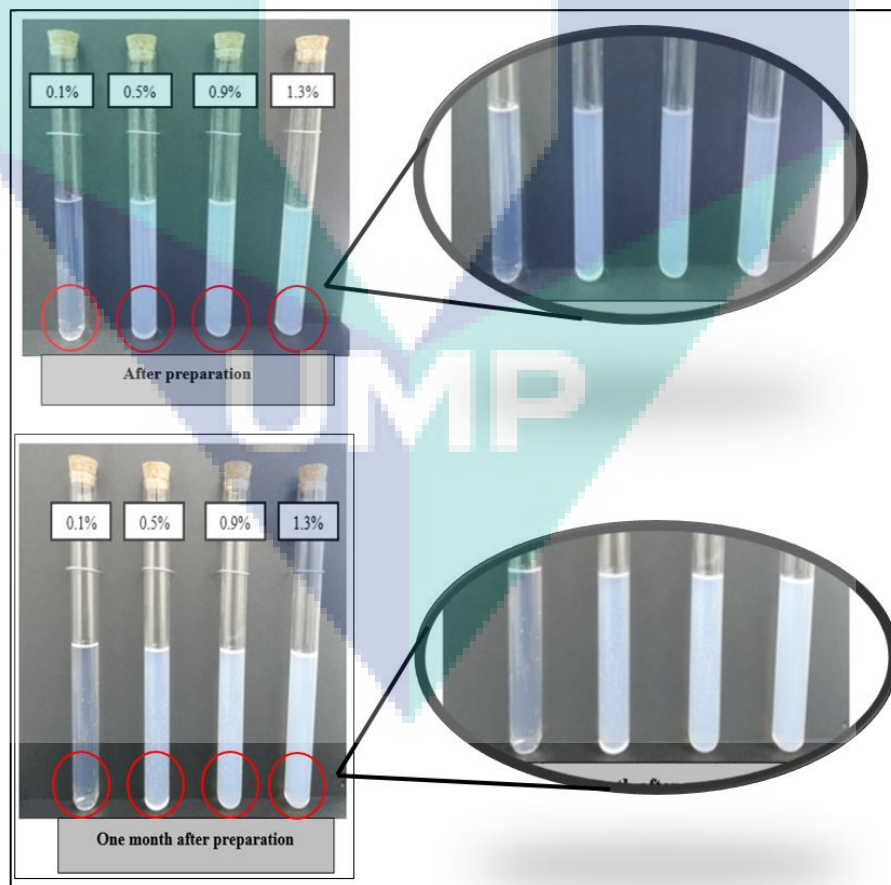


Figure 4.1 Photographs shows comparison of appearance taken at different timeline which shows no settlement of nanosubstance at bottom of test tube

4.2.2 Ultra Violet-Visible Spectrophotometry

Absorbance drop evaluation is another stability validation method used to prove stable of nanofluid scientifically. Foremost, peak absorbance wave length need to be determined for all the volume concentration and the results are as shown in Figure 4.2. From the graph, it is noted that the peak absorbance for entire volume concentration occurs at wavelength of 254nm. Thus, this peak wavelength value is used in Shimadzu UV-2600 Spectrophotometry to measure absorbance drop for one month. The absorbance drop evaluation is measured only for the lowest volume concentration (0.1%) and highest volume concentration (1.3%) as depicts in Figure 4.3 and Figure 4.4 respectively.

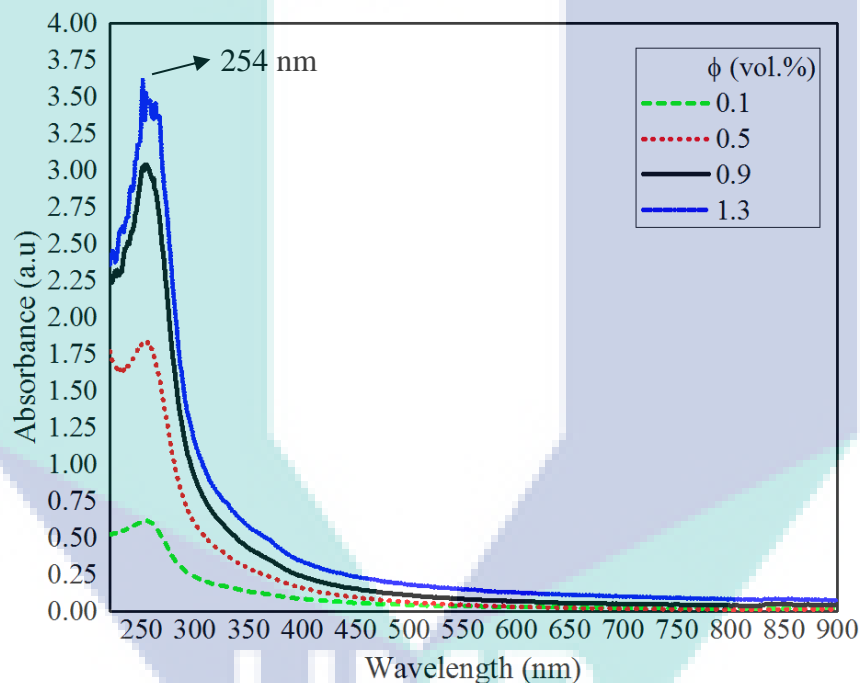


Figure 4.2 Peak absorbance value is measured at 254 nm for all the volume concentration

Graph in Figure 4.3 shows absorbance drop for 0.1% volume concentration. The measured absorbance drop after one month is 5.51%. Literature disclose that absorbance drop more than 30% after a month indicate that nanofluid is instable (Sharif et al., 2017). Thus, dispersion of nanocellulose in EGW produces a highly stable nanofluid.

Meanwhile, absorbance drop for 1.3% volume concentration as illustrates in Figure 4.4. It achieves absorbance drop of 1.14% after one month of evaluation. Thus, nanofluid with lowest volume concentration records the highest absorbance drop

compared to highest volume concentration (Mehrali et al., 2014). This best explanation for this phenomenon is known as effect of adjacent particle. Once colloidal suspension is achieved, base fluid generates an upward flow which pushes the nanoparticle and prevents it from falling due to gravity acceleration. Thus, the upward flow effect is greater in high concentration nanofluid compared to low concentration nanofluid which reduces absorbance drop in the colloidal suspension (Richardson & Zaki, 1954).

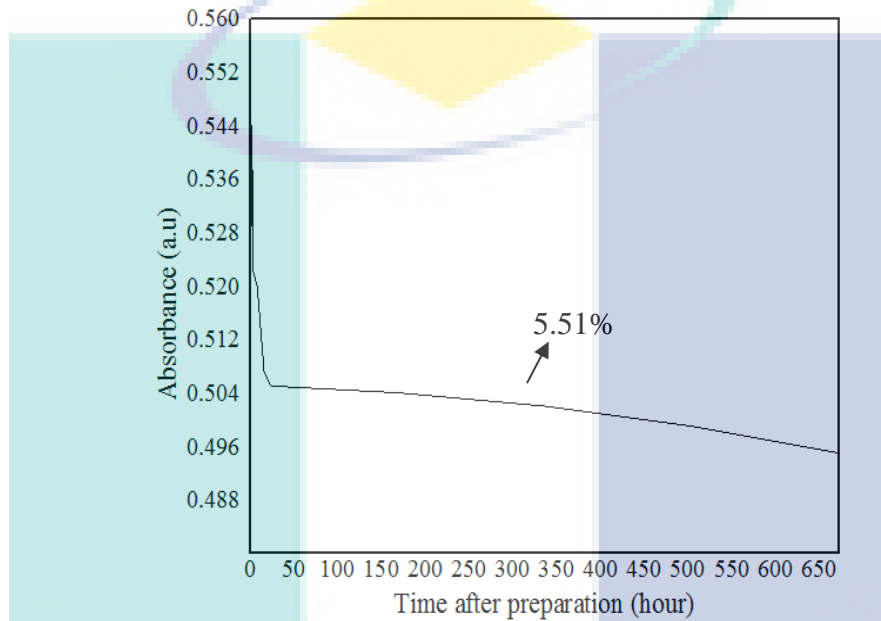


Figure 4.3 Absorbance drop of 5.51% is measured for volume concentration 0.1% after one month of nanofluid preparation

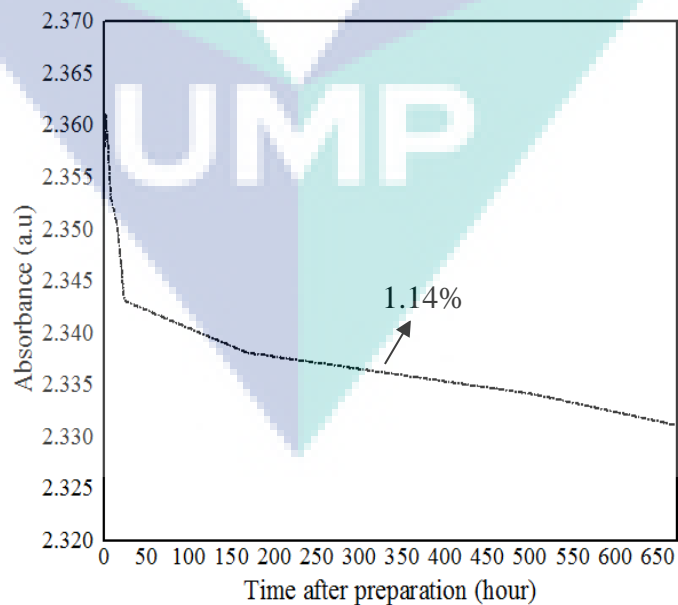


Figure 4.4 Absorbance drop of 1.14% is measured for volume concentration 1.3% after one month of nanofluid preparation

4.3 Thermophysical Property of Nanofluid

Characteristics of nanofluid for thermal application is determined through thermophysical property measurement which comprises of thermal conductivity, dynamic viscosity, density and specific heat capacity. A small enhancement in thermophysical property greatly effects the heat transfer performance especially to be used in heat transfer applications. The optimized nanofluid should have highest thermal conductivity and specific heat capacity value hence minimal dynamic viscosity and density value. Statistical analytical tool can be used to determine the optimized nanofluid among various volume concentration.

4.3.1 Thermal Conductivity

Results for thermal conductivity measurement for nanofluid (CNC) and conventional ethylene glycol-distilled water mixture (EGW) at varying volume concentration and temperature as shown in Figure 4.5. The maximum thermal conductivity acquired is 0.566 W/m.K at volume concentration of 1.3% and 80°C meanwhile lowest thermal conductivity measured is 0.44 W/m.K at volume concentration of 0.1% and 30°C. Thus, thermal conductivity results has proportional relation with temperature and volume concentration (Dardan et al., 2016).

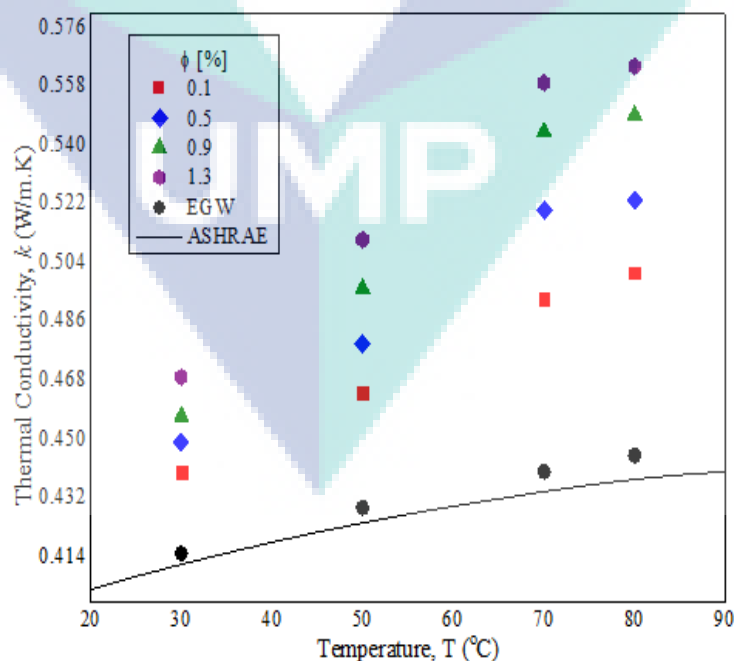


Figure 4.5 Comparison of thermal conductivity at varying temperature and volume concentration

Meanwhile, comparison of thermal conductivity enhancement among CNC and EGW is as shown in Figure 4.6. Maximum thermal conductivity enhancement occurs is 28.19% at volume concentration of 1.3% and 80°C. Conversely, the minimum thermal conductivity enhancement is 7.02% at volume concentration of 0.1% and 30°C. Overall, thermal conductivity enhancement is 7.02% - 13.01% at 30°C, 8.16% - 19.11% at 50°C, 12.05% - 27.05% at 70°C and 12.58% - 28.19% at 80°C with varying volume concentration ranged from 0.1% to 1.3%. Thus, thermal conductivity enhancement has proportional relation with temperature and volume concentration too.

In experiment conducted by Koblinski et al. (2002) and Teng et al. (2010) found similar trend for thermal conductivity which is thermal conductivity increases as temperature and concentration increases. In addition, Das et al. (2003) used Al₂O₃ nanoparticle in their research and proves that temperature has significant effect on thermal conductivity enhancement. Thus, colloidal suspension of nanocellulose into the basefluid help to produce maximum thermal conductivity enhancement of 28.19%, compared to EGW.

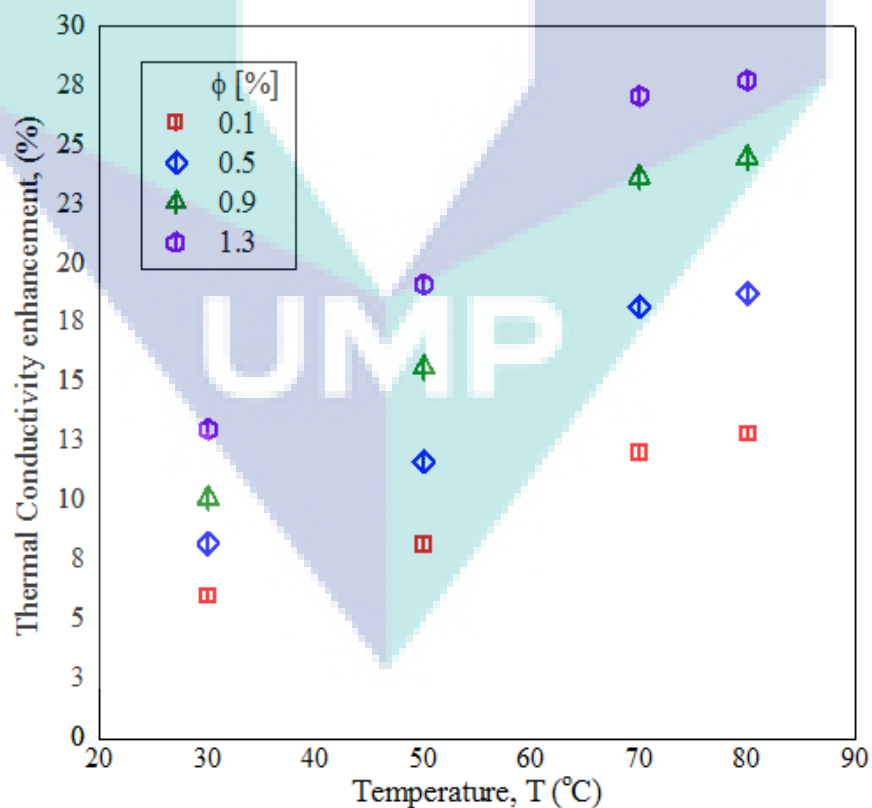


Figure 4.6 Comparison of thermal conductivity enhancement at varying temperature and volume concentration

As mentioned earlier, thermal conductivity has proportional relation with temperature and volume concentration (Dardan et al., 2016; Soltanimehr & Afrand, 2016). As temperature increases, a phenomenon known as Brownian motion, increases kinetic energy of the particles eventually influences for thermal conductivity enhancement (W. Li et al., 2017). Besides, nanomaterial dispersant forms interfacial layer between nanomaterial and basefluid. This interfacial layer act as a thermal bridge which reduces thermal resistance hence improves thermal conductivity (Timofeeva et al., 2010).

In addition, physical appearance of nanosubstance such as size, shape, type and preparation of nanofluid causes significant effects on thermal conductivity enhancement. In experiment conducted by Hong et al. (2006), they found metallic nanoparticle produces better thermal conductivity than non-metallic particle and ceramic nanoparticle under same circumstances. According to Asadi et al. (2017), increasing sonication time helps to enhance thermal conductivity value by achieving more stable nanofluid. Nanofluid with highest thermal conductivity is preferable for thermal transport applications since it helps to enhance heat removal rate (Abdul Hamid et al., 2014).

4.3.2 Dynamic viscosity

Dynamic viscosity results for CNC and EGW at varying temperature and volume concentration is as illustrated in Figure 4.7. The maximum dynamic viscosity measured is 0.00822 kg/m.s at 30°C with volume concentration of 1.3%. The graph in Figure 4.7 shows dynamic viscosity has increasing trend with volume concentration and decline trend with temperature. Reported research study by Anoop et al. (2009) and Usri et al. (2014) agrees with the obtained trend in this research (Turgut et al., 2009).

In high volume concentration, friction factor appears to be high because large amount of nanomaterial had been dispersed. Literally, friction factor promotes dynamic viscosity value. On the other hand, temperarute rise in nanofluid weaken the inter molecular adhesion force and responsible for lower dynamic viscosity value (C. Nguyen et al., 2007).

In addition, relative viscosity results at varying volume concentration and temperature is as shown in Figure 4.8. Overall, calculated relative dynamic viscosity value at 30°C is within 1.093 – 3.468, at 50°C is within 1.127 – 3.745, at 70°C is within 1.298- 3.946 and at 80°C is within 1.512 – 4.424 for varying volume concentration ranged

from 0.1% to 1.3%. Thus, relative dynamic viscosity has proportional relation with volume concentration and temperature. Nanofluid has relatively higher dynamic viscosity ratio. The colloidal suspension of nanosubstance increases internal shearing force and related with relative dynamic viscosity enhancement (C. Nguyen et al., 2007).

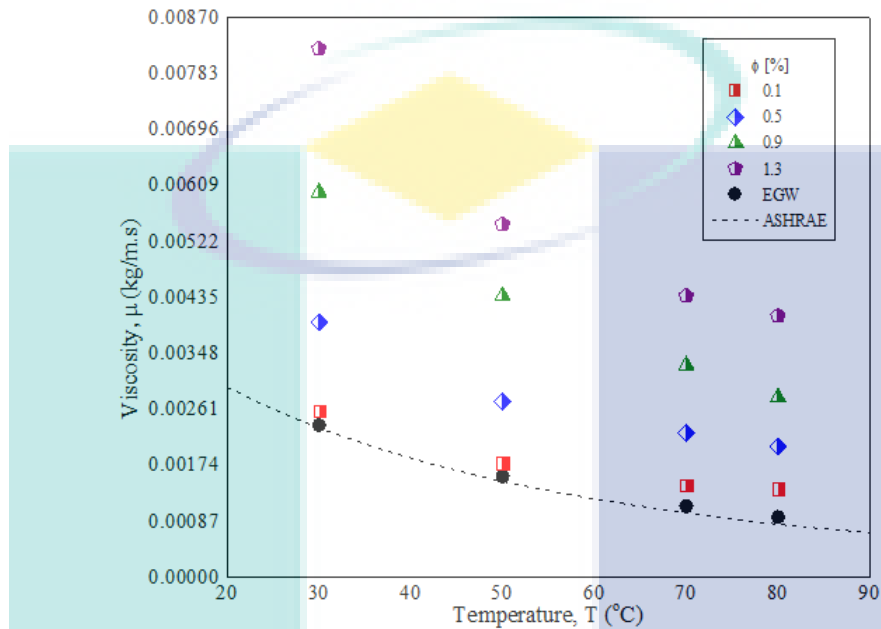


Figure 4.7 Comparison of dynamic viscosity measurement at varying temperature and volume concentration

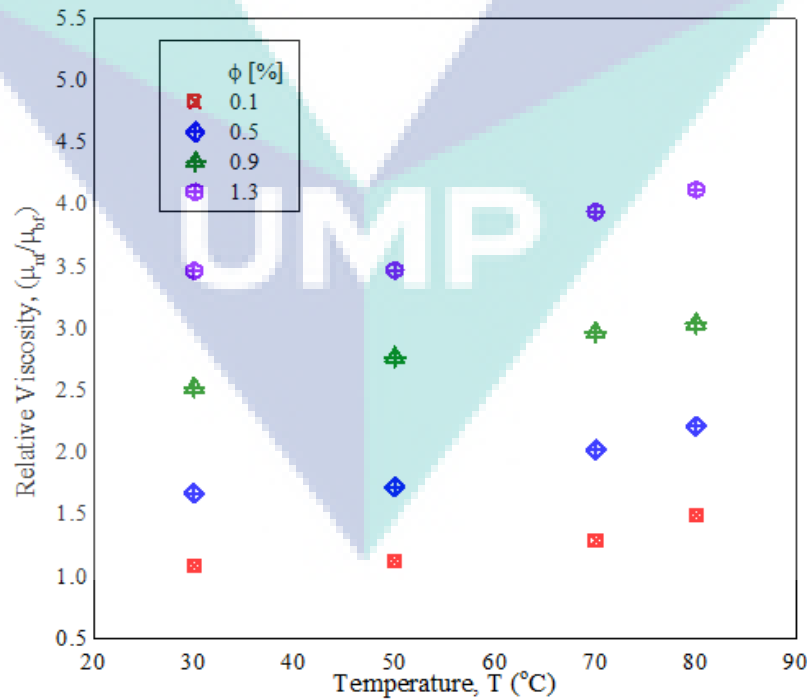


Figure 4.8 Comparison of relative dynamic viscosity measurement at varying temperature and volume concentration

Dynamic viscosity enhancement is related with physical condition of nanomaterial such as size, shape, type of nanomaterial and nanofluid preparation method (Timofeeva et al., 2011; Wei et al., 2017). Meanwhile, C. T. Nguyen et al. (2007) studied effect of particle size on viscosity by using Al_2O_3 with 36nm and 47nm. Apparently, smaller size nanoparticle produces low viscosity value. This is because resistance forms in small sized nanomaterial is lower and internal shearing stress acting onto it is minimal too (Agarwal et al., 2013). Nanofluid with lower dynamic viscosity help to reduce required pumping power which is literally increases performance factor of cooling system (Azmi et al., 2016).

4.3.3 Density

Comparison of density results for CNC and EGW at varying temperature and volume concentration is as depicted in Figure 4.9. The maximum density measured is 1063.05 kg/m^3 at 30°C and volume concentration of 1.3%. Meanwhile, the lowest density obtained is 1036.31 kg/m^3 at 80°C and volume concentration 0.1%. Overall, at temperature 30°C , density varies from 1059.31 kg/m^3 to 1063.05 kg/m^3 , at 50°C varies from 1052.31 kg/m^3 to 1056.36 kg/m^3 , at 70°C varies from 1041.31 kg/m^3 to 1048.56 kg/m^3 is acquired and at 80°C density of 1036.31 kg/m^3 to 1043.06 kg/m^3 is measured for nanofluid with volume concentration ranged 0.1 – 1.3%. Density results reveals that it has a decline trend with temperature and increasing trend with volume concentration.

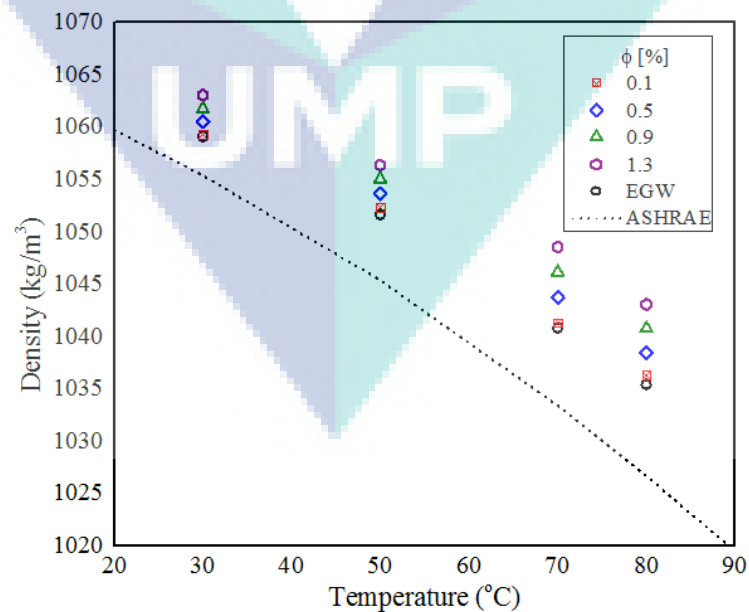


Figure 4.9 Comparison of density measurement at varying temperature and volume concentration

Thus, density has proportional relation with volume concentration and inverse relation with temperature. Density measurement by Said et al., (2013) using TiO_2 , SiO_2 and TiSiO_4 nanoparticles obtained the same trend as in this research. Research by Mostafizur et al., (2015) using Al_2O_3 nanoparticle also obtained the same trend. Colloidal suspension of nanocellulose spontaneously fills the gaps in the basefluid. Thus, nanofluid density increases as volume concentration increases.

Meanwhile, during heating, kinetic energy weakens the intermolecular adhesion force which is responsible for decline in density value. Besides, density is an important thermophysical property that influences Reynolds number and friction factor in fluid flow. Thus, enhancement in density value increases pressure drop of cooling system and eventually reduces overall performance factor (Mahbubul et al., 2013). Thus, nanofluid with minimum density value is preferred for an efficient thermal transport fluid which has lower resistance.

4.3.4 Specific Heat Capacity

Specific heat capacity is another vital thermophysical property that influences heat transfer performance. Specific heat capacity results for CNC and EGW at varying temperature and volume concentration is as depicted in Figure 4.10. The maximum specific heat capacity value achieved is $3972 \text{ J/kg}\cdot^\circ\text{C}$ at 90°C and volume concentration of 0.1%. Meanwhile, the minimum specific heat capacity achieved is $3432 \text{ J/kg}\cdot^\circ\text{C}$ at 30°C and volume concentration of 1.3%.

It is observed from Figure 4.10, at temperature 30°C , specific heat capacity of $3592 \text{ J/kg}\cdot^\circ\text{C}$ - $3432 \text{ J/kg}\cdot^\circ\text{C}$ is obtained, at temperature 60°C specific heat capacity of $3813 \text{ J/kg}\cdot^\circ\text{C}$ - $3532 \text{ J/kg}\cdot^\circ\text{C}$ is achieved, at temperature 80°C specific heat capacity of $3945 \text{ J/kg}\cdot^\circ\text{C}$ - $3629 \text{ J/kg}\cdot^\circ\text{C}$ is obtained and at 90°C , specific heat capacity of $3972 \text{ J/kg}\cdot^\circ\text{C}$ - $3644 \text{ J/kg}\cdot^\circ\text{C}$ is measured at varying volume concentration ranged from 0.1 to 1.3%.

From the scatter plot, it is observed that specific heat capacity has proportional relation with temperature and inverse relation with volume concentration. Same trend is reported by Zhou & Ni, (2008) in their research for specific heat capacity study. Meanwhile, in specific heat capacity enhancement, volume concentration has great influence than temperature (Zhou & Ni, 2008). Experiments conducted for specific heat

capacity measurement involving nanofluid is very limited which makes difficult to explain the anomaly behind this trend.

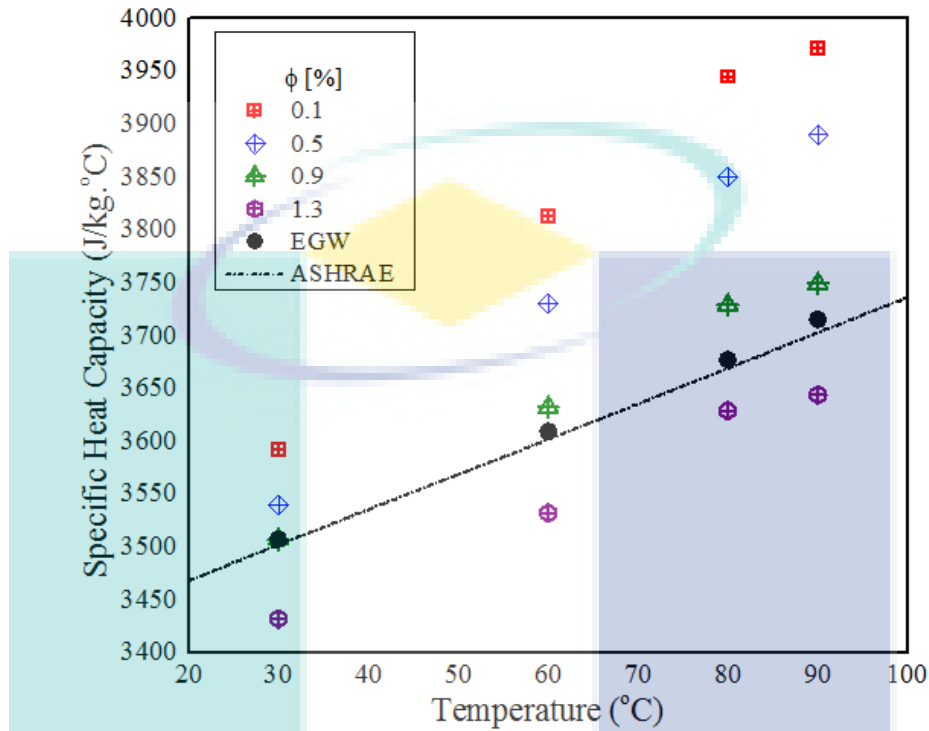


Figure 4.10 Comparison of specific heat capacity measurement at varying temperature and volume concentration

Nevertheless, it is expected that the interaction between bulk liquid and nanomaterial alter crystallization structure in colloidal suspension which is related with reduction of specific heat capacity value at higher concentrations. According to recent research study by P. Gopal, (2016), specific heat capacity plays a major role and influences more than thermal conductivity in automotive radiator. Thus, nanofluid with high specific heat capacity value is required for an efficient thermal exchange application.

4.4 Nanofluid optimization

Nanofluid optimization helps to find the optimized nanofluid to be used as thermal transport fluid in radiator test rig. Thermophysical property measurement is used in statistical analytical tool, Minitab 17 to determine this optimized nanofluid. By using only one nanofluid (optimized nanofluid) the number of experiment and expenses can be reduced. As mentioned in the methodology part, inlet temperature (operating temperature) is kept constant at 80°C. Table 4.1 shows lists of thermophysical property measurement at each volume concentration at temperature 80°C.

Table 4.1 Thermophysical property measurement of varying volume concentration at temperature 80°C

Volume concentration (%)	Thermal Conductivity (W/m.K)	Dynamic Viscosity (kg/m.s)	Density (kg/m ³)	Specific Heat Capacity (J/kg.°C)
0.1	0.5011	0.00138	1036.31	3945
0.5	0.5232	0.00204	1038.43	3850
0.9	0.5491	0.00280	1040.75	3729
1.3	0.5640	0.00407	1043.06	3629

Thermophysical property results as is Table 4.1 is used to determine optimized nanofluid by response optimizer function in statistical analytical software, Minitab 17. Optimized nanofluid should have maximize thermal conductivity and specific heat capacity. Meanwhile, to obtain acceptable rheological behaviour nanofluid should have minimize dynamic viscosity and density. The optimized volume concentration obtained from the analytical software is 0.4893%. Thus, it is impossible to prepare nanofluid for this volume concentration accurately. Thus, the optimized volume concentration is round off to the nearest value which is 0.5%.

Figure 4.11 depicts results obtained from the response optimizer function for composite desirability, D. Composite desirability indicates the value of closeness on a scale from 0 to 1 that used to determine favourable results is achievable or not for all responses in a single value. Meanwhile, individual desirability value, d, determines the level of closeness as a single response. Thus, inverse parabolic graph as depicts in Figure 4.11 shows that closeness to favourable result is achievable with composite desirable value of 0.6112 which indicates the optimized response analysis is in good agreement.

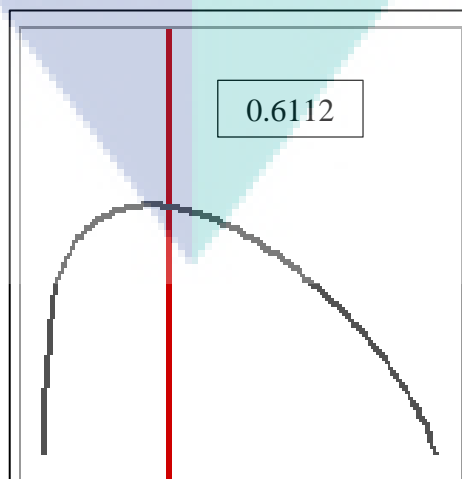


Figure 4.11 Results from statistical analysis for composite desirability, D

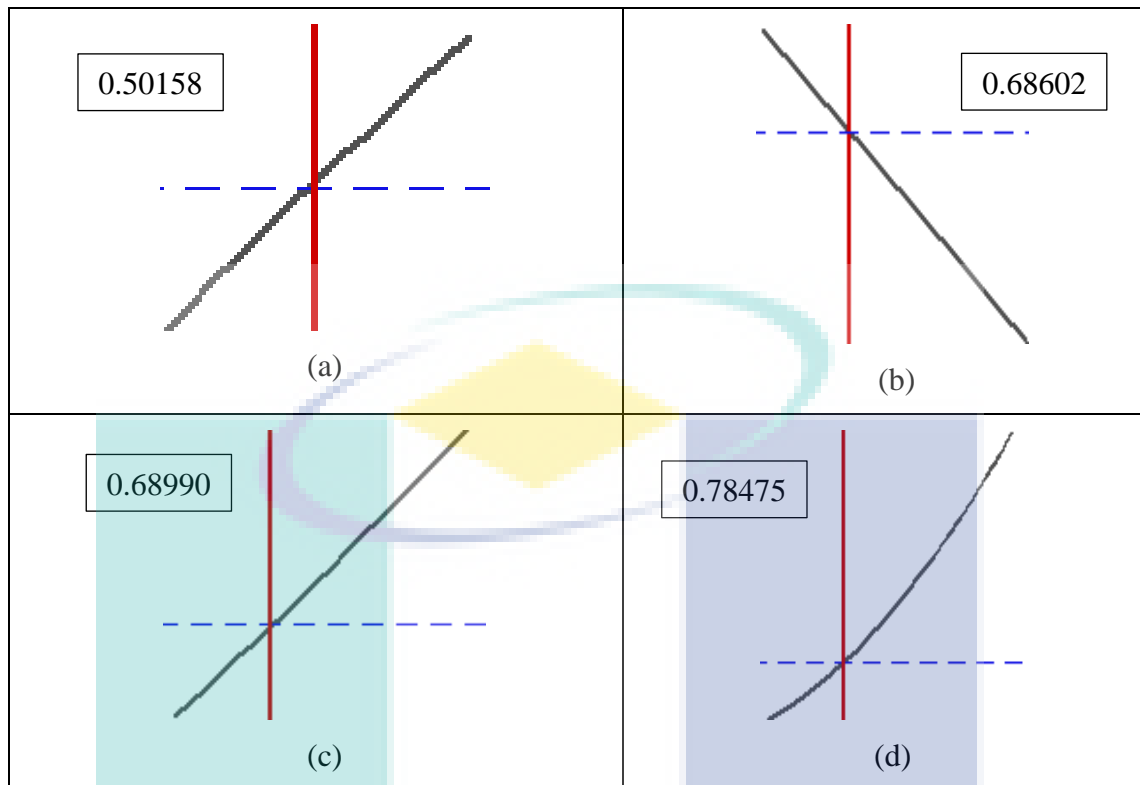


Figure 4.12 Results from statistical analysis for individual desirability for; (a) thermal conductivity; (b) Specific heat capacity; (c) Density (d) Dynamic viscosity

Meanwhile, Figure 4.12 shows individual desirability for individual thermophysical property, d scaled from 0 to 1. Thus, all the individual desirability achieves favourable response value. From the literature study, increment in specific heat capacity value is important than thermal conductivity enhancement for automotive cooling application (Bhanu Pratap Singh Tomar, 2015). From the statistical analysis, specific heat capacity has good response value which shows the optimized nanofluid concentration in acceptable agreement. Thus, nanofluid volume concentration with 0.5% (CNC) is selected as thermal transport fluid to be compared with convective ethylene glycol-water mixture (EGW).

4.5 Analysis of Heat Transfer Performance in Radiator Test Rig

Heat transfer performance analysis is validated with the aid of fabricated radiator test rig. Conventional ethylene glycol water mixture (EGW) and nanofluid (CNC) were used as thermal transport fluid to measure and compare heat transfer performance among them. In heat transfer analysis, convection heat transfer, experimental heat transfer coefficient, heat transfer enhancement and temperature distribution profile in radiator surface is measured. In addition, some of the flow behaviour characteristics such as

Reynolds number, Nusselt number and friction factor is calculated to study flow behaviour between CNC and EGW. Heat transfer enhancement and overall performance factor of CNC relative to EGW sum up this research's result. Experiments in this is conducted under two different circumstances; without the influence of fan (forced heat transfer convection through fluid only) and with influence of fan (forced heat transfer convection through fluid flow and air).

4.5.1 Experimental Heat Transfer Coefficient

According to Newton's law of cooling, convective heat transfer has proportional relation with heat transfer coefficient value (Bejan, 2013). Thus, enhancement in heat transfer coefficient increases convective heat transfer. Figure 4.13 shows experimental heat transfer coefficient value (without the influence of fan) against varying flow rate which is calculated by using formula in Equation (3.9). From the graph, the maximum experimental heat transfer coefficient obtained at flow rate of 5.5 LPM. The calculated experimental heat transfer coefficient value at this flow rate for nanofluid (CNC) is $36.172 \text{ W/m}^2\cdot\text{°C}$ and for conventional ethylene glycol (EGW) is $19.995 \text{ W/m}^2\cdot\text{°C}$.

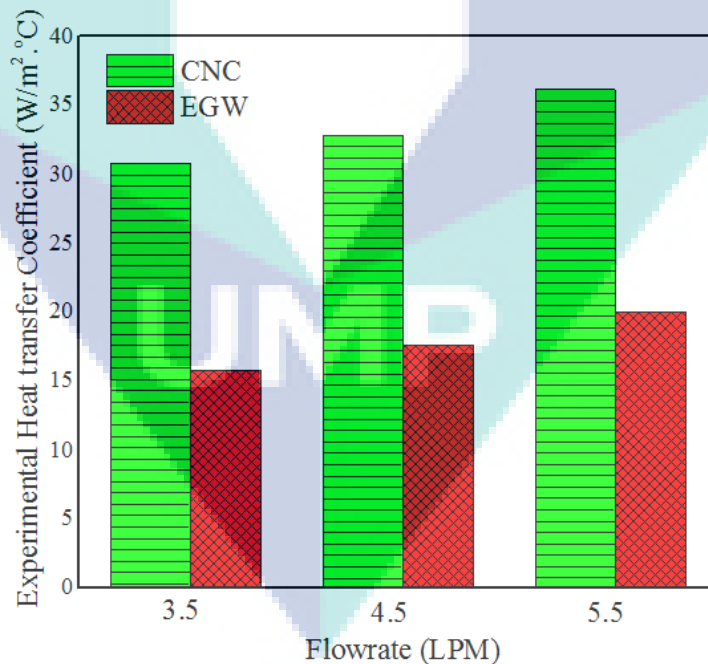


Figure 4.13 Comparison of experimental heat transfer coefficient results for CNC and EGW against flow rate (without influence of fan)

Meanwhile, measurement for relative heat transfer coefficient against flow rate (LPM) for without the influence of fan is as illustrated in Figure 4.14. The maximum

calculated relative experimental heat transfer coefficient is 1.809 at flow rate of 5.5 LPM. Meanwhile, the minimum experimental heat transfer coefficient obtained at flow rate of 3.5 LPM for nanofluid (CNC) is 30.797 W/m².°C and for conventional ethylene glycol (EGW) is 15.788 W/m².°C. Under this circumstance, the measured relative experimental heat transfer coefficient is 1.951. Thus, heat transfer coefficient has proportional relation with flow rate meanwhile relative heat transfer coefficient has inverse relation with flow rate for without the influence of fan circumstance.

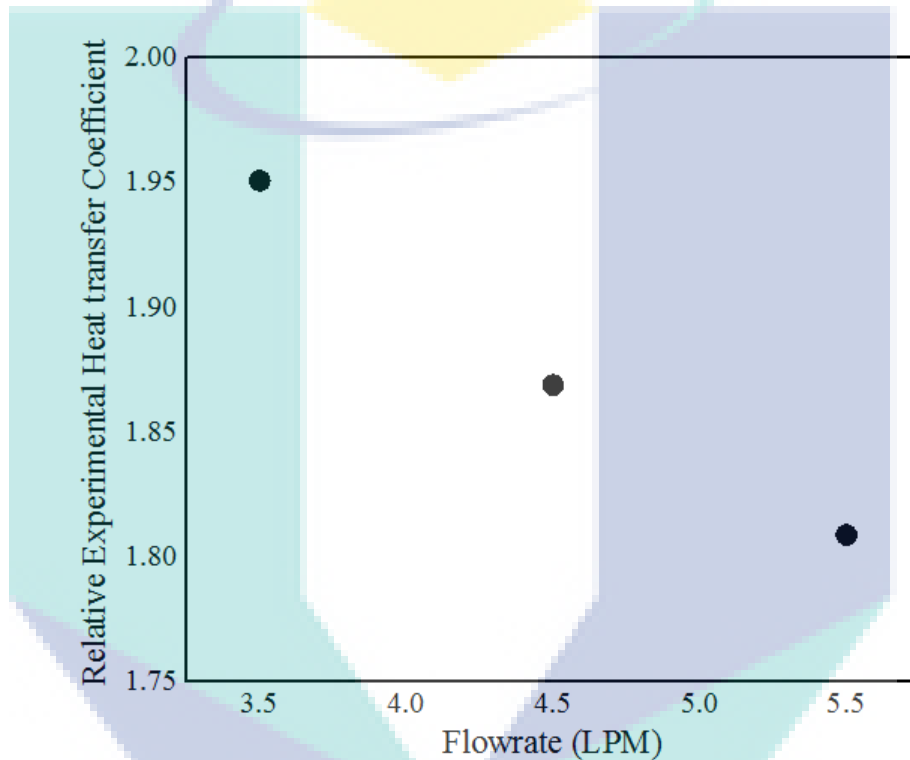


Figure 4.14 Relative experimental heat transfer coefficient results against varying flow rate (without influence of fan)

Meanwhile, Figure 4.15 shows bar chart for experimental heat transfer coefficient against flow rate (LPM) under the influence of fan. The maximum experimental heat transfer coefficient obtained at flow rate of 5.5 LPM. At this flow rate, the experimental heat transfer coefficient value for nanofluid (CNC) is 92.997 W/m².°C and for conventional ethylene glycol (EGW) is 46.322 W/m².°C. The relative experimental heat transfer coefficient obtained under this circumstance is 2.0076 as depicts in Figure 4.16. On the other side, minimum experimental heat transfer coefficient obtained is at 3.5 LPM whereas for nanofluid (CNC) is 84.293 W/m².°C and for conventional ethylene glycol (EGW) is 40.71 W/m².°C. Relative experimental heat transfer coefficient obtained at this parameter is 2.0706.

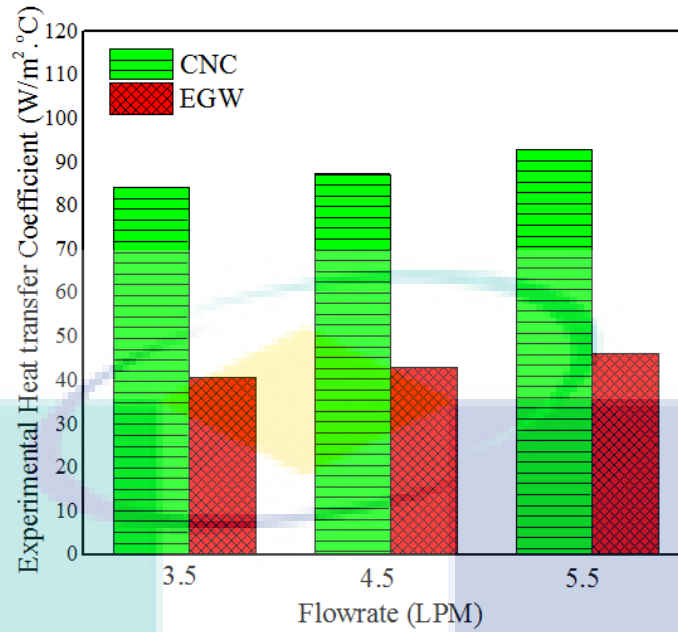


Figure 4.15 Comparison of experimental heat transfer coefficient results for CNC and EGW against flow rate (with influence of fan)

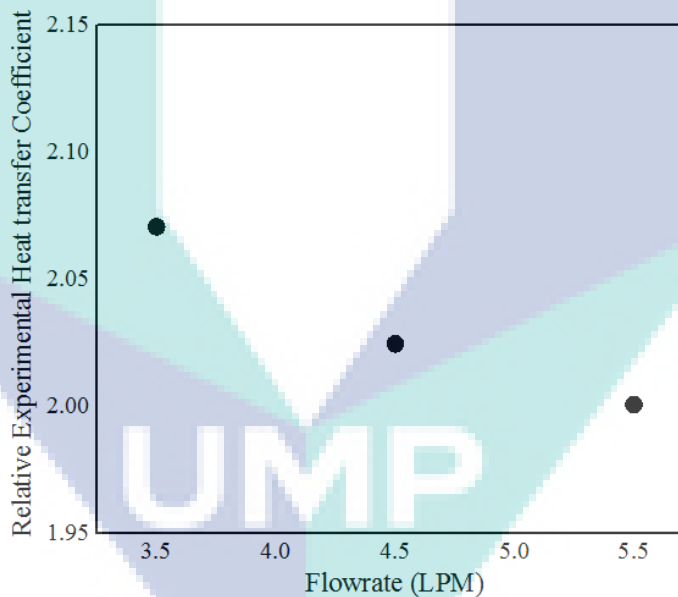


Figure 4.16 Results of relative experimental heat transfer coefficient against flow rate (with influence of fan)

Thus, experimental heat transfer coefficient value has proportional relation with flow rate (LPM). Conversely, relative experimental heat transfer coefficient has inverse relation with flow rate (LPM) under the influence of fan. In a similar research conducted by Ali et al., (2015), they produce same trend as this research when compared basefluid with nanofluid. In an experiment conducted by Namburu et al., (2009), they disperse copper oxide (CuO) in ethylene glycol-water mixture to study heat transfer performance

in radiator test rig. The author reported that at 20,000 Reynolds number, the heat transfer coefficient enhanced 1.35 times than basefluid. Besides, under the influence of fan circumstances high experimental heat transfer coefficient is measured compared to without the influence of fan circumstances.

The anomaly behind high heat transfer coefficient value measured in nanofluid can be explained with high specific heat capacity and thermal conductivity value in CNC compared to EGW. As reported in literature, specific heat capacity influences rate of heat removal in thermal transport application. Besides, high relative heat transfer coefficient value at low flow rates indicates that at low volumetric flow rate, high heat removal can be achieved in CNC than EGW. Besides, heat transfer coefficient value with the influence of fan has higher value than without the influence of fan circumstances. Indeed, air velocity used in the experiment accelerates the rate of heat removal in radiator test rig. Thus, combination of heat removal through forced heat transfer convection mechanism by fluid and air has high efficient than fluid alone.

4.5.2 Convection Heat Transfer

Another vital heat transfer performance analysis is convective heat transfer as shown in Figure 4.17. The graph is plotted against varying flow rate (LPM) under the influence of fan circumstance. Maximum convective heat transfer value obtained is 338.603 W for CNC and 219.837 W for EGW at 5.5 LPM. The convection heat transfer enhancement under this parameter is 54.02 %. At flow rate of 4.5 LPM, convective heat transfer enhancement of 55.323 % is measured. Meanwhile, Figure 4.19 illustrates comparison of convection heat transfer enhancement under two different circumstances.

On the other hand, lowest convective heat transfer measured is 326.095 W for CNC and 195.44 W for EGW. Convection heat transfer enhancement of 66.85 % is recorded under the influence of without fan circumstance. It can be concluded that convective heat transfer without the influence of fan has proportional relation with flow rate. Hence, convective heat transfer enhancement has inverse relation with volumetric flow rate under the same circumstance.

On the other side, Figure 4.18 depicts graph of convective heat transfer against flow rate (LPM) with the influence of fan. The maximum convection heat transfer reported is 874.334 W for CNC and 566.316 W for EGW at 5.5 LPM. Convective heat

transfer enhancement obtained at this parameter is 54.39 % as shown in Figure 4.19. Meanwhile, minimum convective heat transfer measured is 815.238 W for CNC and 525.018 W for EGW at 3.5 LPM. Convective heat transfer enhancement of 55.27 % is measured among them at the same flow rate. Meanwhile, at flow rate of 4.5 LPM, convective heat transfer enhancement of 54.47 % is measured. It can be concluded that convective heat transfer has proportional relation with volumetric flow rate under the influence of draft fan.

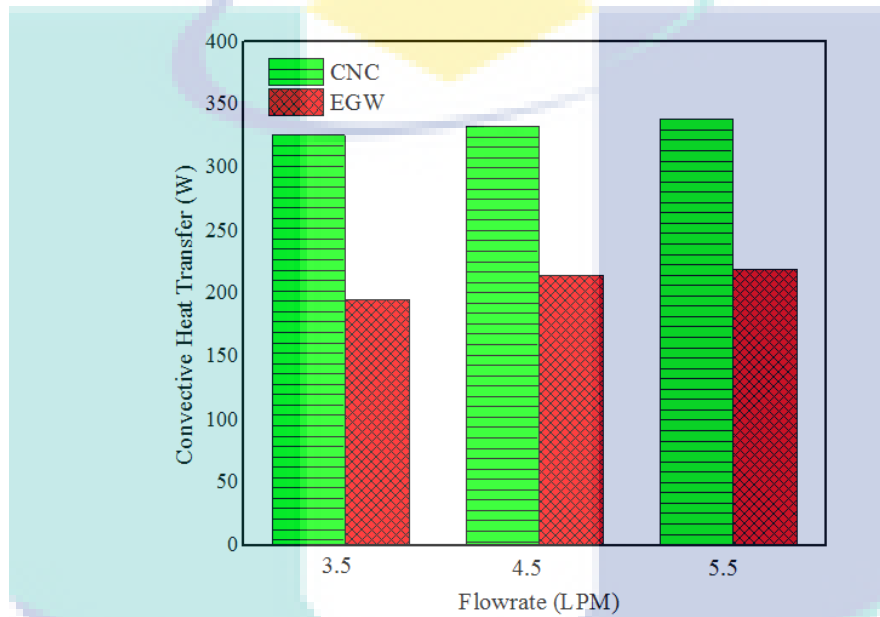


Figure 4.17 Comparison of convective heat transfer results for CNC and EGW against varying flow rate (without influence of fan)

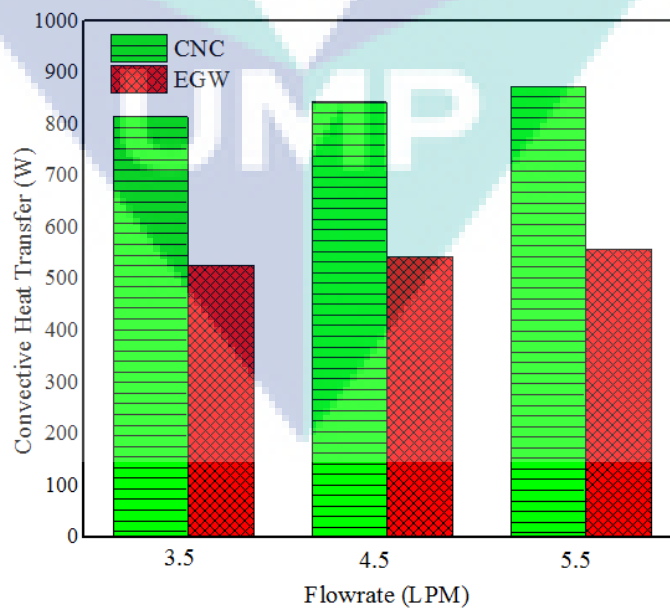


Figure 4.18 Comparison of convective heat transfer results for CNC and EGW against varying flow rate (with influence of fan)

The reason for high convective heat transfer in CNC can be related with high experimental heat transfer coefficient value, thermal conductivity and specific heat capacity. According to Newton's law of cooling, enhancement in heat transfer coefficient value increases the rate of heat removal (Bejan, 2013). Thus, convective heat transfer enhancement has inverse relation with volumetric flow rate under both circumstances. So, CNC has better heat removal capacity and shows an excellent heat transfer enhancement as depicted in Figure 4.19.

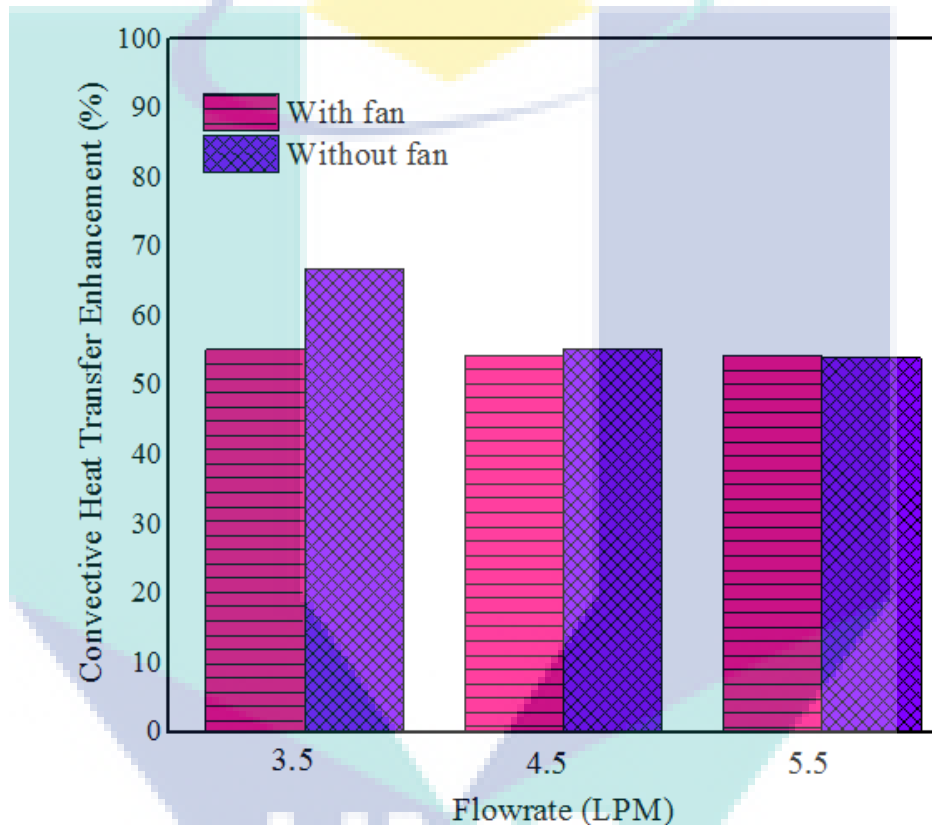


Figure 4.19 Overall convective heat transfer enhancement comparison at two experiment circumstances (with and without influence of fan)

4.5.3 Reynolds Number

Reynolds number need to be calculated in this research because it is important to identify type of flow regime in the radiator test rig. Graph of Reynolds number against flow rate for conventional ethylene glycol (EGW) is as shown in Figure 4.20. Reynolds number is calculated by using Equation 3.11. The maximum Reynolds number measured for EGW is 8931.55 at 5.5 LPM and the minimum Reynolds number is 5678.41 at 3.5 LPM. So, turbulent flow regime is achieved for conventional ethylene glycol. The graph trend shows Reynolds number for EGW has proportional relation with flow rate.

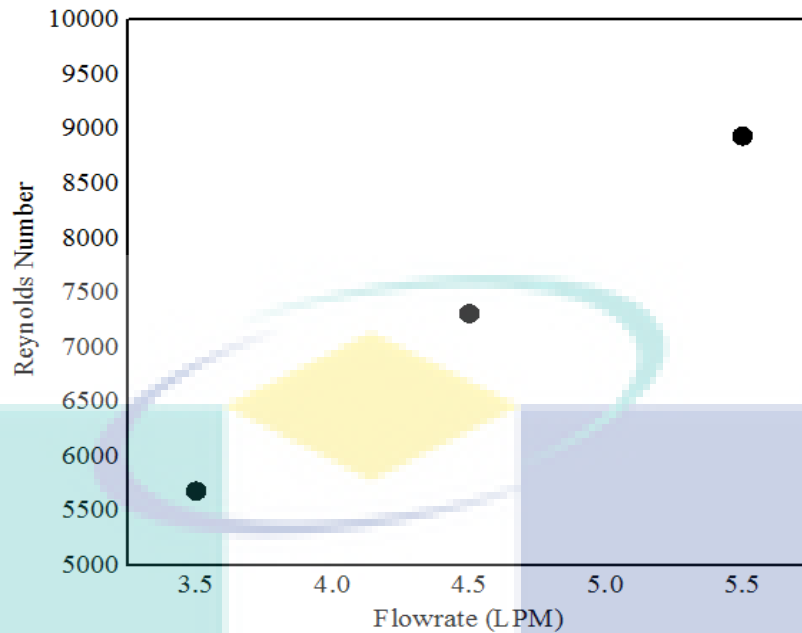


Figure 4.20 Results for Reynolds number against varying flow rate (conventional ethylene glycol - EGW)

Meanwhile, Reynolds number against flow rate for nanofluid (CNC) is as illustrated in Figure 4.21. The maximum Reynolds number measured for CNC is 3850.93 at 5.5 LPM and the minimum Reynolds number is 2448.31 at 3.5 LPM. So, CNC also achieved same flow regime (turbulent) as EGW. Thus, Reynolds number for CNC has proportional relation with flow rate. Thus, both thermal transport fluid has turbulent flow regime inside the radiator at varying flow rate between 3.5 LPM to 5.5 LPM. Furthermore, nanofluid (CNC) achieved smaller Reynold number than conventional ethylene glycol-water mixture (EGW).

On the other hand, in an experiment conducted by Heris et al., (2007) by using Al_2O_3 nanofluid, they obtained Reynolds number less than base fluid. In addition, research conducted by Ali et al., (2015) which involves ZnO based nanofluid produces same trend as in this research. Lower Reynolds number in nanofluid can be explained with influence of high viscous force than inertial force (Batchelor, 2000).

Since CNC has high dynamic viscosity value compared to EGW, it reduces the Reynolds number of the flow. In addition, high density value in CNC than EGW causes it to have a high inertial effect on nanofluid which also plays a major role in Reynolds number reduction. Meanwhile, Reynolds number has increasing trend with flow rate. This can be best explained by fundamental theory behind this formula. Literally, as

velocity increase, high inertial force effect on fluid causes Reynolds number enhancement.

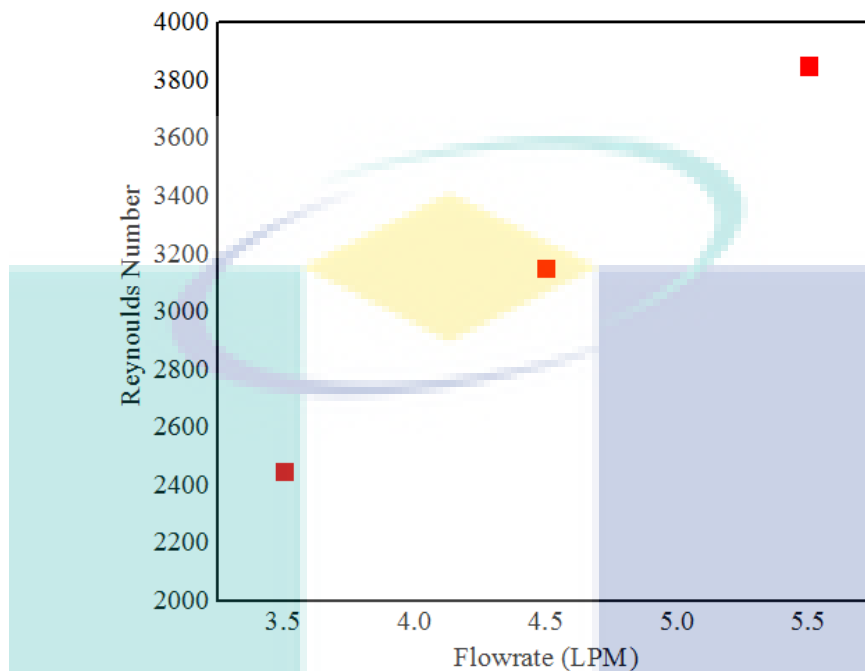


Figure 4.21 Results for Reynolds number against varying flow rate (Nanofluid - CNC)

4.5.4 Nusselt Number

Nusselt number is a dimensionless value which is defined as ratio of convective heat transfer to conductive heat transfer. Nusselt number in this experiment is calculate by using Equation 3.12. Figure 4.22 shows graph of Nusselt number against flow rate without the influence of fan. The highest Nusselt number achieved is 36.164 for CNC and 19.97 for EGW with Nusselt number enhancement of 80.868% at 5.5 LPM. Meanwhile, the lowest Nusselt number measured is 30.797 for CNC and 15.787 for EGW with Nusselt number enhancement of 95.071 % at 3.5 LPM. Thus, Nusselt number has proportional relation with flow rate without the influence of fan.

Meanwhile, graph in Figure 4.23 shows Nusselt number against flow rate under influence of fan. The highest Nusselt number achieved is 92.997 for CNC and 46.322 for EGW with Nusselt number enhancement of 100.06 % at 5.5 LPM. Meanwhile, the minimum Nusselt number measured is 84.29 for CNC and 40.709 for EGW with Nusselt number enhancement of 40.71 %. Nusselt number shows proportional relation with flow rate under influence of velocity from draft fan.

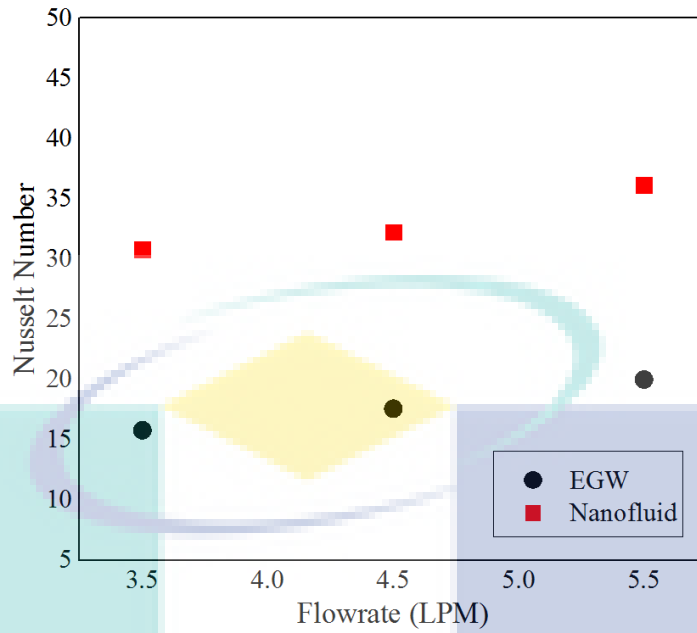


Figure 4.22 Comparison of nusselt number against varying flow rate for nanofluid and EGW under without fan circumstance

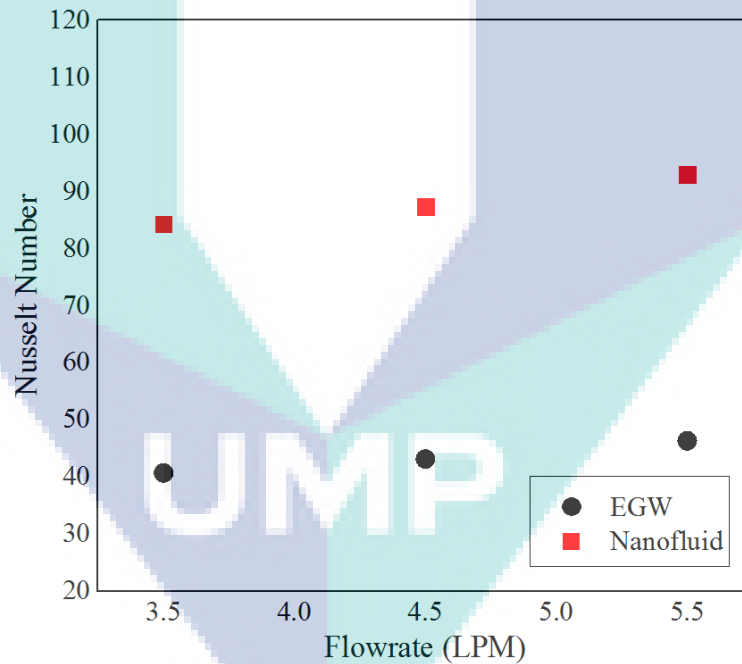


Figure 4.23 Comparison of nusselt number against varying flow rate for nanofluid and EGW under with fan circumstance

The obtained Nusselt number results for EGW and CNC is compared as shown in Figure 4.24 and Figure 4.25 respectively. Nusselt number is increasing as Reynold number increases. This trend tallies with S.Peyghambarzadeh et al., (2011) experiment results. On the other side, CNC achieves high Nusselt number under both circumstances compared to EGW (Peyghambarzadeh et al., 2013).

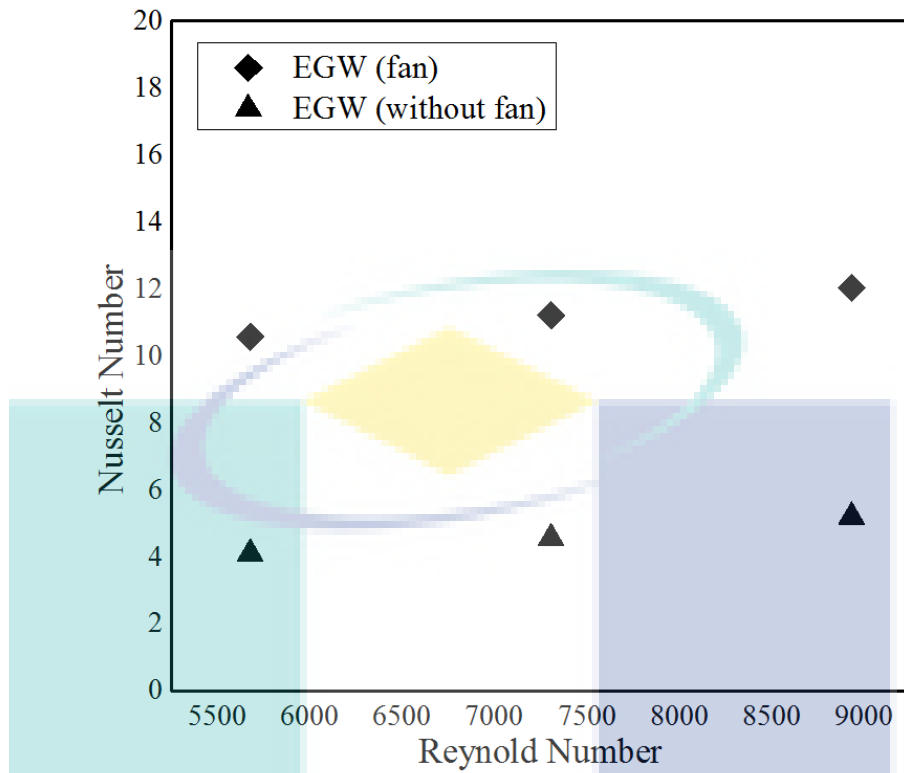


Figure 4.24 Results for Nusselt number against varying Reynold number for EGW under two different circumstances

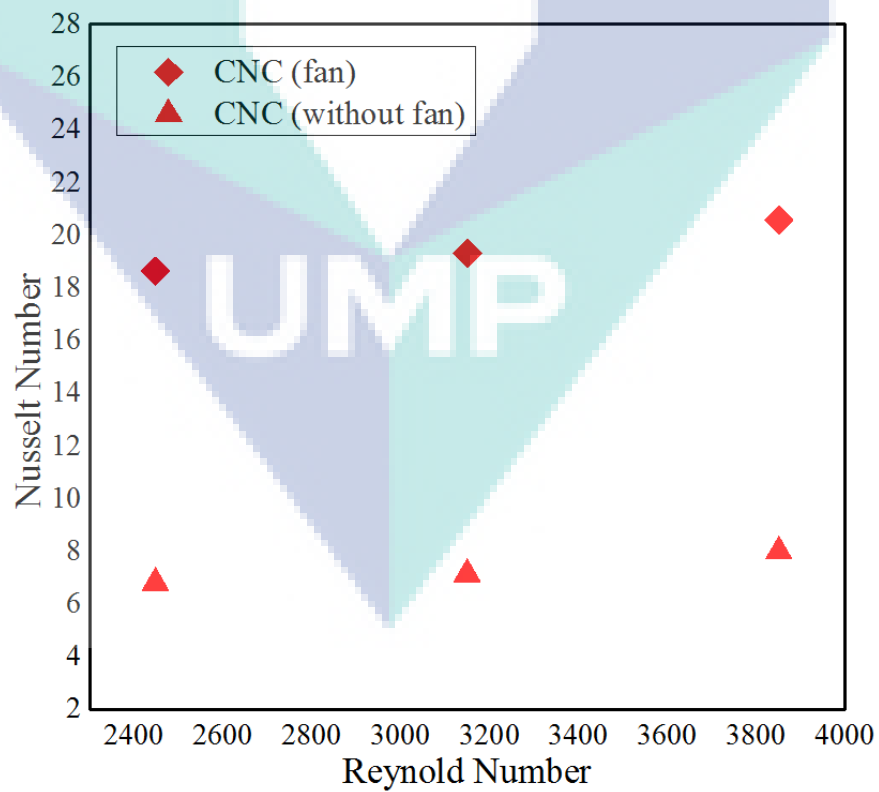


Figure 4.25 Results for Nusselt number against varying Reynold number for CNC under two different circumstances

The anomaly behind high Nusselt number in CNC than EGW can be explained with high influence of convective heat transfer than conductive heat transfer (Wen & Ding, 2004). It is related with high experimental heat transfer coefficient value in nanofluid (CNC) compared to conventional ethylene glycol-water mixture (EGW). Thus, heat transfer coefficient value has proportional relation with Nusselt number.

4.5.5 Friction Factor

Friction factor is influenced by pressure drop between inlet and outlet of flow in radiator. Friction factor in this research is calculated by using Equation 3.14. Graph plotted in Figure 4.26 depicted friction factor against Reynolds number for EGW. The highest friction factor measured is 0.092 at Reynolds number of 5678.39 for EGW. Meanwhile, the lowest friction factor obtained is 0.058 at Reynolds number of 8931.55 for EGW. In between them, at Reynolds number of 7304.97, friction factor of 0.071 is recorded. Thus, friction factor has inverse relation with Reynolds number for EGW.

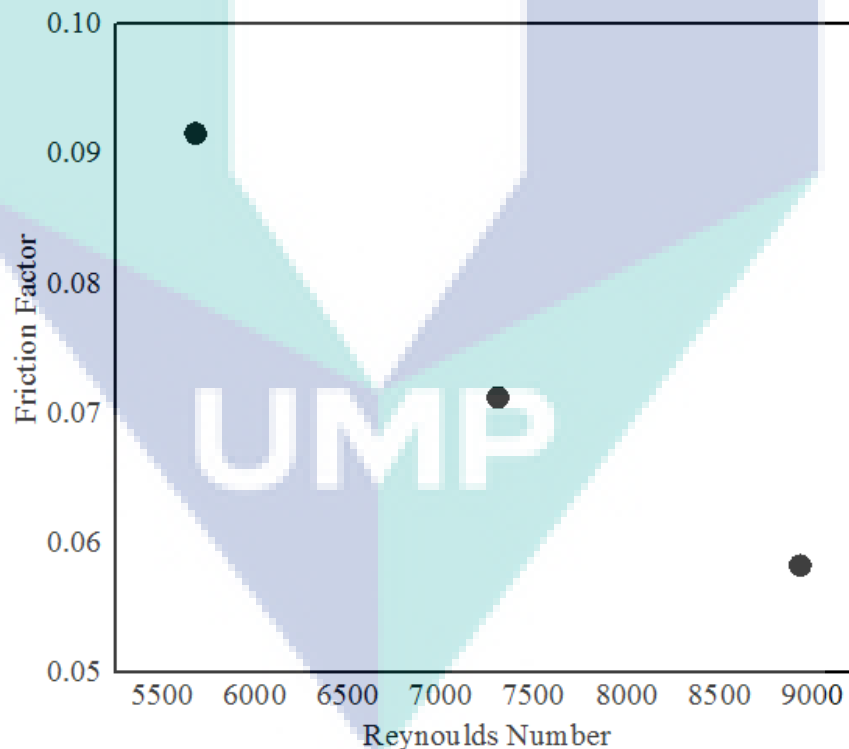


Figure 4.26 Results for friction factor against varying Reynolds number for EGW

Meanwhile, Figure 4.27 depicts friction factor against Reynolds number for CNC. The highest friction factor measured is 0.212 at Reynolds number of 2448.31 for CNC. Meanwhile, the lowest friction factor obtained is 0.135 at Reynolds number of 3850.93

for CNC. In between them at Reynolds number 3149.62, friction factor of 0.165 is recorded. Thus, friction factor has inverse relation with Reynolds number for CNC (Ko et al., 2007).

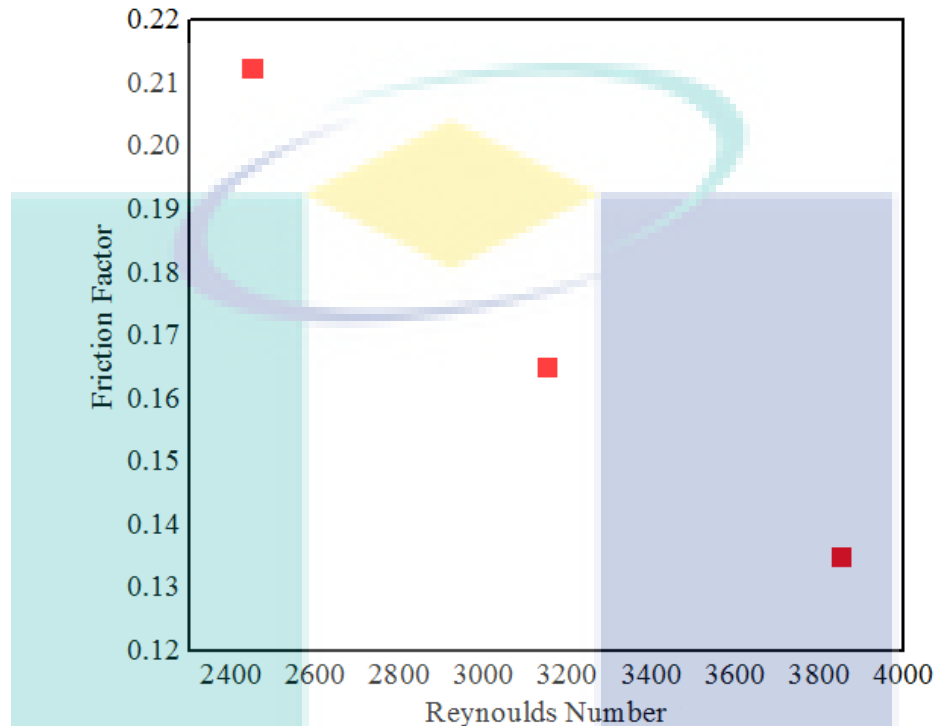


Figure 4.27 Results for friction factor against varying Reynolds number for CNC

According to literature, under turbulent flow regime, friction factor has inverse relation with Reynolds number which shows the same trend as in this research (Naraki et al., 2013). Presence of high friction factor in CNC (nanofluid) than EGW (conventional ethylene glycol-water mixture) thermal transport fluid is because of high dynamic viscosity in nanofluid (Duangthongsuk & Wongwises, 2010). This phenomenon can also be explained by the increase of internal shearing stress in nanofluid. Meanwhile, as Reynolds number increases, resistance acting between boundary layer and walls of the radiator reduces. Thus, friction factor has inverse relation with Reynolds number.

4.5.6 Heat Transfer Enhancement

Heat transfer enhancement using nanofluid in automotive radiator is computed by using Equation 3.15. As shown in Figure 4.28, the highest heat transfer enhancement calculated is 39.75 % at flow rate of 3.5 LPM. Meanwhile, the lowest heat transfer enhancement achieved is 33.02% at flow rate of 5.5 LPM. Thus, heat transfer

enhancement has inverse relation trend with flow rate under without the influence of fan circumstance.

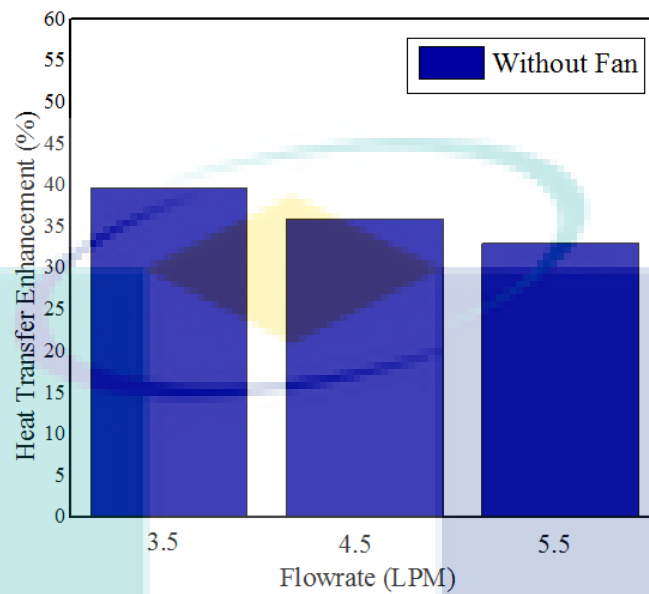


Figure 4.28 Results of heat transfer enhancement against flow rate (without influence of fan)

Meanwhile, Figure 4.29 shows heat transfer enhancement against flow rate with the influence of draft fan. The highest heat transfer enhancement is occurred is 43.24 % at 3.5 LPM flow rate. Meanwhile, the lowest heat transfer enhancement achieved is 39.46 % at 5.5 LPM flow rate. Thus, heat transfer enhancement has inverse relation trend with flow rate under with the influence of fan circumstance.

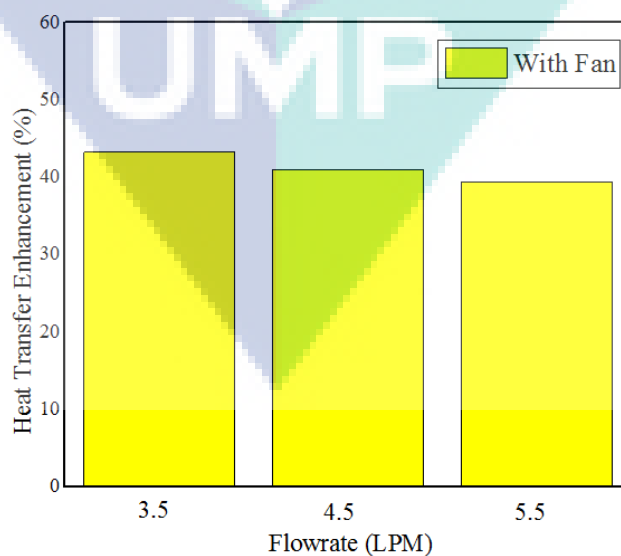


Figure 4.29 Results of heat transfer enhancement against flow rate (with influence of fan)

Comparison of heat transfer enhancement for both circumstances as depicts in Figure 4.30. The bar graph shows that heat transfer enhancement has inverse relation with flow rate. Under turbulent regime, lowest flow rate able to remove heat efficiently from the automotive radiator. This result can be related with convective heat transfer enhancement as mentioned at early of the chapter. Thus, the effect of forced convection heat transfer through combined effect of air and fluid removes heat efficiently. The anomaly behind high heat transfer enhancement is high thermal conductivity and specific heat capacity value with acceptable dynamic viscosity and density value.

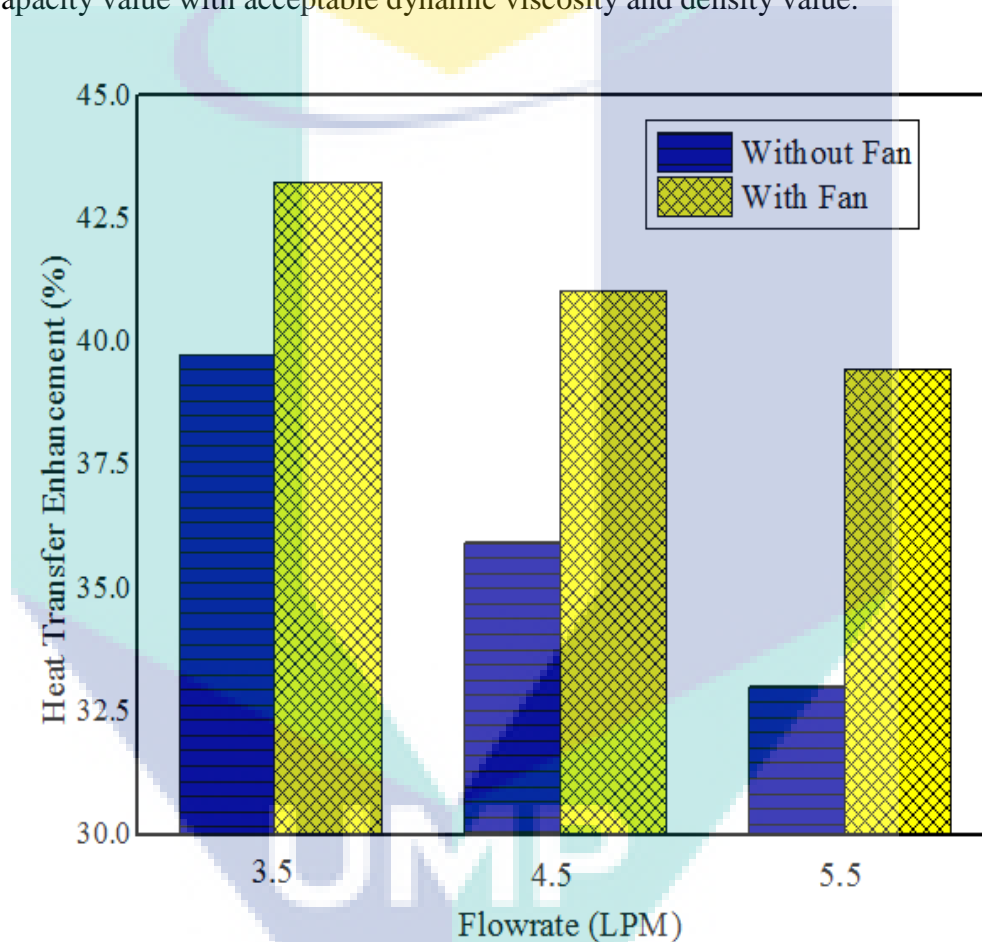


Figure 4.30 Overall comparison of heat transfer enhancement against varying flow rate under two different circumstances

4.5.7 Thermal and Hydraulic Performance Factor

Finally, thermal and hydraulic performance factor is calculated by using Equation 3.15. Meanwhile, Figure 4.31 depicts thermal and hydraulic performance factor against flow rate without the influence of fan. The highest performance factor measured is 2.15 at flow rate 3.5 LPM meanwhile the lowest is achieved is 1.99 at flow rate of 5.5 LPM. In between of 4.5 LPM, performance factor of 2.02 is recorded.

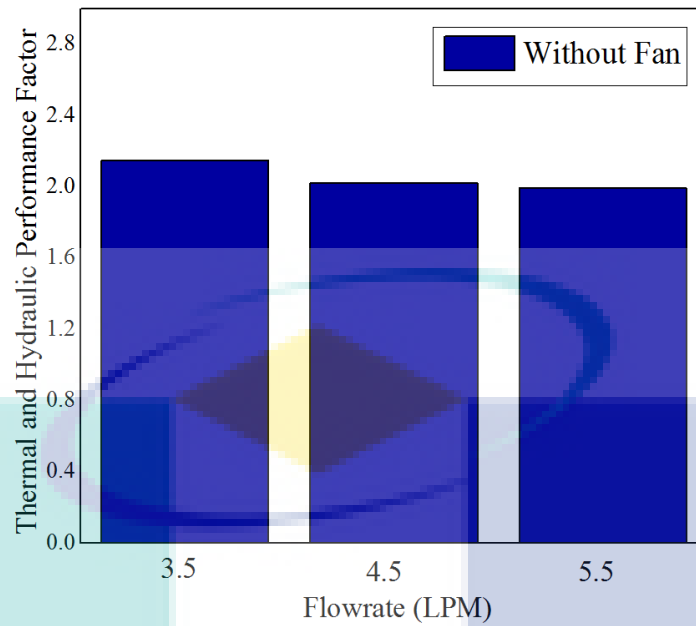


Figure 4.31 Results of overall cooling system efficiency against flow rate (without influence of fan)

In addition, Figure 4.32 depicts thermal and hydraulic performance factor against flow rate flow rate with the influence of fan. The performance factor is measured is 2.28 at flow rate 3.5 LPM meanwhile lowest value achieved is 2.21 at flow rate 5.5 LPM. Meanwhile, at 4.5 LPM, performance factor of 2.23 is measured.

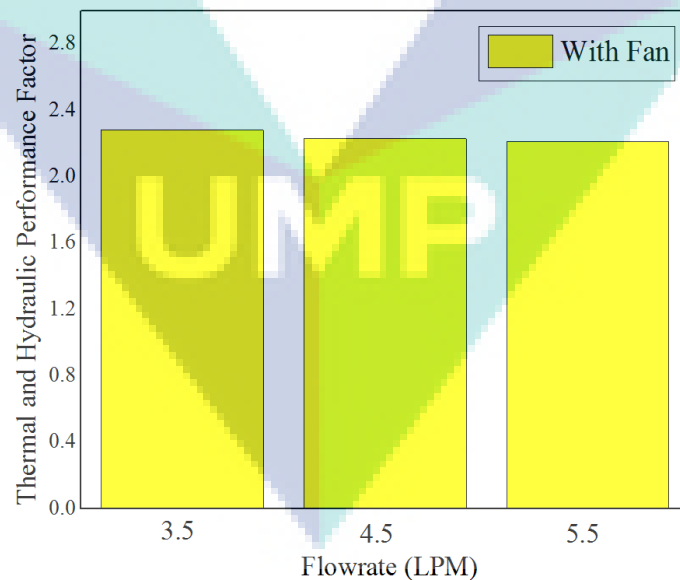


Figure 4.32 Results of overall cooling system efficiency against flow rate (with influence of fan)

Finally, Figure 4.33 illustrates comparison for thermal and hydraulic performance factor against flow rate flow rate. It is observed that thermal and hydraulic performance

factor has proportional relation with flow rate. This is best explained by under turbulent regime; lowest flow rate removes heat efficiently from the cooling system.

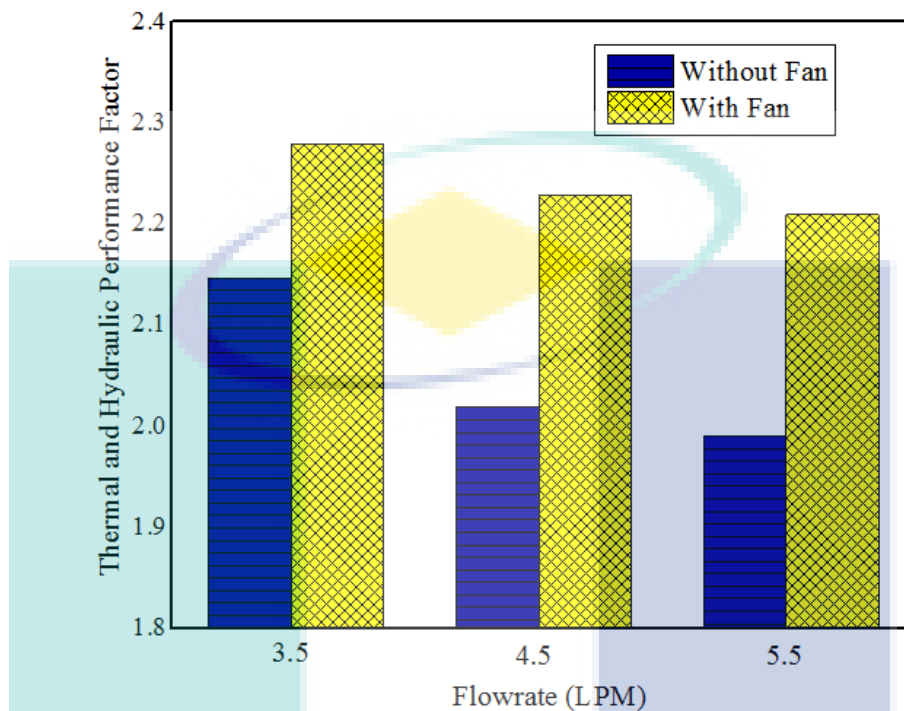


Figure 4.33 Overall comparison of performance factor against varying flow rate under two circumstances

We can conclude that the overall performance factor has inverse relation with volumetric flow rate. This can be explained with reduction of friction factor value at increasing flow rate. Besides, the higher the performance factor value, the more efficient it is in heat removal from automotive radiator. Thus, the combined effect of forced convection heat transfer through air and fluid influencing the rate of heat removal which produces high performance factor value. From the graph in Figure 4.33, we can observe that at all parameter, performance factor more than 1 is achieved. This means that influence of heat transfer enhancement is greater than frictional factor. Even though, friction factor in nanofluid quite high than EGW, the overall performance of CNC is better than EGW.

4.5.8 Temperature Distribution Analysis on Automotive Radiator

Figure 4.34 until Figure 4.39 shows temperature distribution profile without the influence of fan. Meanwhile, from Figure 4.40 to 4.45 shows temperature distribution profile under the influence of fan.

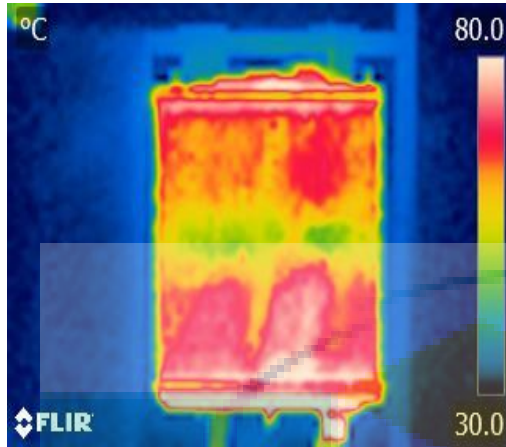


Figure 4.34 Temperature distribution at flow rate of 3.5 LPM – EGW (without influence of fan)

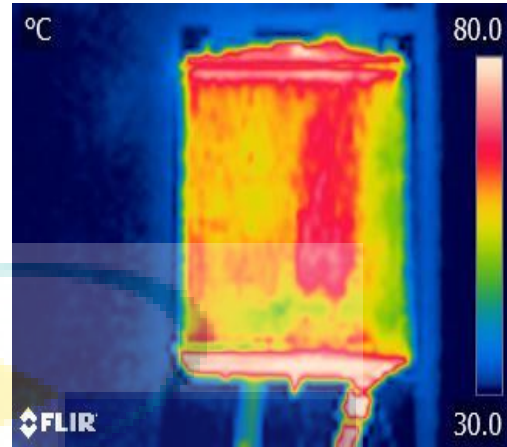


Figure 4.35 Temperature distribution at flow rate of 3.5 LPM – CNC (without influence of fan)

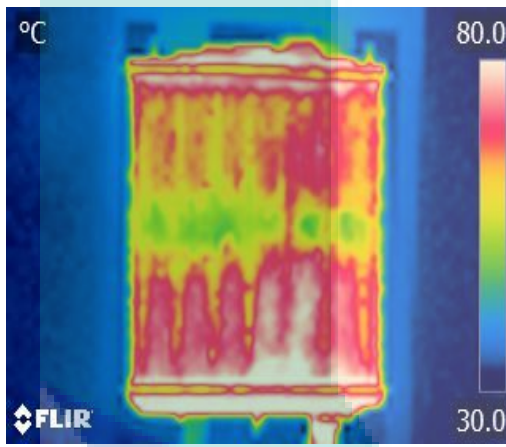


Figure 4.36 Temperature distribution at flow rate of 4.5 LPM – EGW (without influence of fan)

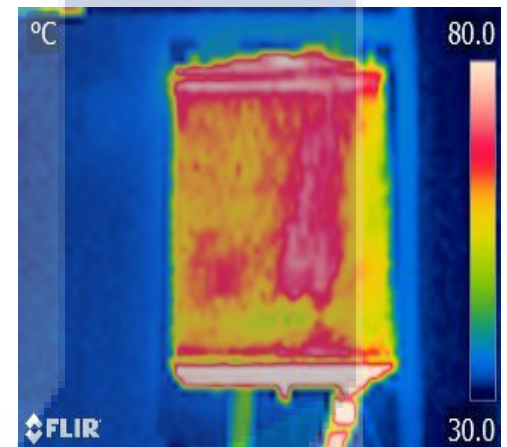


Figure 4.37 Temperature distribution at flow rate of 4.5 LPM – CNC (without influence of fan)

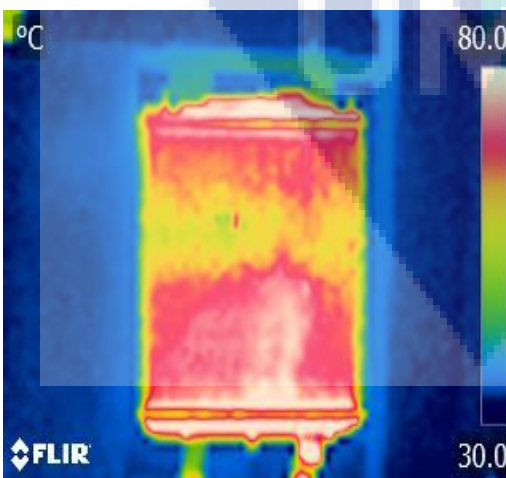


Figure 4.38 Temperature distribution at flow rate of 5.5 LPM – EGW (without influence of fan)

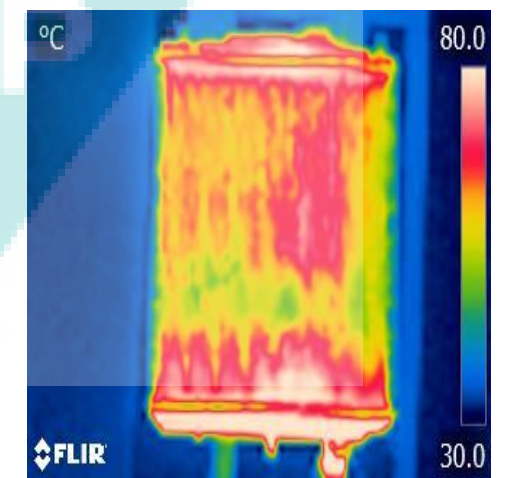


Figure 4.39 Temperature distribution at flow rate of 5.5 LPM – CNC (without influence of fan)

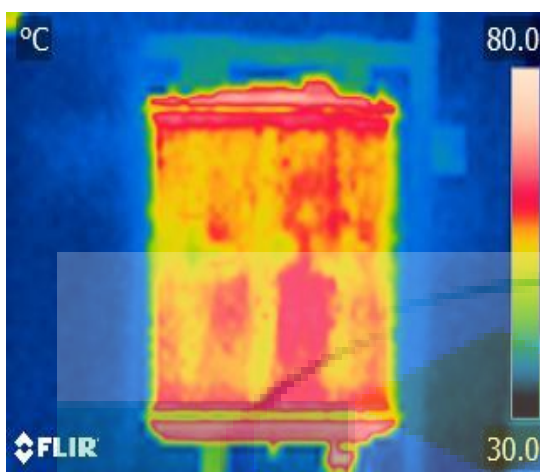


Figure 4.40 Temperature distribution at flow rate of 3.5 LPM – EGW (with influence of fan)

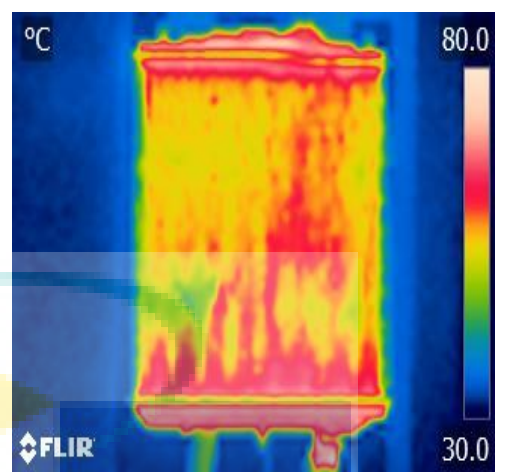


Figure 4.41 Temperature distribution at flow rate of 3.5 LPM – CNC (with influence of fan)

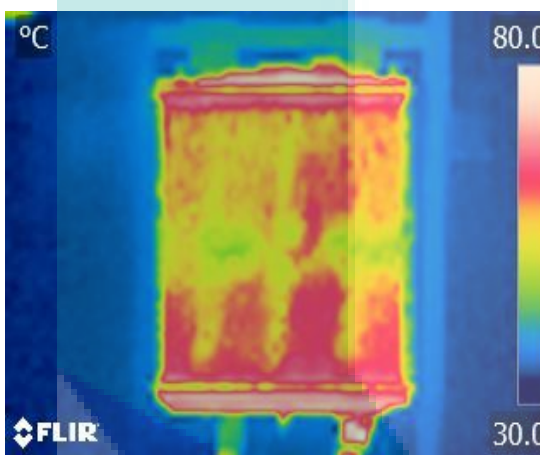


Figure 4.42 Temperature distribution at flow rate of 4.5 LPM – EGW (with influence of fan)

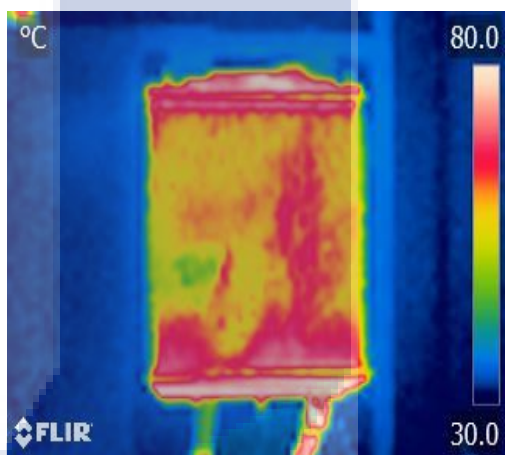


Figure 4.43 Temperature distribution at flow rate of 4.5 LPM – CNC (with influence of fan)

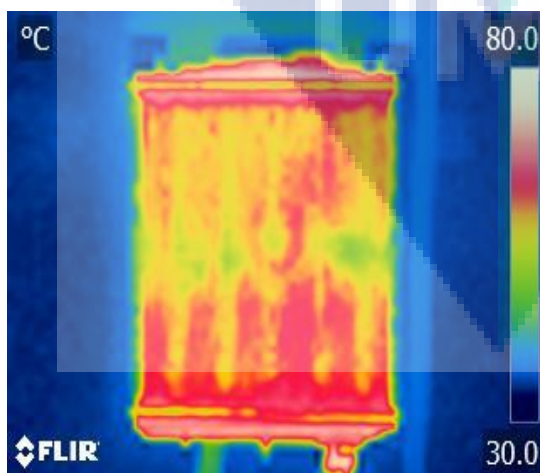


Figure 4.44 Temperature distribution at flow rate of 5.5 LPM – EGW (with influence of fan)

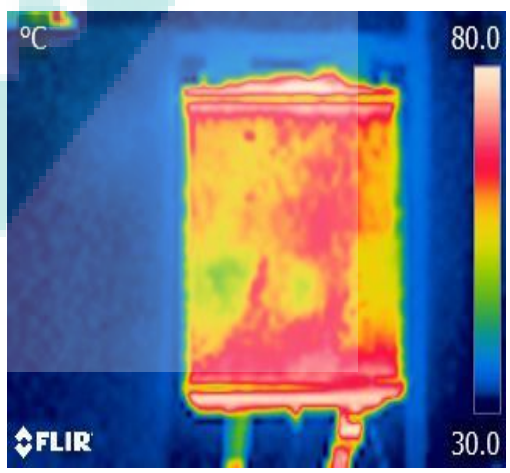


Figure 4.45 Temperature distribution at flow rate of 5.5 LPM – CNC (with influence of fan)

From the temperature distribution profile, we can observe that nanofluid has better heat profile compared to conventional ethylene glycol-water mixture. Nanofluid also has more cooled areas (green colour). The highest heat dissipation occurs at the middle of the radiator. Besides, images taken by using EGW thermal transport fluid is mostly covered with red area which has high temperature exposure.

On the other side, heat dissipation with the influence of fan has better temperature distribution profile compared to without the influence of fan. The temperature profile proves that nanofluid is efficient in removing heat from the automotive radiator. Thus, thermophysical property enhancement especially thermal conductivity and specific heat capacity is significant in increasing heat removal from the radiator. This temperature distribution profile results supports the results discussed in this chapter previously. Nanofluid produces high heat transfer coefficient value which helps to enhance heat transfer far better than conventional ethylene glycol-water mixture.



UMP

CHAPTER 5

CONCLUSION AND RECOMMENDATIONS

5.1 Introduction

In this chapter, conclusion is drawn and future recommendations is highlighted. In nutshell, dispersion of nanocellulose with weight concentration of 8.0% in ethylene glycol-water mixture at volume ratio of 40:60 enhances convective heat transfer compared to conventional ethylene glycol-water mixture. The prepared nanocellulose based nanofluid able to produce high stability characteristics and promotes for the thermophysical enhancement. Nanofluid with high thermal conductivity is suitable to be used in automotive cooling system as novel thermal transport fluid. In future, other type of nanocellulose can be used to study heat transfer performance in automotive cooling system.

5.2 Conclusion

Dispersion of nanocellulose which is extracted from Western Hemlock plant with weight concentration of 8% in ethylene glycol-distilled water mixture at volume ratio of 40:60 able to produce stable nanofluid and proven by stability results. Sedimentation observation for one month shows there are no settlement of nanosubstance at the bottom of test tube and least absorbance drop is recorded using spectrophotometry. Thus, high stability in nanofluid can be achieved because nanocellulose has a good physical and morphology characteristic. Besides, nanocellulose can dispersed well in ethylene glycol-distilled water mixture since it is hydrophilic.

The prepared stable nanofluid is used to measure thermophysical property measurement such as thermal conductivity, dynamic viscosity, density and specific heat capacity. Nanocellulose based nanofluid enhances thermophysical property especially thermal conductivity and specific heat capacity. The anomaly behind thermal

conductivity enhancement is related with Brownian motion and interfacial layer formation. Besides, enhancement in specific heat capacity is due to combined effect of bulk fluid and nanomaterial. This colloidal suspension alter crystallization which is responsible for enhancement in specific heat capacity. Meanwhile, both relative density and dynamic viscosity has linear relation with volume concentration and inverse relation with temperature. This is because of weakening of adhesion force when temperature increases. In addition, it is believed that nanocellulose fills the gaps in the nanofluid spontaneously which causes increases in mass and friction.

Once thermophysical property is measured, statistical analytical tool, Minitab is used to optimize volume concentration of nanofluid. The optimized nanofluid should have maximum value of thermal conductivity and specific heat capacity. On the other hand, it should be least value of density and dynamic viscosity. From the optimization response result, nanofluid with 0.5% is selected as optimized nanofluid and is been used as thermal transport fluid (CNC) and compared with conventional thermal transport fluid (EGW).

Experimental result shows that, experimental heat transfer coefficient, convective heat transfer, Reynolds number, Nusselt number produces proportional relation with volumetric flow rate. Meanwhile, maximum convective heat transfer enhancement is 66.85% under without the fan influence circumstance and 55.27% for with the influence of fan circumstance. Thus, nanocellulose based nanofluid removes heat from radiator efficiently. On the other side, maximum heat transfer enhancement involving overall effect of convective heat transfer and conductive heat transfer in radiator is 39.75% for without the influence of fan circumstance and 43.24% for with the influence of fan circumstance.

Besides, maximum thermal and hydraulic performance factor without and with the influence of fan is 2.15 and 2.28 respectively. These high values indicate nanocellulose based nanofluid has a better heat transfer performance compared to conventional thermal transport fluid. Meanwhile, rise in friction factor for nanocellulose based nanofluid in acceptable level. Better heat transfer performance of nanocellulose based nanofluid can be seen from temperature distributed profile image where CNC has large cooled area compared to EGW. In nutshell, Thus, nanocellulose based nanofluid is suitable for automotive cooling application since it has a better heat transfer performance.

REFERENCES

- Abdul Hamid, K., Azmi, W. H., Mamat, R., & Usri, N. A. (2014). *Thermal conductivity enhancement of aluminium oxide nanofluid in ethylene glycol*. Paper presented at the Applied Mechanics and Materials.
- Abitbol, T., Rivkin, A., Cao, Y., Nevo, Y., Abraham, E., Ben-Shalom & Shoseyov, O. (2016). Nanocellulose, a tiny fiber with huge applications. *Current opinion in biotechnology*, 39, 76-88.
- Adnan Mohammed, H. (2014). *Heat transfer enhancement using nanofluids in the automotive cooling system*. Doctoral thesis, Universiti Malaysia Pahang.
- Afrand, M. (2017). Experimental study on thermal conductivity of ethylene glycol containing hybrid nano-additives and development of a new correlation. *Applied Thermal Engineering*, 110, 1111-1119.
- Agarwal, D. K., Vaidyanathan, A., & Kumar, S. S. (2013). Synthesis and characterization of kerosene–alumina nanofluids. *Applied Thermal Engineering*, 60(1), 275-284.
- Ali, H. M., Ali, H., Liaquat, H., Maqsood, H. T. B., & Nadir, M. A. (2015). Experimental investigation of convective heat transfer augmentation for car radiator using ZnO–water nanofluids. *Energy*, 84, 317-324.
- Anoop, K., Kabelac, S., Sundararajan, T., & Das, S. K. (2009). Rheological and flow characteristics of nanofluids: influence of electroviscous effects and particle agglomeration. *Journal of Applied Physics*, 106(3), 034909.
- Aravind, S. S. J., & Ramaprabhu, S. (2013). Graphene-multiwalled carbon nanotube-based nanofluids for improved heat dissipation. *RSC Advances*, 3(13), 4199-4206. doi:10.1039/C3RA22653K
- Asadi, A., Asadi, M., Siahmargoi, M., Asadi, T., & Andarati, M. G. (2017). The effect of surfactant and sonication time on the stability and thermal conductivity of water-based nanofluid containing Mg(OH)₂ nanoparticles: An experimental investigation. *International Journal of Heat and Mass Transfer*, 108, 191-198.
- Azmi, W. H., Abdul Hamid, K., Mamat, R., Sharma, K. V., & Mohamad, M. S. (2016). Effects of working temperature on thermo-physical properties and forced convection heat transfer of TiO₂ nanofluids in water – Ethylene glycol mixture. *Applied Thermal Engineering*, 106, 1190-1199.
- Batchelor, G. K. (2000). *An introduction to fluid dynamics*: Cambridge university press.
- Bejan, A. (2013). *Convection heat transfer*: John wiley & sons.
- Bhanu Pratap Singh Tomar, A. T. (2015). Experimental Study of Heat Transfer of a Car Radiator with Nano fluid- Al₂O₃/Water mixture as Coolant. *International Journal of Advanced Research in Science, Engineering and Technology*, 2(9).
- Cengel, Y. A., & Cimbala, J. M. (2006). *Fundamental and applications*: McGraw Hill, New York.
- Chandrasekar, M., Suresh, S., & Chandra Bose, A. (2010). Experimental investigations and theoretical determination of thermal conductivity and viscosity of Al₂O₃/water nanofluid. *Experimental Thermal and Fluid Science*, 34(2), 210-216. doi:10.1016/j.expthermflusci.2009.10.022
- Chen, R., Lu, M.-C., Srinivasan, V., Wang, Z., Cho, H. H., & Majumdar, A. (2009). Nanowires for Enhanced Boiling Heat Transfer. *Nano Letters*, 9(2), 548-553. doi:10.1021/nl8026857
- Choi, C., Yoo, H., & Oh, J. (2008). Preparation and heat transfer properties of nanoparticle-in-transformer oil dispersions as advanced energy-efficient coolants. *Current Applied Physics*, 8(6), 710-712.

- Choi, S., Jaluria, Y., Manca, O., & Wang, L. (2011). Nanofluids. *Nanoscale research letters*, 6.
- Dardan, E., Afrand, M., & Meghdadi Isfahani, A. H. (2016). Effect of suspending hybrid nano-additives on rheological behavior of engine oil and pumping power. *Applied Thermal Engineering*, 109, Part A, 524- 34.
- Das, S. K., Putra, N., Thiesen, P., & Roetzel, W. (2003). Temperature Dependence of Thermal Conductivity Enhancement for Nanofluids. *Journal of Heat Transfer*, 125(4), 567. doi:10.1115/1.1571080
- Duangthongsuk, W., & Wongwises, S. (2009). Measurement of temperature-dependent thermal conductivity and viscosity of TiO₂-water nanofluids. *Experimental Thermal and Fluid Science*, 33(4), 706-714. doi:10.1016/j.expthermflusci.2009.01.005
- Duangthongsuk, W., & Wongwises, S. (2010). An experimental study on the heat transfer performance and pressure drop of TiO₂-water nanofluids flowing under a turbulent flow regime. *International Journal of Heat and Mass Transfer*, 53(1), 334-344.
- Duran, N., Paula Lemes, A., & B Seabra, A. (2012). Review of cellulose nanocrystals patents: preparation, composites and general applications. *Recent patents on nanotechnology*, 6(1), 16-28.
- Eastman, J. A., Choi, S., Li, S., Yu, W., & Thompson, L. (2001). Anomalous increased effective thermal conductivities of ethylene glycol-based nanofluids containing copper nanoparticles. *Applied Physics Letters*, 78(6), 718-720.
- Esfé, M. H., Saedodin, S., & Mahmoodi, M. (2014). Experimental studies on the convective heat transfer performance and thermophysical properties of MgO–water nanofluid under turbulent flow. *Experimental Thermal and Fluid Science*, 52, 68-78.
- Fakoor Pakdaman, M., Akhavan-Behabadi, M. A., & Razi, P. (2012). An experimental investigation on thermo-physical properties and overall performance of MWCNT/heat transfer oil nanofluid flow inside vertical helically coiled tubes. *Experimental Thermal and Fluid Science*, 40, 103-111.
- Ferrouillat, S., Bontemps, A., Poncelet, O., Soriano, O., & Gruss, J.-A. (2013a). Influence of nanoparticle shape factor on convective heat transfer and energetic performance of water-based SiO₂ and ZnO nanofluids. *Applied Thermal Engineering*, 51(1–2), 839-851.
- Ferrouillat, S., Bontemps, A., Poncelet, O., Soriano, O., & Gruss, J.-A. (2013b). Influence of nanoparticle shape factor on convective heat transfer and energetic performance of water-based SiO₂ and ZnO nanofluids. *Applied Thermal Engineering*, 51(1), 839-851.
- Fotukian, S., & Esfahany, M. N. (2010). Experimental study of turbulent convective heat transfer and pressure drop of dilute CuO/water nanofluid inside a circular tube. *International Communications in Heat and Mass Transfer*, 37(2), 214-219.
- Garg, J., Poudel, B., Chiesa, M., Gordon, J., Ma, J., Wang, J., Nanda, J. (2008). Enhanced thermal conductivity and viscosity of copper nanoparticles in ethylene glycol nanofluid. *Journal of Applied Physics*, 103(7), 074301.
- Ghadimi, A., Saidur, R., & Metselaar, H. (2011). A review of nanofluid stability properties and characterization in stationary conditions. *International Journal of Heat and Mass Transfer*, 54(17), 4051-4068.
- Godson, L., Raja, B., Lal, D. M., & Wongwises, S. (2010). Enhancement of heat transfer using nanofluids—an overview. *Renewable and sustainable energy reviews*, 14(2), 629-641.

- Gupta, M., Singh, V., Kumar, R., & Said, Z. (2017). A review on thermophysical properties of nanofluids and heat transfer applications. *Renewable and sustainable energy reviews*, 74, 638-670.
- Halefadi, S., Estellé, P., & Maré, T. (2014). Heat transfer properties of aqueous carbon nanotubes nanofluids in coaxial heat exchanger under laminar regime. *Experimental Thermal and Fluid Science*, 55, 174-180.
- He, Y., Jin, Y., Chen, H., Ding, Y., Cang, D., & Lu, H. (2007). Heat transfer and flow behaviour of aqueous suspensions of TiO₂ nanoparticles (nanofluids) flowing upward through a vertical pipe. *International Journal of Heat and Mass Transfer*, 50(11), 2272-2281.
- Heris, S. Z., Esfahany, M. N., & Etemad, S. G. (2007). Experimental investigation of convective heat transfer of Al₂O₃/water nanofluid in circular tube. *International Journal of Heat and Fluid Flow*, 28(2), 203-210.
- Hong, K., Hong, T.-K., & Yang, H.-S. (2006). Thermal conductivity of Fe nanofluids depending on the cluster size of nanoparticles. *Applied Physics Letters*, 88(3), 031901.
- Horrocks, J., & McLaughlin, E. (1963). *Non-steady-state measurements of the thermal conductivities of liquid polyphenyls*. Paper presented at the Proceedings of the Royal Society of London A: Mathematical, Physical and Engineering Sciences.
- Hussein, A. M., Bakar, R., & Kadrigama, K. (2014). Study of forced convection nanofluid heat transfer in the automotive cooling system. *Case Studies in Thermal Engineering*, 2, 50-61.
- Jang, S. P., & Choi, S. U. (2004). Role of Brownian motion in the enhanced thermal conductivity of nanofluids. *Applied physics letters*, 84(21), 4316-4318.
- Joseph, E. A. O., & Isaac, B. (2016). Effect of Heat Expansion in an Internal Combustion Automotive Engine.
- Keblinski, P., Phillpot, S., Choi, S., & Eastman, J. (2002). Mechanisms of heat flow in suspensions of nano-sized particles (nanofluids). *International Journal of Heat and Mass Transfer*, 45(4), 855-863.
- Ko, G. H., Heo, K., Lee, K., Kim, D. S., Kim, C., Sohn, Y., & Choi, M. (2007). An experimental study on the pressure drop of nanofluids containing carbon nanotubes in a horizontal tube. *International Journal of Heat and Mass Transfer*, 50(23), 4749-4753.
- Kulkarni, D. P., Vajjha, R. S., Das, D. K., & Oliva, D. (2008). Application of aluminum oxide nanofluids in diesel electric generator as jacket water coolant. *Applied Thermal Engineering*, 28(14), 1774-1781.
- Kumaresan, V., & Velraj, R. (2012). Experimental investigation of the thermo-physical properties of water–ethylene glycol mixture based CNT nanofluids. *Thermochimica Acta*, 545, 180-186.
- Lee, J., & Mudawar, I. (2007). Assessment of the effectiveness of nanofluids for single-phase and two-phase heat transfer in micro-channels. *International Journal of Heat and Mass Transfer*, 50(3), 452-463.
- Lee, J. H. (2009). *Convection performance of nanofluids for electronics cooling*: Stanford University.
- Lee, S. W., Park, S. D., Kang, S., Bang, I. C., & Kim, J. H. (2011). Investigation of viscosity and thermal conductivity of SiC nanofluids for heat transfer applications. *International Journal of Heat and Mass Transfer*, 54(1), 433-438.
- Leong, K., Yang, C., & Murshed, S. (2006). A model for the thermal conductivity of nanofluids—the effect of interfacial layer. *Journal of nanoparticle research*, 8(2), 245-254.

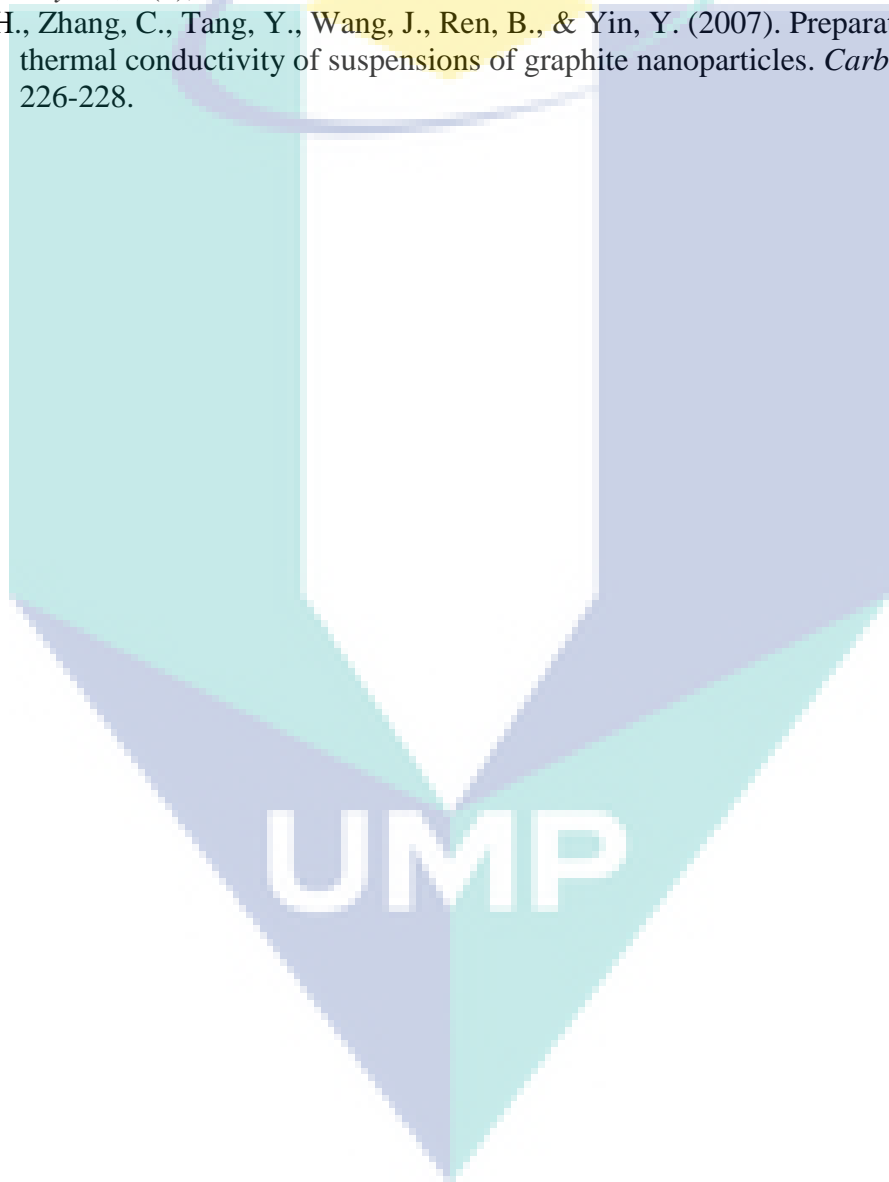
- Leong, K. Y., Saidur, R., Kazi, S. N., & Mamun, A. H. (2010). Performance investigation of an automotive car radiator operated with nanofluid-based coolants (nanofluid as a coolant in a radiator). *Applied Thermal Engineering*, 30(17–18), 2685-2692.
- Li, Q., Xuan, Y., & Wang, J. (2003). Investigation on convective heat transfer and flow features of nanofluids. *Journal of Heat Transfer*, 125(2003), 151-155.
- Li, W., Zou, C., & Li, X. (2017). Thermo-physical properties of waste cooking oil-based nanofluids. *Applied Thermal Engineering*, 112, 784-792.
- Li, Y., Tung, S., Schneider, E., & Xi, S. (2009). A review on development of nanofluid preparation and characterization. *Powder Technology*, 196(2), 89-101.
- Lin, C.-Y., Wang, J.-C., & Chen, T.-C. (2011). Analysis of suspension and heat transfer characteristics of Al₂O₃ nanofluids prepared through ultrasonic vibration. *Applied Energy*, 88(12), 4527-4533.
- Mahbubul, I., Elcioglu, E. B., Saidur, R., & Amalina, M. (2017). Optimization of ultrasonication period for better dispersion and stability of TiO₂–water nanofluid. *Ultrasonics Sonochemistry*, 37, 360-367.
- Mahbubul, I., Saidur, R., & Amalina, M. (2012). Latest developments on the viscosity of nanofluids. *International Journal of Heat and Mass Transfer*, 55(4), 874-885.
- Mahbubul, I., Saidur, R., & Amalina, M. (2013). Thermal conductivity, viscosity and density of R141b refrigerant based nanofluid. *Procedia Engineering*, 56, 310-315.
- Masuda, H., Ebata, A., & Teramae, K. (1993). Alteration of thermal conductivity and viscosity of liquid by dispersing ultra-fine particles. Dispersion of Al₂O₃, SiO₂ and TiO₂ ultra-fine particles.
- Mathivanan, E., Gasior, D., Liu, L., Yee, K., & Li, Y. (2017). *Experimental Investigation of the Impact of Nanofluids on Heat Transfer Performance of a Motorcycle Radiator* (0148-7191). Retrieved from
- Maxwell, J. C. (1881). *A treatise on electricity and magnetism* (Vol. 1): Clarendon press.
- Mehrali, M., Sadeghinezhad, E., Latibari, S. T., Kazi, S. N., Mehrali, M., Zubir, M. N. B. M., & Metselaar, H. S. C. (2014). Investigation of thermal conductivity and rheological properties of nanofluids containing graphene nanoplatelets. *Nanoscale research letters*, 9(1), 15.
- Mostafizur, R., Saidur, R., Aziz, A. A., & Bhuiyan, M. (2015). Thermophysical properties of methanol based Al₂O₃ nanofluids. *International Journal of Heat and Mass Transfer*, 85, 414-419.
- Mui, J., Ngo, J., & Kim, B. (2016). Aggregation and colloidal stability of commercially available Al₂O₃ nanoparticles in aqueous environments. *Nanomaterials*, 6(5), 90.
- Murshed, S., Leong, K., & Yang, C. (2005). Enhanced thermal conductivity of TiO₂–water based nanofluids. *International Journal of Thermal Sciences*, 44(4), 367-373.
- Murshed, S., Leong, K., & Yang, C. (2008). Thermophysical and electrokinetic properties of nanofluids—a critical review. *Applied Thermal Engineering*, 28(17), 2109-2125.
- Namburu, P. K., Das, D. K., Tanguturi, K. M., & Vajjha, R. S. (2009). Numerical study of turbulent flow and heat transfer characteristics of nanofluids considering variable properties. *International Journal of Thermal Sciences*, 48(2), 290-302.
- Naraki, M., Peyghambarzadeh, S. M., Hashemabadi, S. H., & Vermahmoudi, Y. (2013). Parametric study of overall heat transfer coefficient of CuO/water nanofluids in a car radiator. *International Journal of Thermal Sciences*, 66, 82-90.
- Nguyen, C., Desgranges, F., Galanis, N., Roy, G., Maré, T., Boucher, S., & Mintsa, H. A. (2008). Viscosity data for Al₂O₃–water nanofluid—hysteresis: Is heat transfer

- enhancement using nanofluids reliable? *International Journal of Thermal Sciences*, 47(2), 103-111.
- Nguyen, C., Desgranges, F., Roy, G., Galanis, N., Maré, T., Boucher, S., & Mintsa, H. A. (2007). Temperature and particle-size dependent viscosity data for water-based nanofluids–hysteresis phenomenon. *International Journal of Heat and Fluid Flow*, 28(6), 1492-1506.
- Nguyen, C. T., Desgranges, F., Roy, G., Galanis, N., Maré, T., Boucher, S., & Angue Mintsa, H. (2007). Temperature and particle-size dependent viscosity data for water-based nanofluids – Hysteresis phenomenon. *International Journal of Heat and Fluid Flow*, 28(6), 1492-1506.
- P. Gopal, C. R. K., Vadivelu. (2016). *Experimental Investigation On Heat Transfer Enhancement In Automotive Radiator Using Copper Nano Particles In Engine Coolant*. Paper presented at the International Conference on Energy Efficient Technologies For Automobiles (EETA' 15).
- Pak, B. C., & Cho, Y. I. (1998). Hydrodynamic and heat transfer study of dispersed fluids with submicron metallic oxide particles. *Experimental Heat Transfer an International Journal*, 11(2), 151-170.
- Palabiyik, I., Musina, Z., Witharana, S., & Ding, Y. (2011). Dispersion stability and thermal conductivity of propylene glycol-based nanofluids. *Journal of Nanoparticle Research*, 13(10), 5049.
- Pastoriza-Gallego, M., Casanova, C., Legido, J. a., & Piñeiro, M. (2011). CuO in water nanofluid: influence of particle size and polydispersity on volumetric behaviour and viscosity. *Fluid Phase Equilibria*, 300(1), 188-196.
- Pastoriza-Gallego, M., Casanova, C., Páramo, R., Barbés, B., Legido, J., & Piñeiro, M. (2009). A study on stability and thermophysical properties (density and viscosity) of Al₂O₃ in water nanofluid. *Journal of Applied Physics*, 106(6), 064301.
- Peyghambarzadeh, S., Hashemabadi, S., Hoseini, S., & Jamnani, M. S. (2011). Experimental study of heat transfer enhancement using water/ethylene glycol based nanofluids as a new coolant for car radiators. *International Communications in Heat and Mass Transfer*, 38(9), 1283-1290.
- Peyghambarzadeh, S. M., Hashemabadi, S. H., Jamnani, M. S., & Hoseini, S. M. (2011). Improving the cooling performance of automobile radiator with Al₂O₃/water nanofluid. *Applied Thermal Engineering*, 31(10), 1833-1838.
- Peyghambarzadeh, S. M., Hashemabadi, S. H., Naraki, M., & Vermahmoudi, Y. (2013). Experimental study of overall heat transfer coefficient in the application of dilute nanofluids in the car radiator. *Applied Thermal Engineering*, 52(1), 8-16.
- Powell, R. (1957). Experiments using a simple thermal comparator for measurement of thermal conductivity, surface roughness and thickness of foils or of surface deposits. *Journal of Scientific Instruments*, 34(12), 485.
- Putra, N., Thiesen, P., & Roetzel, W. (2003). Temperature dependence of thermal conductivity enhancement for nanofluids. *J Heat Transf*, 125, 567-574.
- Rashmi, W., Ismail, A. F., Sopyan, I., Jameel, A. T., Yusof, F., Khalid, M., & Mubarak, N. (2011). Stability and thermal conductivity enhancement of carbon nanotube nanofluid using gum arabic. *Journal of Experimental Nanoscience*, 6(6), 567-579.
- Richardson, J. F., & Zaki, W. N. (1954). The sedimentation of a suspension of uniform spheres under conditions of viscous flow. *Chemical Engineering Science*, 3(2),
- Rodionova, G., Eriksen, Ø., & Gregersen, Ø. (2012). TEMPO-oxidized cellulose nanofiber films: effect of surface morphology on water resistance. *Cellulose*, 19(4), 1115-1123.

- Saeedinia, M., Akhavan-Behabadi, M., & Razi, P. (2012). Thermal and rheological characteristics of CuO–Base oil nanofluid flow inside a circular tube. *International Communications in Heat and Mass Transfer*, 39(1), 152-159.
- Said, Z., Kamyar, A., & Saidur, R. (2013). *Experimental investigation on the stability and density of TiO₂, Al₂O₃, SiO₂ and TiSiO₄*. Paper presented at the IOP Conference Series: Earth and Environmental Science.
- Saidur, R., Leong, K. Y., & Mohammad, H. A. (2011). A review on applications and challenges of nanofluids. *Renewable and sustainable energy reviews*, 15(3), 1646-1668.
- Sakamoto, M., Kanda, Y., Miyahara, M., & Higashitani, K. (2002). Origin of long-range attractive force between surfaces hydrophobized by surfactant adsorption. *Langmuir*, 18(15), 5713-5719.
- Seyf, H. R., & Mohammadian, S. K. (2011). Thermal and hydraulic performance of counterflow microchannel heat exchangers with and without nanofluids. *Journal of Heat Transfer*, 133(8), 081801.
- Sharif, M. Z., Redhwan, A., & Zawawi, N. (2017). *Preparation and stability of silicone dioxide dispersed in polyalkylene glycol based nanolubricants*. Paper presented at the MATEC Web of Conferences.
- Sharma, S., & Gupta, S. M. (2016). Preparation and evaluation of stable nanofluids for heat transfer application: A review. *Experimental Thermal and Fluid Science*, 79, 202-212.
- Shi, J., Zhao, W., Li, J., & Liu, Z. (2017). Heat Transfer Performance of Heat Pipe Radiator with SiO₂/Water Nanofluids. *Heat Transfer—Asian Research*.
- Singh, D., Bhalla, V., Mathur, A., Wan, M., Dhawan, P. K., Jaiswal, A. K., & Yadav, R. R. (2015). Experimental Investigation On the Thermal Conductivity and Ultrasonic Velocity of Propylene Glycol Based TiO₂ Nanofluids.
- Siró, I., & Plackett, D. (2010). Microfibrillated cellulose and new nanocomposite materials: a review. *Cellulose*, 17(3), 459-494.
- Soltanimehr, M., & Afrand, M. (2016). Thermal conductivity enhancement of COOH-functionalized MWCNTs/ethylene glycol–water nanofluid for application in heating and cooling systems. *Applied Thermal Engineering*, 105, 716-723.
- Sundar, L. S., Singh, M. K., Bidkin, I., & Sousa, A. C. (2014). Experimental investigations in heat transfer and friction factor of magnetic Ni nanofluid flowing in a tube. *International Journal of Heat and Mass Transfer*, 70, 224-234.
- Sundar, L. S., Singh, M. K., & Sousa, A. C. M. (2013). Thermal conductivity of ethylene glycol and water mixture based Fe₃O₄ nanofluid. *International Communications in Heat and Mass Transfer*, 49, 17-24. doi:10.1016/j.icheatmasstransfer.2013.08.026
- Syam Sundar, L., Singh, M. K., & Sousa, A. C. M. (2013). Investigation of thermal conductivity and viscosity of Fe₃O₄ nanofluid for heat transfer applications. *International Communications in Heat and Mass Transfer*, 44, 7-14.
- Teng, T.-P., Hung, Y.-H., Teng, T.-C., Mo, H.-E., & Hsu, H.-G. (2010). The effect of alumina/water nanofluid particle size on thermal conductivity. *Applied Thermal Engineering*, 30(14-15), 2213-2218. doi:10.1016/j.applthermaleng.2010.05.036
- Teng, T.-P., & Yu, C.-C. (2013). Heat dissipation performance of MWCNTs nanocoolant for vehicle. *Experimental Thermal and Fluid Science*, 49, 22-30.
- Thomas, S., & Sobhan, C. B. P. (2011). A review of experimental investigations on thermal phenomena in nanofluids. *Nanoscale Research Letters*, 6(1), 377.
- Timofeeva, E. V., Smith, D. S., Yu, W., France, D. M., Singh, D., & Routbort, J. L. (2010). Particle size and interfacial effects on thermo-physical and heat transfer

- characteristics of water-based α -SiC nanofluids. *Nanotechnology*, 21(21), 215703.
- Timofeeva, E. V., Yu, W., France, D. M., Singh, D., & Routbort, J. L. (2011). Nanofluids for heat transfer: an engineering approach. *Nanoscale research letters*, 6(1), 182.
- Ting, F. C. K., & Kirby, J. T. (1996). Dynamics of surf-zone turbulence in a spilling breaker. *Coastal Engineering*, 27(3), 131-160.
- Tiznobaik, H., & Shin, D. (2013). Enhanced specific heat capacity of high-temperature molten salt-based nanofluids. *International Journal of Heat and Mass Transfer*, 57(2), 542-548.
- Turgut, A., Tavman, I., Chirtoc, M., Schuchmann, H., Sauter, C., & Tavman, S. (2009). Thermal conductivity and viscosity measurements of water-based TiO₂ nanofluids. *International Journal of Thermophysics*, 30(4), 1213-1226.
- Usri, N. A., Azmi, W. H., Mamat, R., & Abdul Hamid, K. (2014). *Viscosity of aluminium oxide (Al₂O₃) nanoparticle dispersed in ethylene glycol*. Paper presented at the Applied Mechanics and Materials.
- Vajjha, R., Das, D., & Mahagaonkar, B. (2009). Density measurement of different nanofluids and their comparison with theory. *Petroleum Science and Technology*, 27(6), 612-624.
- Van Trinh, P., Anh, N. N., Thang, B. H., Quang, L. D., Hong, N. T., Hong, N. M., Hong, P. N. (2017). Enhanced thermal conductivity of nanofluid-based ethylene glycol containing Cu nanoparticles decorated on a Gr-MWCNT hybrid material. *RSC Advances*, 7(1), 318-326. doi:10.1039/C6RA25625B
- Wang, J., Zhu, J., Zhang, X., & Chen, Y. (2013). Heat transfer and pressure drop of nanofluids containing carbon nanotubes in laminar flows. *Experimental Thermal and Fluid Science*, 44, 716-721.
- Wang, K.-J., Ding, G.-L., & Jiang, W. (2006). *Nano-scale thermal transporting and its use in engineering*. Paper presented at the Proceedings of the 4th Symposium on Refrigeration and Air Conditioning Southeast University Press, Nanjing, China.
- Wang, R., Hao, B., Xie, G., & Li, H. (2003). *A refrigerating system using HFC134a and mineral lubricant appended with n-TiO₂ (R) as working fluids*. Paper presented at the Proceedings of the 4th International Symposium on HVAC, Tsinghua University Press, Beijing, China.
- Wang, X., Xu, X., & S. Choi, S. U. (1999). Thermal conductivity of nanoparticle-fluid mixture. *Journal of thermophysics and heat transfer*, 13(4), 474-480.
- Wei, B., Zou, C., Yuan, X., & Li, X. (2017). Thermo-physical property evaluation of diathermic oil based hybrid nanofluids for heat transfer applications. *International Journal of Heat and Mass Transfer*, 107, 281-287.
- Wen, D., & Ding, Y. (2004). Experimental investigation into convective heat transfer of nanofluids at the entrance region under laminar flow conditions. *International Journal of Heat and Mass Transfer*, 47(24), 5181-5188.
- Wen, D., & Ding, Y. (2005). Experimental investigation into the pool boiling heat transfer of aqueous based γ -alumina nanofluids. *Journal of Nanoparticle Research*, 7(2), 265-274.
- Witharana, S., Palabiyik, I., Musina, Z., & Ding, Y. (2013). Stability of glycol nanofluids—the theory and experiment. *Powder Technology*, 239, 72-77.
- Yadav, J., & Singh, B. R. (2011). Study on Performance Evaluation of Automotive Radiator. *S-JPSET*, 2(2), 47-56.
- Yousefi, T., Shojaeizadeh, E., Veysi, F., & Zinadini, S. (2012). An experimental investigation on the effect of pH variation of MWCNT–H₂O nanofluid on the efficiency of a flat-plate solar collector. *Solar Energy*, 86(2), 771-779.

- Yu, W., & Xie, H. (2012). A Review on Nanofluids: Preparation, Stability Mechanisms, and Applications. *Journal of Nanomaterials*, 2012, 1-17. doi:10.1155/2012/435873
- Yu, W., Xie, H., Li, Y., & Chen, L. (2011). Experimental investigation on thermal conductivity and viscosity of aluminum nitride nanofluid. *Particuology*, 9(2), 187-191.
- Zhou, S.-Q., & Ni, R. (2008). Measurement of the specific heat capacity of water-based Al₂O₃ nanofluid. *Applied Physics Letters*, 92(9), 093123.
- Zhu, D., Li, X., Wang, N., Wang, X., Gao, J., & Li, H. (2009). Dispersion behavior and thermal conductivity characteristics of Al₂O₃-H₂O nanofluids. *Current Applied Physics*, 9(1), 131-139.
- Zhu, H., Zhang, C., Tang, Y., Wang, J., Ren, B., & Yin, Y. (2007). Preparation and thermal conductivity of suspensions of graphite nanoparticles. *Carbon*, 45(1), 226-228.



APPENDIX A
EXPERIMENTAL DATA MEASURED

Table A.1 Thermophysical measurement of nanofluid at 30°C

Thermophysical property	ASHRAE	EGW	0.1	0.5	0.9	1.3
Thermal conductivity (W.mK)	0.412	0.415	0.44	0.449	0.457	0.469
Dynamic viscosity (kg/m.s)	0.0023	0.0024	0.0026	0.00397	0.00599	0.00822
Density (kg/m ³)	1055.39	1059.12	1059.32	1060.52	1061.74	1063.05

Table A.2 Thermophysical measurement of nanofluid at 50°C

Thermophysical property	ASHRAE	EGW	0.1	0.5	0.9	1.3
Thermal conductivity (W.mK)	0.425	0.429	0.464	0.479	0.496	0.511
Dynamic viscosity (kg/m.s)	0.00143	0.00158	0.00178	0.00273	0.00438	0.00549
Density (kg/m ³)	1045.35	1051.645	1052.312	1053.6243	1055.0366	1056.3596

Table A.3 Thermophysical measurement of nanofluid at 70°C

Thermophysical property	ASHRAE	EGW	0.1	0.5	0.9	1.3
Thermal conductivity (W.mK)	0.434	0.44	0.493	0.52	0.544	0.559
Dynamic viscosity (kg/m.s)	1.00E-03	0.00111	0.00144	0.00225	0.0033	0.00438
Density (kg/m ³)	1033.37	1040.82	1041.31	1043.72	1046.145	1048.558

Table A.4 Thermophysical measurement of nanofluid at 80°C

Thermophysical property	ASHRAE	EGW	0.1	0.5	0.9	1.3
Thermal conductivity (W.mK)	0.438	0.445	0.501	0.523	0.54912	0.564
Dynamic viscosity (kg/m.s)	8.20E-04	9.20E-04	0.00138	0.00204	0.0028	0.00407
Density (kg/m ³)	1026.65	1035.413	1036.31	1038.4331	1040.7451	1043.057

APPENDIX B
SPECIFIC HEAT CAPACITY MEASUREMENT

Table B.1 Specific heat capacity measurement of nanofluid

Temperature (°C)	ASHRAE	EGW	0.1	0.5	0.9	1.3
30	3502	3507	3592	3540	3507	3432
60	3602	3609	3813	3730	3632	3532
80	3669	3677	3945	3850	3729	3629
90	3703	3715	3972	3890	3749	3644

*Unit = J/kg.°C

